

PETROLOGY, DIAGENESIS, AND GENETIC STRATIGRAPHY OF THE
EOCENE BACA FORMATION, ALAMO NAVAJO RESERVATION
AND VICINITY, SOCORRO COUNTY, NEW MEXICO

APPROVED:

Robert L. Folk

Alan J. Brooks
John E. Chapin

PETROLOGY, DIAGENESIS, AND GENETIC STRATIGRAPHY OF THE
EOCENE BACA FORMATION, ALAMO NAVAJO RESERVATION
AND VICINITY, SOCORRO COUNTY, NEW MEXICO

by

STEVEN MARTIN CATHER, B.S.

THESIS

Presented to the Faculty of the Graduate School of
The University of Texas at Austin
in Partial Fulfillment
of the Requirements
for the Degree of

MASTER OF ARTS

THE UNIVERSITY OF TEXAS AT AUSTIN

August 1980

ACKNOWLEDGMENTS

I wish to sincerely thank Drs. R. L. Folk and C. E. Chapin for their enthusiasm toward this study and their patience in tutoring a novice geologist in their respective fields of expertise. Dr. A. J. Scott provided many helpful comments concerning lacustrine sedimentation and thesis illustrations. Discussions with Bruce Johnson contributed greatly to my understanding of the distribution of facies and paleoenvironments within the Baca-Eagar basin. I would also like to thank my colleagues in Austin and Socorro for their helpful comments and criticisms. Bob Blodgett served as student editor. Finally, I would like to acknowledge Jerry Garcia, who provided unending inspiration and motivation throughout the course of this study.

Financial support for field work and the writing of this manuscript was generously provided by the New Mexico Bureau of Mines and Mineral Resources. The University of Texas Geology Foundation also provided funds for travel expenses and field work.

This thesis was submitted to the committee in June, 1980.

PETROLOGY, DIAGENESIS, AND GENETIC STRATIGRAPHY OF THE
EOCENE BACA FORMATION, ALAMO NAVAJO RESERVATION
AND VICINITY, SOCORRO COUNTY, NEW MEXICO

by

Steven M. Cather

ABSTRACT

The Eocene Baca Formation of New Mexico and correlative Eagar Formation and Mogollon Rim gravels of Arizona comprise a redbed sequence of conglomerate, sandstone, mudstone, and claystone which crops out from near Socorro, New Mexico, to the Mogollon Rim of Arizona. These sediments were deposited in a large intermontane basin present in western New Mexico and eastern Arizona during Laramide time. The Baca-Eagar basin is bounded to the north by the Defiance, Zuni, and Lucero uplifts, to the southwest by the Mogollon Highland, to the east by the Sierra-Sandia uplift, and to the southeast by the Morenci uplift. The study area consists of an approximately 12 mi^2 (31 km^2) exposure of the Baca Formation located along the north end of the Gallinas Mountains about 20 mi (32 km) northwest of Magdalena, New Mexico. In the study area, the Baca is about 940 ft (289 m) thick and can be subdivided into three

informal members (lower red, middle sandstone, and upper red units) which are genetically related to large-scale lake-level fluctuations in a large, closed lacustrine system present in the Bear-Gallinas Mountains vicinity during Baca time. Three component facies were recognized within the Baca in the study area. These are the distal braided alluvial-plain, fine-grained lacustrine delta, and lacustrine basinal facies. The regional paleocurrent direction in the Gallinas Mountains vicinity appears to be toward the northeast. Baca sediments in the study area were derived predominantly from the Morenci uplift and from the western flank of that portion of the Sierra-Sandia uplift which lies to the south of the area.

Three episodes of structural development took place in the study area: (a) formation of a Laramide (?) monoclinial flexure in the southeastern portion of the area, (b) Neogene extensional faulting, drag folding, and dike intrusion, and (c) uplift of the Colorado Plateau in Neogene time, which resulted in the shallow southward dip of the strata in the area.

Lithologies present within Baca conglomerate clasts include metaquartzite, limestone, chert, granite, sandstone, siltstone, schist, mudstone, and volcanics. The majority of the sandstones in the study area are lithic arkoses, feldspathic litharenites, and sublitharenites. Two genetic

quartz types, common and metamorphic quartz, are present in subequal proportions. Orthoclase is the dominant feldspar, followed by microcline and plagioclase. Rock fragment varieties include metamorphic, chert, mudstone, granite/gneiss, volcanic, carbonate, siltstone and sandstone rock fragments. Upsection changes in sandstone mineralogy suggest the progressive "unroofing" of Precambrian source terranes during basal Baca sedimentation. Heavy-mineral suites from non-red Baca sandstones show evidence of alteration by negative-Eh groundwaters associated with Miocene dike intrusion and dolomite cementation. Illite is the dominant detrital clay mineral in the study area.

Four types of cements (calcite, kaolinite, quartz, and dolomite) are present in the Baca sediments. The environment of deposition strongly controlled the diagenetic history of the sediments in the study area. The widespread red coloration of the Baca was produced diagenetically, by intrastratal dissolution of unstable iron-bearing heavy minerals, precipitation of limonite, and subsequent dehydration of this limonite to form the hematite colorant. Yellow-gray coloration is restricted to permeable sandstones located near mafic dikes, and occurred by oxidation during recent outcrop weathering of reduced iron which was primarily incorporated within dolomite cements that formed synchronously with dike intrusion in Miocene time.

TABLE OF CONTENTS

TEXT

	<u>Page</u>
INTRODUCTION	1
Study Area	1
Purpose and Methods of Study	3
GENERAL STRATIGRAPHY	5
Late Cretaceous Crevasse Canyon Formation	6
Eocene Baca Formation	7
Correlation and previous work	7
Lower Tertiary equivalents	9
Age and fossils	12
Contacts	15
General description and informal units	17
Lower red unit	20
Middle sandstone unit	21
Upper red unit	21
Oligocene Spears Formation	22
Miocene Dikes	23
Pliocene (?) to Holocene Piedmont Gravels	24
Quaternary Alluvium	25
LARAMIDE TECTONICS	26
Styles of Deformation	26
Cordilleran foldbelt	26
Basement uplifts of the Laramide	
Rocky Mountains	29
Colorado Plateau monoclinial flexures	33
Baca-Eagar Basin Tectonic Framework	35
Mogollon Highland	37
Lucero uplift	38
Zuni uplift	38
Defiance uplift	39
Sierra-Sandia uplift	40
Morenci uplift	43
Plate Tectonics and the Development of the Laramide Foreland	47
STRUCTURAL GEOLOGY	53
Laramide Folding	53
Early Rift Faults, Drag Folds, and Dikes	55
Colorado Plateau Uplift	57

	<u>Page</u>
DEPOSITIONAL SYSTEMS	58
Braided Alluvial-Plain System	58
Distal braided alluvial-plain facies	59
Facies characteristics	59
Depositional processes	62
Braided alluvial plain model	65
Lacustrine System	68
Lacustrine fine-grained delta facies	69
Facies characteristics	69
Depositional processes	78
Basinal facies	80
Facies characteristics	80
Depositional processes	80
General characteristics of the lacustrine system	82
Lacustrine model	87
DEPOSITIONAL RECONSTRUCTION	91
Sediment Dispersal Patterns	91
Depositional History	95
PETROLOGY	102
Conglomerate Petrology	102
Clast composition	102
Clast morphology	106
Sandstone Petrology	110
Quartz	111
Common quartz	113
Metamorphic quartz	114
Feldspar	120
Orthoclase	128
Microcline	128
Plagioclase	128
Rock fragments	129
Metamorphic rock fragments	129
Chert	134
Granite and gneiss rock fragments	137
Volcanic rock fragments	137
Mudstone rock fragments	140
Sandstone and siltstone rock fragments	141
Carbonate rock fragments	142
Heavy minerals	144
Mudstone Petrology	150
PROVENANCE	156

	<u>Page</u>
DIAGENESIS	160
Cements	160
Calcite	160
Quartz	171
Kaolinite	178
Dolomite	182
Source of Coloration	187
Red coloration	187
Soil-derived red coloration	187
Diagenetic red coloration	189
Source of red coloration in the	
Baca Formation	190
Yellow-gray coloration	198
Porosity	199
Primary porosity	199
Secondary porosity	200
Diagenesis Summary	201
PALEOCLIMATE	205
ECONOMIC GEOLOGY	207
Uranium Occurrences	207
Ore Genesis	208
SUMMARY OF BACA-EAGAR BASIN DEPOSITIONAL SYSTEMS	210
SUMMARY AND CONCLUSIONS	212
APPENDIX A: Baca Formation Measured Section	218
APPENDIX B: Summary of Point-Count Data for	
Study-Area Sandstone Thin Sections	229
REFERENCES CITED	231
VITA	244

LIST OF TABLES

<u>Table</u>		<u>Page</u>
1	Summary of Previous Studies	10
2	Summary of Fossil Age Determinations	13
3	Distal Braided Alluvial-Plain Characteristics	60
4	Lacustrine Fine-Grained Delta Facies Characteristics	71
5	Lacustrine Basinal Facies Characteristics	81
6	Summary of Pebble Composition Data	103
7	Distribution of Coloration, Cements, Porosity, and Heavy Minerals in Relation to the Various Baca Facies	203

LIST OF FIGURES

<u>Figure</u>		<u>Page</u>
1	Location of study area and Baca, Eagar, and Mogollon Rim gravels	2
2	Map showing outcrop areas of lower Tertiary units in New Mexico and adjacent areas	11
3	Cloven hoof prints found in a Baca delta- plain sandstone. Lens cap is approximately seven cm in diameter.	14
4	Hematitic mudstone-filled ostracod test in sample 49. Field width=0.8 mm, crossed nicols.	16
5	Comparison of generalized Baca stratigraphic sections measured in the Gallinas and Bear Mountains, showing similarity of lithofacies and probable correlation of informal units. Sections are separated by about 10 mi (16 km). Bear Mountains section modified from Massingill (1979).	19

<u>Figure</u>		<u>Page</u>
6	Map showing distribution and structural styles of Laramide uplifts in western North America, and the location of the Baca-Eagar basin. Modified from Eardley (1962) and Drewes (1978).	27
7	Section across Spring Mountains, southern Nevada, showing typical Cordilleran-foldbelt style of deformation. Note imbricate, east-verging thrust plates. . . .	28
8	Two hypothetical styles of deformation in Laramide Rocky mountain uplifts. (a) Uplift caused by vertical forces acting along range-bounding faults which steepen with depth. Section through Owl Creek uplift, Wyoming. From Couples and Stearns (1978). (b) Uplift created by horizontal stresses acting along thrust faults. Cross section through the Wind River Mountains, Wyoming. Modified from Sales (1968).	31
9	Experimental deformational model showing probable style of Colorado Plateau monoclinal flexures, using "strata" of kaolinite and modeling clay resting on rigid "basement" of pine board. Davis (1978).	34
10	Laramide tectonic framework in eastern Arizona and western New Mexico. Heavy barbed line is northeastward limit of Cordilleran foldbelt (according to Drewes, 1978). Baca-Eagar-Mogollon Rim gravel outcrop areas are also shown. Reference points: S=Socorro, M=Magdalena, D=Datil, Sp=Springerville, SL=Show Low, SC=Silver City, T=Tucson. Modified from Eardley (1962).	36
11	Location of Morenci lineament and distribution of Laramide plutons adjacent to the Baca-Eagar basin. Presumably the majority of these plutons (circled) were associated with coeval volcanic centers. Reference points same as Figure 10, except Mo=Morenci. Lineament and pluton data from Chapin and others (1978).	44

<u>Figure</u>		<u>Page</u>
12	Distribution of lineaments (stippled) in the Four Corners area which controlled the development of monoclines (heavy lines). The coalescing Cow Springs (CS), Organ Rock (OR), and Comb Ridge (CR) monoclines are about the same length and trend the same direction as the proposed Morenci uplift. Modified from Davis (1978).	46
13	Map showing plate positions and relative motion vectors prior to Laramide orogeny. F=Farallon plate, K=Kula plate, P=Pacific plate, NA=North American plate. Vectors show motion of Farallon (Far) and North American (NA) plates relative to hot-spot frame of reference. Resultant shows direction and magnitude of plate convergence. Spreading centers shown by stippled areas between parallel lines, subduction zones by heavy barbed lines, thrust belts by light barbed lines, metamorphic core complexes by fine wavy lines, and arc terranes by short, dashed lines. Modified from Coney (1978).	49
14	Map showing plate positions and relative motion vectors during Laramide orogeny. Uplifts shown by small, elongate, closed areas. Other symbols same as Figure 13. Modified from Coney (1978).	50
15	Map showing plate positions and relative motion vectors during post-Laramide, middle-Tertiary ignimbrite flare-up. CP=Colorado Plateau. Dotted areas are large caldera complexes. Other symbols same as Figure 11. From Coney (1978).	52
16	Structure index map of study area.	54
17	Typical vertical section of distal braided alluvial-plain facies. Modified from Johnson (1978).	61

<u>Figure</u>		<u>Page</u>
18	Map showing distribution of bar types and sedimentary structures in proximal and mid-fan facies of Scott glacial outwash fan, Alaska. From Johnson (1978).	67
19	Typical vertical section of lacustrine fine-grained delta facies, showing upward-coarsening cycles. Modified from Johnson (1978).	70
20	Branching horizontal burrows (feeding traces?) in a red, lacustrine sandstone.	73
21	Baca fine-grained delta deposit exhibiting unusually steeply inclined prodelta foreset beds.	75
22	Gently inclined prodelta foreset beds overlain by quasi-spheroidally weathering delta front deposits. Hammer handle points in direction of delta progradation.	76
23	Exceptionally large deltaic distributary-channel deposit. Note the low width-to-depth ratio (less than 10:1) and the highly symmetrical nature, which are characteristic of distributary channel deposits in marine deltas.	77
24	Map showing crude, concentric zonation of facies in Eocene Lake Gosiute, Wyoming, during a high stand (Tipton Shale time). Marginal facies is composed of calcareous sandstones and siltstones, somewhat similar to the lacustrine system rocks in the study area. Surdam and Wolfbauer (1975).	89
25	Well-developed parting-step lineation in a fine-grained Baca sandstone. Paleoflow was parallel to trend of mechanical pencil.	92
26	Comparison of paleocurrent data in western (a,b) and eastern (c,d) portions of study area. The significant portions of the bidirectional rose diagrams (shaded) were determined by comparison with associated unidirectional data. The area was arbitrarily divided along the line between Indian Spring Canyon and Indian Mesa quadrangles.	94

<u>Figure</u>		<u>Page</u>
27	Generalized Baca stratigraphic section in the study area showing relationships between shoreline migrations, depositional systems, and informal units.	97
28	Generalized stratigraphy of the Green River Formation in Bridger and Washakie basins of Wyoming, showing alternation of high stands (Tipton and Laney Shales) and low stands (Luman Shale, Wilkins Peak) in Eocene Lake Gosiute. From Surdam and Wolfbauer (1975). .	101
29	Ternary plot of Baca pebble compositions. Data from 15 pebble counts within the study area..	105
30	Sphericity-form diagram showing shapes of 71 Baca pebbles. Average effective settling sphericity is 0.754. L=long diameter, I=intermediate diameter, S=short diameter. Sphericity-form diagram from Folk (1974). . .	107
31.	Classification of Baca sandstones based on data from 26 thin sections. Cross shows average composition. After Folk (1974).	112
32	Stretched metamorphic quartz grain. Sample 68, crossed nicols, field width=0.75 mm.	115
33	Schistose metamorphic quartz grain. Note minor amounts of parallel oriented muscovite and elongated quartz crystallites. Sample C, crossed nicols, field width=0.75 mm.	116
34	Recrystallized metamorphic quartz grain. Note equant shape of and simple boundaries between crystallites. Sample 32, crossed nicols, field width=0.75 mm.	117
35	Plot of grain size vs. metaquartz/common quartz for 27 Baca sandstones, showing tendency towards increasing abundances of metaquartz with increasing grain size.	119

<u>Figure</u>		<u>Page</u>
36	Plot of metaquartz/total quartz ratios as a function of stratigraphic position. Mean grain size ranges between 1.6 and 2.9 ϕ	121
37	Cavernous dissolution in an orthoclase grain from a fluvial sandstone (sample 48). Secondary porosity within the grain appears blue, due to impregnation of sample with colored epoxy. Plane light, field width=0.75 mm. . . .	122
38	Orthoclase grain being replaced by calcite. Sample 34, crossed nicols, field width=0.75 mm.	123
39	Plot of feldspar abundance as a function of stratigraphic position. Mean grain size of samples ranges between 1.6 and 2.9 ϕ	127
40	Quartzose metamorphic rock fragment. Note abundant inclusions of muscovite. Sample 48, crossed nicols, field width=0.75 mm.	130
41	Argillaceous metamorphic rock fragment which has been ductilely deformed by adjacent grains during compaction. Sample C, crossed nicols, field width=0.75 mm.	132
42	Plot of abundance of metamorphic rock fragments as a function of stratigraphic position. Mean grain size ranges between 1.6 and 2.9 ϕ	133
43	Chert grain. Sample A, crossed nicols, field width=0.75 mm.	135
44	Plot of chert abundance as a function of stratigraphic position. Mean grain size ranges between 1.6 and 2.9 ϕ	136
45	Volcanic rock fragment showing lath-like plagioclase crystals in dark, aphanitic groundmass. Sample 45, crossed nicols, field width=0.75 mm.	139
46	Well-developed oolite in an upper-delta sandstone. Note both concentric and radial structures. Sample 73, plane light, field width=0.75 mm.	143

<u>Figure</u>		<u>Page</u>
47	Typical heavy-mineral grain mount from a red Baca sandstone (sample 48). Note dominance of magnetite/ilmenite/specular hematite. White grains are leucoxene. Field width=0.8 mm.	146
48	Typical heavy-mineral suite from a yellow Baca sandstone (sample 56), showing dominance of limonite-stained leucoxene grains. Note sub-hedral zircon grain. Field width=0.8 mm . .	147
49	Hexagonal biotite observed in a heavy-mineral grain mount from sample 48. Width of field =0.75 mm.	149
50	Churned, disrupted texture typical of Baca lacustrine mudstones, which was probably produced by intense bioturbation. sample F, crossed nicols, field width=3.0 mm. . . .	152
51	Large, spar-filled void spaces in a sandy lacustrine mudstone (sample 8), which are indicative a very early, pre-compactional cementation. Crossed nicols, field width=3.0 mm.	154
52	Plot of metaquartz/total quartz ratios and abundances of feldspar, chert, and metamorphic rock fragments within Baca sandstones as a function of stratigraphic position. Samples were taken from a section measured by the writer in the study area. Mean grain size of the sandstones ranges between 1.6 and 2.9 ϕ	158
53	Plot of metaquartz/total ratios and abundances of feldspar, chert, and metamorphic rock fragments within Baca sandstones as a function of stratigraphic position. Samples were taken from Massingill's (1979) measured section in the Bear Mountains vicinity. Mean grain size varies widely, therefore caution is advised in the interpretation of this data.	159

<u>Figures</u>	<u>Page</u>
54	Well-developed calichified paleosol showing numerous tube-shaped rhizoconcretions. . . . 161
55	Baca caliche as seen in thin section. Note wide range in calcite crystal sizes and the presence of numerous grains which exhibit hematitic clay cutans. Sample 34, crossed nicols, field width=0.8 mm. 163
56	Coarsely crystalline spar cement in an upper-delta sandstone (sample C). Crossed nicols, field width=0.8 mm 165
57	Coarsely crystalline sparry calcite cement in cigar-shaped sandstone concretion (sample 49). Loosely packed fabric is indicative of very early cementation (prior to compaction). Crossed nicols, field width=0.8 mm. 166
58	Hematite-stained fine-grained sparry calcite in a frontal-splay sandstone (sample 13). Note poorly compacted nature of this early-cemented lacustrine sandstone. Crossed nicols, field width=0.75 mm. 169
59	Syntaxial overgrowth on detrital quartz grain Sample 45, crossed nicols, field width=0.75 mm. 172
60	Flamboyant megaquartz cement. Sample M50, crossed nicols, field width=0.8 mm. 173
61	Inhibition of syntaxial quartz overgrowth by coarsely crystalline sparry calcite cement. Sample B, crossed nicols, width of field=0.75 mm. 174
62	Plot of authigenic quartz content in study-area sandstones as a function of stratigraphic position. 176
63	Plot of authigenic quartz content in Baca sandstones as a function of stratigraphic position. Data from point counts made by the writer on thin sections from Massingill's (1979) measured section in the Bear Mountains area. 177

<u>Figure</u>		<u>Page</u>
64	Authigenic kaolinite. Bluish tint is due to impregnation of kaolinite microporosity with blue epoxy. Sample 48, crossed nicols, field width=0.15 mm.	179
65	Scanning electron photomicrograph of vemicular stacks of kaolinite crystallites on a quartz sand grain. Sample 56, 5,000X.	180
66	Dolomite cement showing alternating iron-rich and iron-poor zones. Sample B, crossed nicols, field width=0.75 mm.	183
67	Dolomite rhombohedron replacing adjacent quartz grain. Sample B, crossed nicols, field width=0.75 mm.	184
68	Generalized map of the study area showing coincidence of occurrence of dikes and areas in which Baca sandstones are yellow-gray in color (stippled areas).	186
69	Distribution of coloration for 52 Baca sandstone samples from the study area. Values were determined by comparison with Munsell Soil Color Chart. Color terminology after Folk (1969).	188
70	Hematite flecks uniformly distributed on Baca sand grains, except at contact points between grains. Sample P, plane light, field width=0.15 mm.	192
71	Scanning electron photomicrograph of euhedrally terminated hematite crystals on quartz sand grain. Sample P, 7,000X.	193
72	Change of color with geologic are shown on a plot of hue vs. saturation. Third color dimension of Lightness shown by the numbers 4/ etc. and degree of darkening of the squares. C, initial unweathered sand; A, Saharan sands, data from Alimen; S _f , Simpson Desert, surface fluff of Holocene age; S _m ,	

FiguresPage

	Simpson Desert, modal color <u>en masse</u> of fine sands; Sp, Simpson Desert, color of hematite-clay cutans in pits, formed during Pleistocene lateritization; P, other Pleistocene sediments Hm, color of powdered pure hematite; Py + M, color of Mesozoic and younger Paleozoic red rocks; Po, Older Paleozoic and Precambrian rocks. Processes that create these changes shown by the "evolutionary" arrows. (Modified from Folk, 1976).	197
73	Diagenesis flowchart for the Baca sediments within the study area.	202
74	Plot of grain size <u>vs.</u> percent cement plus primary porosity <u>showing</u> tendency towards looser packing in the fine-grained lower-delta and lacustrine basinal sediments. Note the presence of yellow-gray coloration only in the coarser grained, non-lacustrine sandstones.	204
75	Hypothetical model for the distribution of facies and paleocurrents in the Baca-Eager basin during early Baca time (high lake stand). Letters in parentheses indicate paleocurrent data sources. J=Johnson (1978), P=Pierce (1979), S=Snyder (1971), C=Cather (this study). Reference points same as Figure 10.	211

INTRODUCTION

Study Area

The Eocene Baca Formation of New Mexico and correlative Eagar Formation and Mogollon Rim gravels of Arizona comprise a redbed sequence of conglomerate, sandstone, mudstone, and claystone which crops out in discontinuous exposures along a west-trending belt from near Socorro, New Mexico to the Mogollon Rim of Arizona. The study area consists of an approximately 12 mi² (31.1 km²) exposure of the Baca Formation at the north end of the Gallinas Mountains about 20 mi (32 km) northwest of Magdalena, New Mexico (Fig. 1). The eastern two-thirds of the study area is located on the southern portion of the Alamo Band Navajo Reservation. Quality of exposure ranges from excellently exposed stream channel incisions to very poorly exposed badlands topography. The best exposures are in the eastern portion of the study area. Maximum relief in the area is about 400 ft (123 m), and the average elevation is approximately 6700 ft (2061 m). The area lies within a semiarid climatic zone and receives most of its annual precipitation during July and August.

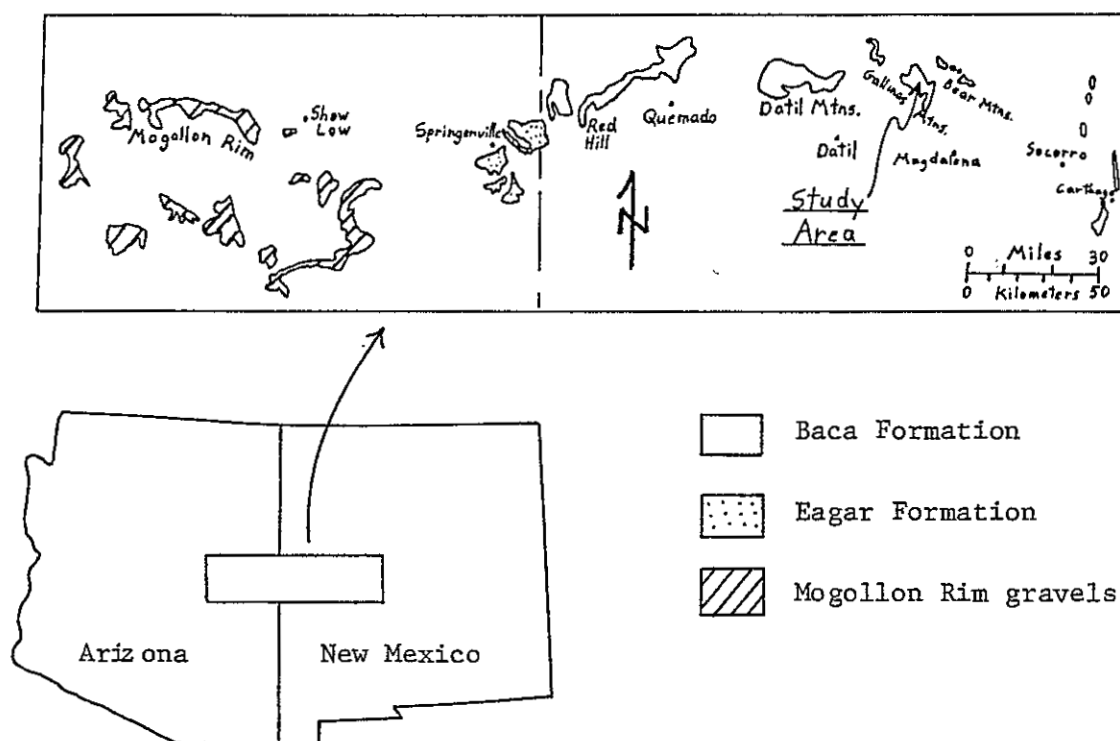


Figure 1. Location of study area and Baca, Eagar, and Mogollon Rim gravels.

Purpose and Methods of Study

The primary objectives of this study were: a) to describe the petrology and provenance of the Baca Formation in the study area; b) to determine the diagenetic history of the Baca sediments; c) to define the environments of deposition and dispersal patterns of the Baca sediments in the study area, and; d) to delineate and summarize the tectonic framework and paleoenvironments for the entire Baca-Eagar basin.

Pebble counts, petrographic examination of sandstones, and petrographic and x-ray mineralogic study of mudstones and claystones were utilized to describe the petrology and determine the provenance of the Baca sediments. Data for reconstruction of the diagenetic history of the sediments was provided by optical and scanning electron microscopy.

Detailed mapping at a scale of 1:24,000 (Plate 1), paleocurrent measurement, and the measurement of one complete and several partial stratigraphic sections provided the basis for reconstruction of paleoenvironments and sediment dispersal patterns. Depositional environments were interpreted using the following criteria: lithofacies geometry, lateral and vertical variation in grain size and sedimentary structures, nature of contacts between

lithofacies, petrographic data, and fossils.

Interpretation of the tectonic and paleo-environmental history of the Baca-Eagar basin was based both on my own data and that of other workers. I have examined on a reconnaissance level the majority of the exposures along the Baca-Eagar outcrop belt. I have relied heavily upon Johnson (1978) for his highly accurate facies analyses, especially in the western portion of the outcrop belt. Additional paleocurrent data was drawn from Snyder (1971), Pierce and others (1979), and Johnson (1978).

GENERAL STRATIGRAPHY

Upper Cretaceous through Quaternary strata are exposed along the northern flank of the Gallinas Mountains. The oldest rocks present are the sandstones and shales of the Late Cretaceous Crevasse Canyon Formation. These are overlain by the Eocene Baca Formation which, in the study area, consists of a redbed sequence of sandstones, mudstones, claystones, and minor conglomerates. The Baca is overlain by the volcaniclastic sedimentary rocks, ash-flow tuffs, and lavas of the Oligocene Spears Formation. Numerous north-trending mafic dikes were emplaced during Miocene time in the eastern portion of the study area. Extensive piedmont gravels of late Pliocene(?) to Holocene age represent coalesced alluvial-fan deposits resulting from the southward erosional retreat of the steep northern flank of the Gallinas Mountains. Quaternary sands and gravels are present in and along modern ephemeral stream channels and as valley fill. Only the Baca Formation was studied in detail.

Late Cretaceous

Crevasse Canyon Formation

The Crevasse Canyon Formation was named by Allen and Balk (1954) for exposures on the west side of the San Juan Basin. It is equivalent to the Dilco and Gibson Members of the Mesa Verde Formation and occupies the stratigraphic interval between the Gallup and Point Lookout Formations. Tonking (1957) was the first to use the term Crevasse Canyon in the Bear-Gallinas Mountains vicinity. Tonking measured a section 1,052 ft (324 m) thick in the Crevasse Canyon Formation directly north of the study area. Winchester (1920) collected floral remains from the Crevasse Canyon which were identified by Knowlton as being of Montanan age. Gardener (1910) tentatively dated the formation as either upper Coloradan or lower Montanan.

The Crevasse Canyon Formation consists of a sequence of yellowish-gray, fine- to medium-grained sandstones, medium-gray to black carbonaceous shales, and a few thin coal beds. The formation was deposited in littoral and paludal environments as the Late Cretaceous epicontinental sea withdrew northeastward from west-central New Mexico for the last time (Tonking, 1957).

Eocene

Baca Formation

In the study area, the Baca Formation overlies the Crevasse Canyon Formation and, in turn, is overlain by the volcanoclastic Spears Formation. The Baca records the first Tertiary sedimentation in the area.

Correlation and Previous Work

Winchester (1920) published one of the first geologic maps of west-central New Mexico. In this bulletin, he proposed the name "Datil Formation" for an approximately 2000-ft (615 m)-thick sequence of Tertiary volcanic and non-volcanic rocks exposed in western Socorro County. Wilpolt and others (1946) defined the Baca Formation as the basal non-volcanic portion of Winchester's Datil Formation. However, the Baca section which they measured and described was in the Joyita Hills, and not where they defined the type section. The Baca type section is 684 ft (210.5 m) thick and is located in the upper part of Baca Canyon on the eastern flank of the Bear Mountains in western Socorro County. Wilpolt and others (1946) also extended the term Baca to equivalent rocks exposed in the Joyita Hills

vicinity about 30 mi (48 km) east of the type locality. Wilpolt and Wanek (1951) further extended the Baca southeast of the type locality into the Carthage area.

Within New Mexico, the Baca Formation has been traced westward along a discontinuous outcrop belt by Tonking (1957), Givens (1957), Willard and Givens (1958), Willard and Weber (1958), Willard (1959), and Foster (1964).

Baca-equivalent rocks have also been described in east-central Arizona. The Mogollon Rim gravels were interpreted by Hunt (1956) to be Late Cretaceous to Eocene in age. Pierce and others (1979) state that these gravels were derived from Precambrian sources to the southwest during Eocene-Oligocene time. The Baca-equivalent sandstones and conglomerates of the Eagar Formation were named and described by Sirrine (1956).

In his regional Baca-Eagar study, Johnson (1978) was the first to correlate the Baca, Eagar, and Mogollon Rim gravels. Based on the continuity of gravel compositions, paleocurrent indicators, lateral facies variations, and the configuration of the early Tertiary tectonic framework in the southwestern United States, I strongly support this correlation.

Very few previous investigations within the study area have been carried out. Tonking (1957) studied the geology of the Puertecito quadrangle, an area which

encompasses the eastern two-thirds of the study area. Givens (1957) studied the western one-third of the study area in his work on the Dog Springs quadrangle. Both of these studies were reconnaissance in nature.

Recently, much detailed work has been performed in areas adjacent to the study area. Mayerson (1979) and Jackson (in progress) have studied and mapped in detail areas to the east and northeast of the study area, respectively. Laroche (in progress) has studied and mapped a portion of the volcanic rocks exposed in the Gallinas Mountains. Snyder (1971) studied the Baca exposed between the Rio Grande and the Arizona-New Mexico state line, including the Baca exposed north of the Gallinas Mountains. A summary of previous work is presented in Table 1.

Lower Tertiary Equivalents

Several lower Tertiary formations are present in New Mexico (Fig. 2). These include the Raton, San Jose, Nacimiento, Galisteo, Cub Mountain, McRae, and Love Ranch Formations. These units were deposited in isolated basins which were created by the Late Cretaceous to Eocene Laramide orogeny.

Table 1

Summary of Previous Studies

Location of Study	Workers
Carthage	Gardener (1910) Wilpolt and Wanek (1951)
Joyita Hills	Wilpolt and others (1946)
Bear Mountains	Winchester (1920) Wilpolt and others (1946) Tonking (1957) Potter (1970) Massingill (1979)
Gallinas Mountains	Tonking (1957) Givens (1957) Mayerson (1979)
Datil Mountains	Willard and Givens (1958) Schiebout, J.A. (ongoing research)
Quemado	Willard and Weber (1958) Schiebout, J.A. (ongoing research) Schrodt, K. (in progress)
Red Hill	O'Brien (1956)
Springerville	Sirrine (1956)
Mogollon Rim	Hunt (1956) Pierce and others (1979)
Regional Studies	Willard (1959) Snyder (1971) Johnson (1978)

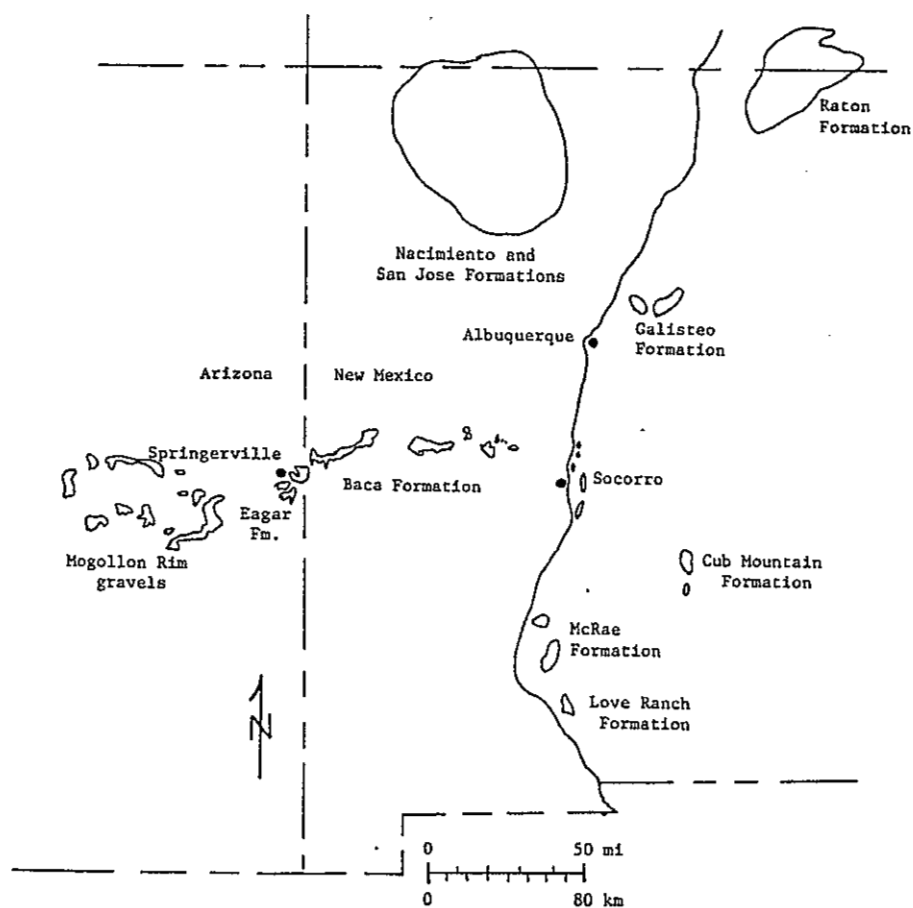


Figure 2. Map showing outcrop areas of lower Tertiary units in New Mexico and adjacent areas.

Age and Fossils

The Baca and Eagar Formations and the Mogollon Rim gravels have been assigned ages ranging from Late Cretaceous to early Oligocene. Most age determinations, however, give an Eocene age for these units. The Laramide orogeny occurred between about 80 and 40 m.y. ago (Coney, 1971). The sediments of the Baca and equivalent units apparently were derived from Laramide uplifts, thus lending support for a Late Cretaceous to Eocene age for these sediments. In the Joyita Hills, a 37.1 m.y. radiometric date has been obtained from a volcanic clast in the Spears Formation which overlies the Baca (Weber, 1971). Therefore, in that area, the Baca must be older than earliest Oligocene. Age determinations for the Baca and Eagar Formations and the Mogollon Rim gravels are summarized in Table 2.

No age determinations for the Baca have been made in the study area. The writer discovered several fossil cloven-hoof prints in the lower red member of the Baca at the NW 1/4, SE 1/4, SE 1/4, sec. 31, T.2N., R.6W. (Fig. 3). Photographs of these prints were shown to several vertebrate paleontologists, including Dr. Wann Langston of the University of Texas at Austin and Dr. Beryl E. Taylor of the American Museum of Natural History, New York. As yet, no one has been able to identify or date these trace

Table 2

Summary of Fossil Age Determinations

Author	Unit	Location	How Dated	Age
Pierce and others (1979)	Mogollon Rim gravels	Mogollon Rim	radiometric	Eocene-Oligocene
Sirrinc (1956)	Eagar	Springerville	pollen, spores	L. Cretaceous
Belcher, R. (pers. comm., Johnson, 1978)	Eagar	Springerville	rhinoceros tooth	Eocene
Gardener (1910)	Baca	Carthage	Palaeosyops, rhinoceros- like mammal	middle Eocene
Schiebout, J.A. (pers. comm.)	Baca	Quemado, Datil, Mountains	titanotheres, turtle, croc- odile, lizard	Eocene-early Oligocene
Snyder (1971)	Baca	Datil Mountains	<u>Protoreodon</u> <u>pumilus</u> , sheep- like mammal	late Eocene
Chaiffetz (1979)	Baca	Bear Mountains	pollen, spores	Eocene



Figure 3. Cloven hoof prints found in a Baca delta-plain sandstone. Lens cap is approximately seven cm in diameter.

fossils. Many ostracods were observed while examining thin sections from the study area (Fig. 4). As I will discuss later, these ostracods provide additional evidence of a largely lacustrine environment of deposition for the Baca, however, I have not been able to use them for dating the unit.

The only other fossil remains observed consist of carbonaceous and siliceous plant and wood fragments. The Galisteo Formation, which is exposed south of Santa Fe, has been dated as Paleocene or Eocene on the basis of fossil plant remains (Lee and Knowlton, 1917). Such dating has not yet been attempted in the Baca.

Contacts

The contact of the Baca with the subjacent Crevasse Canyon Formation is generally poorly exposed in the study area. Where visible, it is a low-relief erosional unconformity of little or no angularity. The lower contact of the Baca was mapped at the base of the first reddish sandstone or mudstone. Rare paleocaliche horizons were observed to be developed in the uppermost portion of the Crevasse Canyon directly below the contact with the Baca Formation. These paleocaliches were produced by soils formed in arid or semi-arid climatic conditions during the

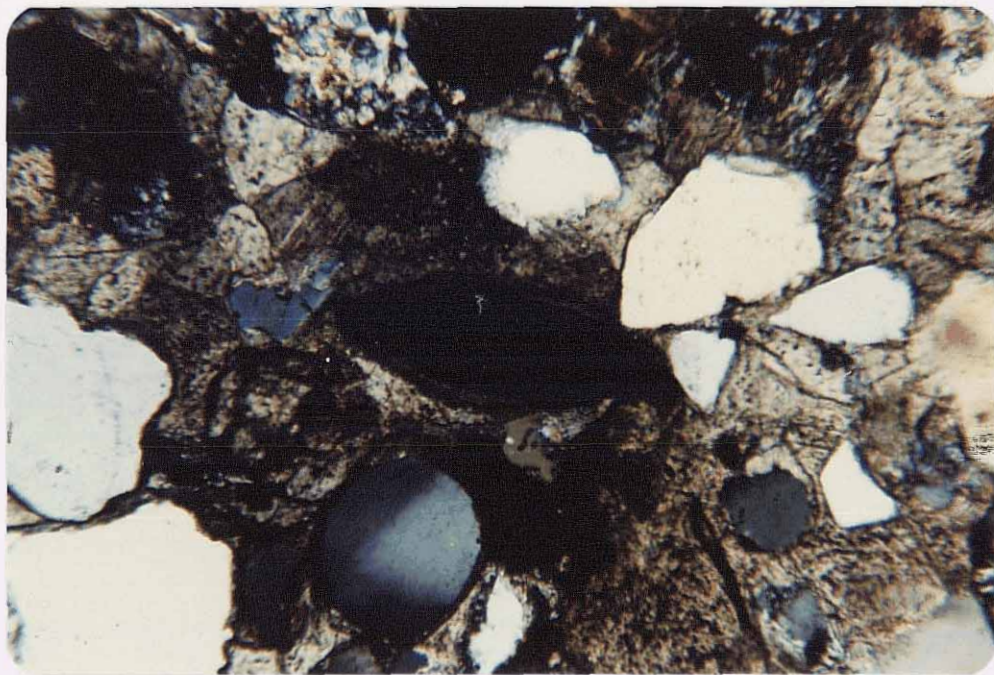


Figure 4. Hematitic mudstone-filled ostracod test in sample 49. Field width=0.8 mm, crossed nicols.

hiatus between final deposition of Crevasse Canyon sediments and the inception of Baca sedimentation. In some areas, a poorly exposed pebble lag appears to be present along the Baca-Crevasse Canyon contact, perhaps representing a paleo-deflation surface which developed on the unconsolidated Crevasse Canyon sediments prior to Baca deposition. In areas outside the study area, the lower contact is reported to be unconformable to apparently conformable (Willard, 1959; Tonking, 1957; Potter, 1970).

The upper contact of the Baca with the Spears Formation generally is gradational, the contact being defined at the first occurrence of megascopically visible volcanic material. The gradation between Baca- and Spears-type lithologies takes place within a few meters.

General Description and Informal Units

In the study area, the Baca Formation consists of a redbed sequence of sandstone, mudstone, claystone, and minor conglomerate. One complete stratigraphic section was measured in the eastern portion of the study area. It has a total thickness of 941.5 ft (289.7 m), and is presented in Appendix A.

In the Bear Mountains area, Potter (1970) divided the Baca into three informal members which he termed, in ascending order, the lower red unit, the middle sandstone unit, and the upper red unit. I found this terminology applicable in the study area, but I must emphasize that these informal units are genetically related to lake-level fluctuations in a large Eocene lacustrine system present in the Bear-Gallinas Mountains area and are not applicable to the predominantly fluvial Baca-Eagar rocks to the west or to the Baca exposed east of the Rio Grande. This subject will be discussed in detail in later sections. On the basis of thickness, stratigraphic position, and similarity of lithofacies, the units defined in the study area are probably directly correlative with the units of Potter (1970) in the Bear Mountains (Fig. 5), although the paleo-continuity of these units has yet to be demonstrated due to late Tertiary structural complications and cover.

In his work in the Bear Mountains area, Massingill (1979) recognized the same three informal units in the Baca as did Potter. However, Massingill chose to abandon Potter's terminology in favor of, in ascending order, the conglomeratic, the gray sandstone, and the red mudstone members. I favor retention of Potter's terminology on the basis of the following criteria: a) the lower red unit in the study area (equivalent to Massingill's conglomeratic

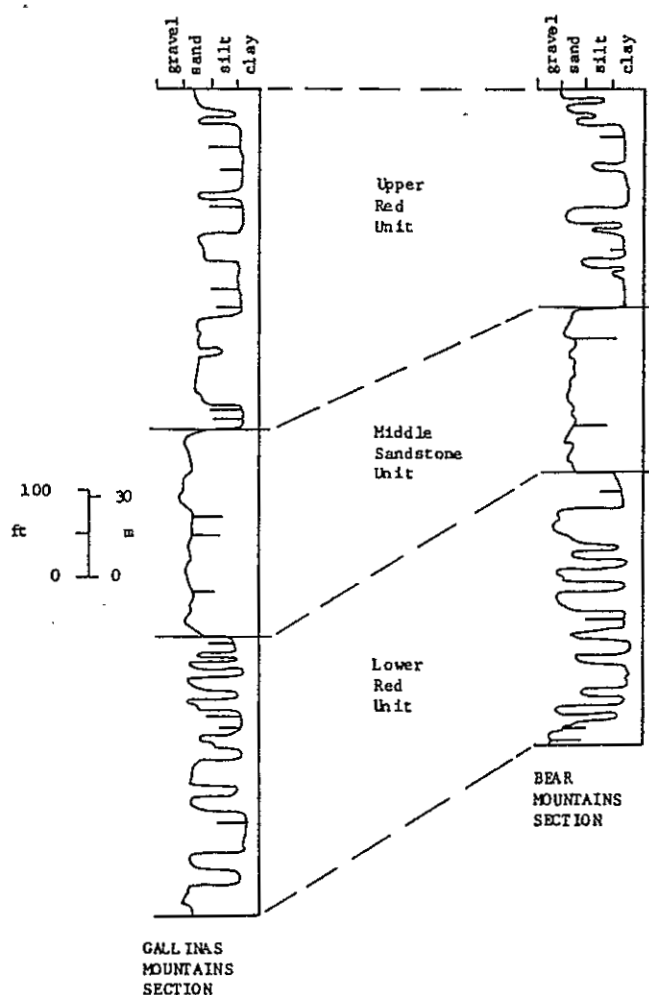


Figure 5. Comparison of generalized Baca stratigraphic sections measured in the Gallinas and Bear Mountains, showing similarity of lithofacies and probable correlation of informal units. Sections are separated by about 10 mi (16 km). Bear Mountains section modified from Massingill (1979).

member) contains very little conglomerate, as will be discussed in a later section. The conglomerates in the Bear Mountain area are present due to the relative proximity of the source area, thus the term lower red unit is more descriptively viable on a regional level; b) the coloration of Massingill's gray sandstone member reflects only the diagenetic history of the sediment. Indeed, the middle sandstone unit in the study area is often red.

The lower red, middle sandstone, and upper red unit terminology will be utilized only for ease of reference and to facilitate generalized lithologic descriptions, as below. For the more detailed descriptions and interpretations in later sections, the principles of genetic stratigraphy will be employed to subdivide the formation into component depositional systems as defined by Fisher and Brown (1972).

Lower Red Unit. The lower red unit is 323 ft (99.4 m) thick at the measured section and is composed of red, gray, and yellow sandstones intercalated with red mudstones and claystones. The ratio of sandstone to mudstone is about 1:1. Minor amounts of conglomerate are present as thin lenses within sandstone units. Sandstone beds in the lower red unit average about 18 ft (5.5 m) thick and range between a few inches to 25 ft (7.7 m) in thickness. Some of the thicker beds can be traced for as much as a mile (1.6 km)

along strike. Mudstone and claystone beds average about 10 ft (3.1 m) thick and range up to 50 ft (15.4 m) in thickness. Mudstone units are calcareous and effervesce in cold, dilute hydrochloric acid.

Middle Sandstone Unit. The middle sandstone unit is 246 ft (75.7 m) thick at the measured section and consists almost entirely of fine- to coarse-grained yellow, gray, or red sandstone. The sandstones are most often horizontally laminated, but frequently display well-developed, medium- to large-scale trough crossbedding and rare tabular crossbedding. Mudstones and claystones are very rare in the middle sandstone unit, occurring primarily as thin, discontinuous clay drapes within the sandstones.

Upper Red Unit. The upper red unit is very similar in appearance to the lower red unit. At the measured section, it consists of a 372.5 ft (114.6 m) sequence of red, yellow, and gray sandstones intercalated with red mudstones and claystones. Conglomerates are rare and occur as thin lenses within sandstone units. The upper red unit contains less conglomerate than the lower. This has also been noted in the Bear Mountains area (Potter, 1970; Johnson, 1978; Massingill, 1979). The sandstone to mudstone ratio is about 1:1. Mudstones are usually

calcareous. Both sandstone and mudstone beds tend to be thicker in the upper red unit than in the lower. Sandstones range in thickness to as much as about 100 ft (30.8 m); mudstones can be as thick as 80 ft (36.9 m).

Oligocene

Spears Formation

Tonking (1957) divided all but the basal Baca portion of Winchester's (1920) Datil Formation into three members. These members are, in ascending order, the Spears, Hells Mesa, and La Jara Peak. The Spears Member was upgraded to formational status by Chapin and others (1978). A section of Spears measured by Tonking (1957) in the Bear Mountains, about 12 mi (19.4 km) east of the study area, indicates a thickness of 1,340 ft (412.3 m). The Spears Formation has been dated radiometrically with dates ranging between 37 and 33 m.y.B.P. (Chapin and others, 1978).

The Spears is composed of a sequence of grayish-purple volcanoclastic sandstones, conglomerates, and mudflow deposits, with interbedded lavas and ash-flow tuffs in the upper part. The formation is latitic to andesitic in composition and represents the early intermediate-composition phase of the Datil-Mogollon volcanic field

(Chapin and Seager, 1975). The Spears contains more volcanic flows to the south, indicating eruptive centers in that direction. Trends of mudflow-filled paleovalleys in the basal Spears directly south of the study area indicate a generally northward transport direction.

Miocene

Dikes

Numerous north-trending dikes are exposed in the eastern portion of the study area. These dikes range in width up to about five feet (1.5 m), dip nearly vertically, and in some cases may be traced for as much as 1.5 mi (2.4 km). The dikes were emplaced along faults and fractures associated with the opening of the Rio Grande rift. Potassium/argon dating of two dikes in the Bear Mountains vicinity yielded dates of 24.3 ± 0.8 and 24.8 ± 0.6 m.y.B.P. (C. E. Chapin, unpublished dates).

Dike rocks are generally greenish-black and range texturally from aphanitic to very-fine-grained holocrystalline. In the Bear Mountains area, these dike rocks have been classified as basaltic andesites (Massingill, 1979). The dikes commonly exhibit fine-grained chilled margins. Baked zones are common in the country rock

adjacent to the dikes, but alteration is usually limited to a zone less than a foot (0.3 m) thick.

Pliocene (?) to Holocene

Piedmont Gravels

Extensive piedmont gravels are present throughout the central and western portions of the study area. Two units of differing ages were mapped. The older unit is topographically higher than the younger and forms isolated deposits capping the higher areas north of the Gallinas Mountains escarpment. The older piedmont gravel ranges up to about 200 ft (61.5 m) in thickness. The younger gravel occupies a large, continuous area in the central portion of the study area. The difference in elevation of the bases of the two units is as much as about 100 ft (30.7 m). However, this elevation difference appears to decrease westward. The thickness of the younger unit is less than that of the older, and ranges up to about 50 ft (15.4 m). Both units locally overlie the Baca with angular unconformity.

Grain size in both units ranges from coarse sand to cobbles. Clast composition of both units is identical, consisting predominantly of subequal proportions of Spears, Hells Mesa, and A-L Peak Tuff lithologies. Pebble

imbrication indicates flow was generally northward. These piedmont gravels represent coalesced alluvial-fan deposits related to the erosional retreat of the steep northern flank of the Gallinas Mountains. Similar piedmont gravels in western Socorro County range in age from late Pliocene(?) to Holocene (J. Hawley, 1979, oral commun.). The difference in elevation of the two gravel units indicates a period of erosion prior to deposition of the younger unit.

Quaternary

Alluvium

Locally derived sands and gravels are present in and near presently active ephemeral stream channels and as valley fill in the northern portions of the study area.

LARAMIDE TECTONICS

Styles of Deformation

The Baca-Eagar basin is one of a multitude of basins and uplifts which formed during the Late Cretaceous to late Eocene Laramide orogeny in western North America (Fig. 6). Three general structural provinces and associated styles of deformation can be delineated. These are the "thin-skinned", low-angle thrusts and folds of the Cordilleran foldbelt, the asymmetric basement-cored anticlinal uplifts of the classic Laramide Rocky Mountains, and the monoclinal flexures of the Colorado Plateau.

Cordilleran Foldbelt

The Cordilleran foldbelt of North America extends from Guatemala to Alaska (Drewes, 1978), and was active predominantly during Late Jurassic to late Eocene time. The dominant style of deformation is one of imbricate east-verging, low-angle thrusting with associated folding within allochthonous plates (Fig. 7). With the notable exception of those in southern Arizona and New Mexico, the thrust sheets generally did not involve Precambrian basement rocks. Amounts of supracrustal transport throughout the Cordilleran

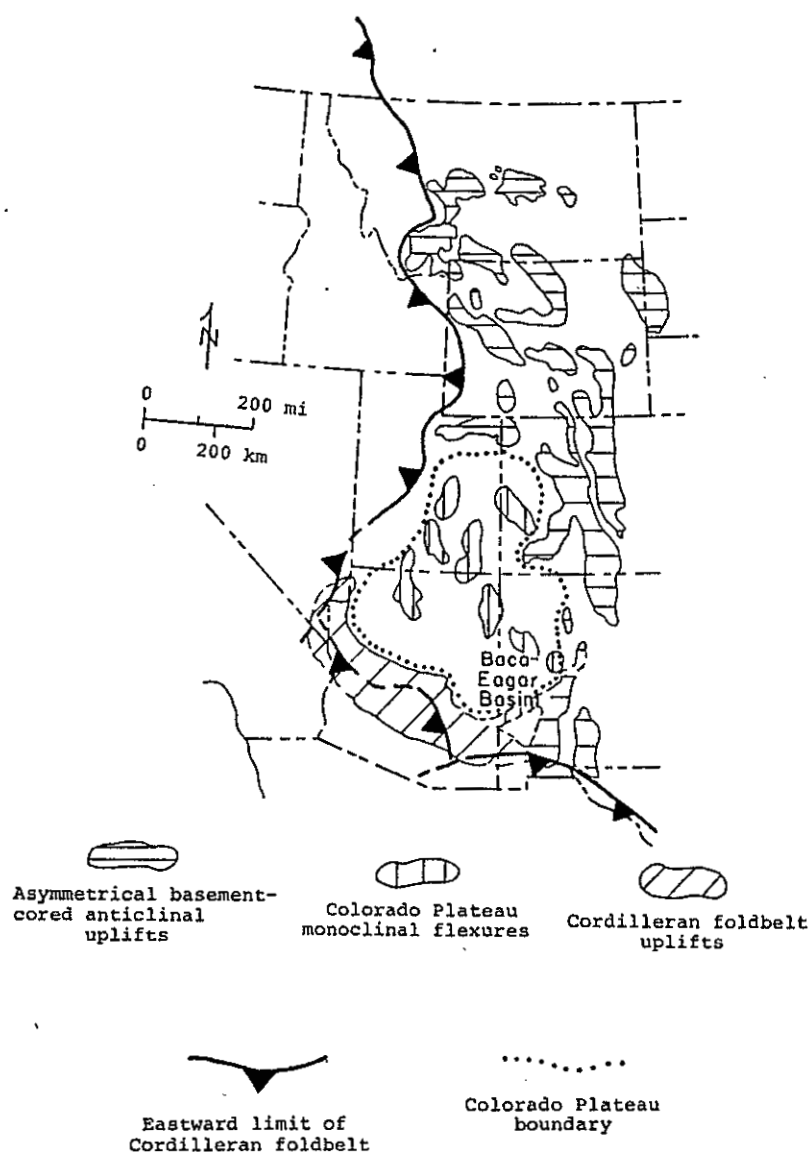


Figure 6. Map showing distribution and structural styles of Laramide uplifts in western North America, and the location of the Baca-Eagar basin. Modified from Eardley (1962) and Drewes (1978).

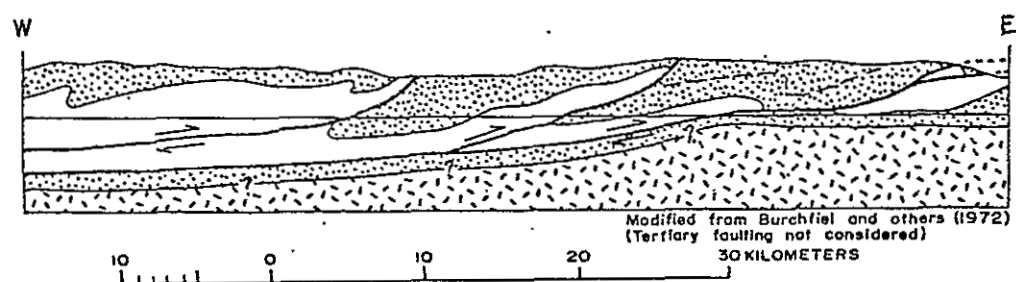


Figure 7. Section across Spring Mountains, southern Nevada, showing typical Cordilleran-foldbelt style of deformation. Note imbricate, east-verging thrust plates.

foldbelt probably averaged between 30 and 60 mi (50 to 100 km), and may be as much as 120 mi (200 km) in some regions (Drewes, 1978). Structures within the foldbelt are indicative of compressional deformation, although the mechanisms by which the stresses were transmitted and the dynamics of thrust plate movements are highly controversial. Thrusting in Nevada and Utah, west of the classic Laramide Rocky Mountains, ceased in Late Cretaceous time (Armstrong, 1968), but major thrust movements in the Cordillera of Mexico and Canada persisted until late Eocene time (Coney, 1976).

Basement Uplifts of the Laramide Rocky Mountains

The geographic distribution, as well as the style of deformation, of the classic Laramide basement uplifts is distinctly different from that of the Cordilleran foldbelt; the former was favored on the thin cratonic shelf while the latter was favored in the Paleozoic miogeosyncline (Coney, 1978). The asymmetrical basement-cored anticlinal uplifts of the Laramide Rocky Mountains form a belt which extends from southern Montana to southern New Mexico. In the northern portion of the belt, the uplifts trend generally northwestward, while in the central and southern portions they trend northward. The uplifts usually contain large

exposures of Precambrian basement and are often bounded on one or more sides by thrust faults. Structural relief between uplifts and adjacent basins may be as much as 49,000 ft (15,000 m) (Coney, 1976).

Theories concerning the origin of the basement uplifts can be broadly divided into two schools of thought: vertical and horizontal tectonism (Fig. 8a, b). Proponents of vertical tectonism suggest that the uplifts were produced by differential vertical movements of high-angle-fault-bounded basement blocks driven by phase changes or plastic flowage in the lower crust or upper mantle, with resultant drape folds and subsidiary thrusts in the overlying strata (Stearns, 1978; Palmquist, 1978; Woodward, 1976). Arguments in favor of vertical tectonism are largely based on evidence against the alternative horizontal-stress-generated basement-upthrust model, such as: (a) space problems resulting from relative thrust-block movement (Stearns, 1978; Palmquist, 1978); (b) necessary major wrench faults bounding lateral edges of thrust blocks have not been observed (Stearns, 1978); (c) non-uniform direction of thrust-block motions throughout the Laramide Rocky Mountains suggests that the uplifts were not formed by unidirectional horizontal compressive stresses (Stearns, 1978). Proponents of vertical tectonism believe the thrust faults in the Laramide Rocky Mountains steepen with depth.

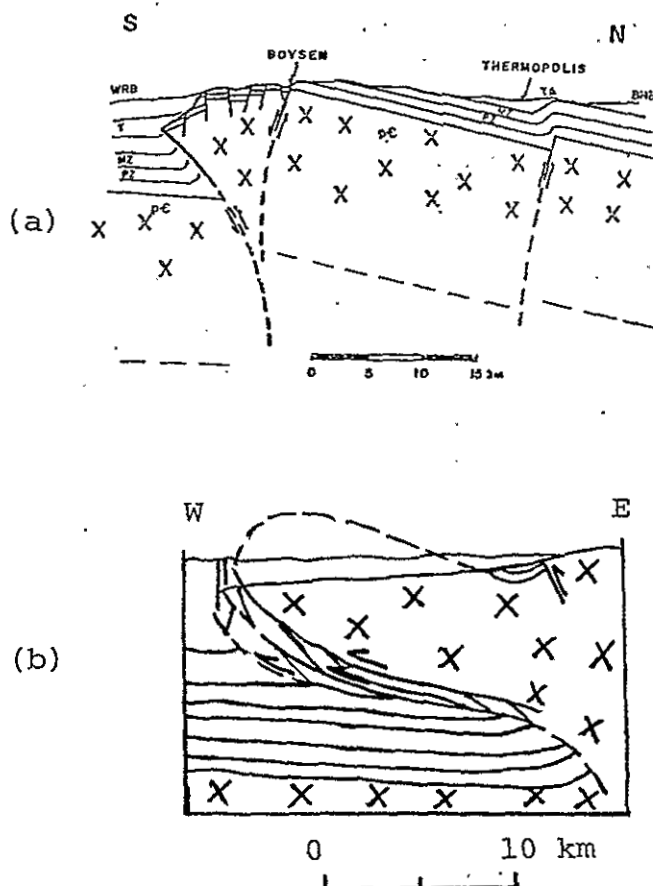


Figure 8. Two hypothetical styles of deformation in Laramide Rocky Mountain basement uplifts. (a) Uplift caused by vertical forces acting along range-bounding faults which steepen with depth. Section through Owl Creek uplift, Wyoming. From Couples and Stearns (1978). (b) Uplift created by horizontal stresses acting along thrust faults. Cross section through Wind River Mountains, Wyoming. Modified from Sales (1968).

The contrasting point of view is that the uplifts of the classic Laramide foreland were created by horizontal stresses, either horizontally directed compression (e.g. Coney, 1976; Thom, 1955) or a combination of horizontally directed compression and left-lateral shear (Sales, 1968). These horizontal stresses resulted in uplifted basement-cored blocks which were upthrust along moderate-angle thrust faults or were uplifted due to underthrusting by another thrust block. Evidence for creation of basement uplifts by horizontal stresses includes: (a) rapid oblique subduction of the Farallon plate under the North American plate resulted in strong southwest-northeast-directed compressive stresses throughout the foreland during Late Cretaceous to late Eocene time (Coney, 1976); (b) COCORP seismic profiling indicates that the southwestern boundary of the Wind River uplift, Wyoming, is a thrust fault which extends at about a 30 to 35 degree angle to a depth of at least 24 km, which suggests horizontal motions were more important than vertical in the development of the uplift (Smithson and others, 1978); (c) thrust faults are widespread throughout the Laramide Rocky Mountains structural province; (d) superincumbent folding commonly associated with basement uplifts is easily explained by large-scale horizontal movements of the basement.

Deformation in the Laramide Rocky Mountains foreland was initiated in Late Cretaceous time and ended by late Eocene time (Tweto, 1975), and may account for as much as 60 mi (100 km) of crustal shortening (Coney, 1976), but generally more modest amounts are visualized.

Colorado Plateau Monoclinial Flexures

The generally flat-lying strata of the Colorado Plateau are locally interrupted by large monoclinial flexures of Laramide age (Kelley, 1955) (Fig. 9). The monoclines are curvilinear, often branching in shape and may be hundreds of kilometers long. Trends are variable, but Davis (1978) recognizes two dominant trend directions of $N20^{\circ}W$ and $N55^{\circ}E$. Structural relief is generally less than that in the classic Laramide Rocky Mountains to the north and east. Precambrian basement is usually not exposed along the monoclines. Monoclines of the Colorado Plateau owe their origin to draping of strata over basement relief created by high-angle reverse faults formed in the northeast-southwest Laramide compressive stress field (Davis, 1978). Davis also states that these monoclines can be fit to a systematic, interdependent network of regional lineaments which are inferred to represent basement-fracture zones which were re-activated as reverse faults during Laramide time.

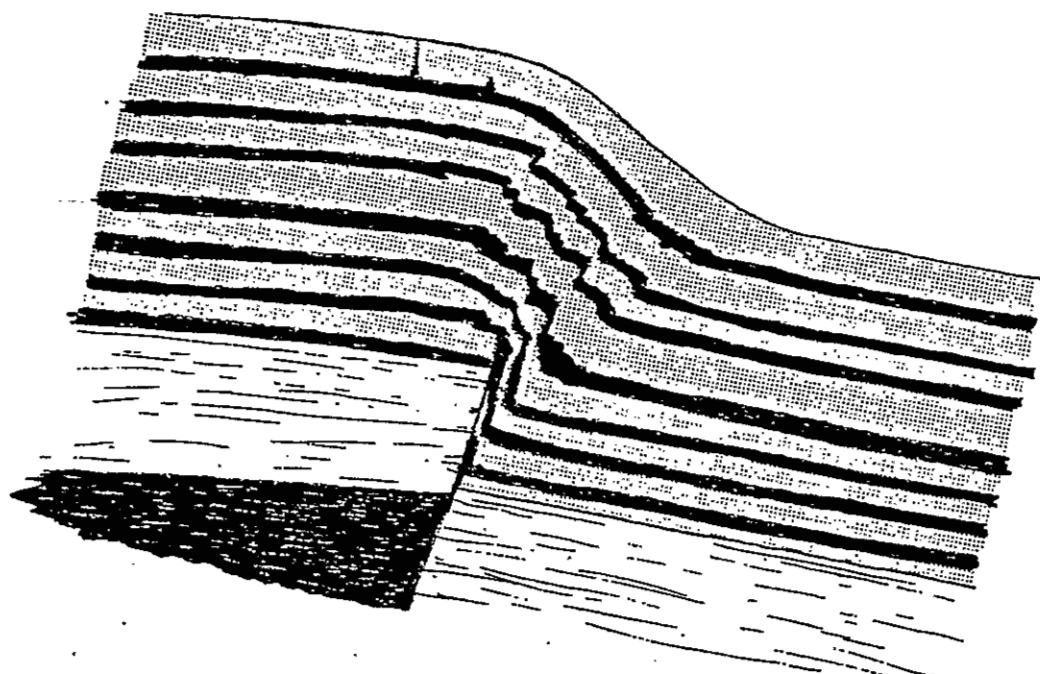


Figure 9. Experimental deformational model showing probable style of Colorado Plateau monoclinial flexures, using "strata" of kaolinite and modeling clay resting on rigid "basement" of pine board. Davis (1978).

The reasons for the differences in style and degree of deformation between the Colorado Plateau and the Laramide Rocky Mountains is not well understood. The greater degree of deformation in the Laramide Rocky Mountains may have occurred due to the presence of previously deformed basement produced during uplifting of the Late Paleozoic ancestral Rocky Mountains in that area (Coney, 1978). Basement uplifts may initially develop as monoclines which are later cut by faults as the uplift continues to rise (Woodward and others, 1972).

Baca-Eagar Basin Tectonic Framework

The Baca-Eagar basin was a west-trending structural depression which formed in the southwestern portion of the Colorado Plateau during Paleogene time. The sediments deposited in the Baca-Eagar basin were derived from surrounding Laramide uplifts (Fig. 10). Examples of all three styles of Laramide uplifts (Cordilleran foldbelt uplifts, asymmetrical basement-cored anticlinal uplifts, and Colorado Plateau monoclinial flexures) are present adjacent to the basin.

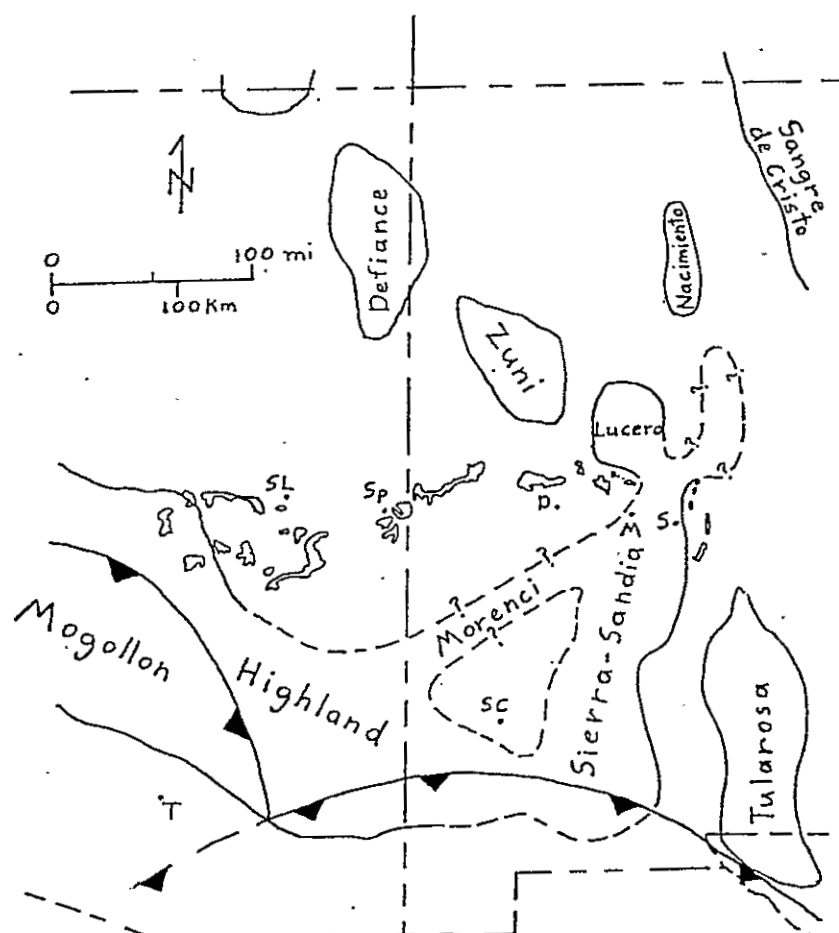


Figure 10. Laramide tectonic framework in eastern Arizona and western New Mexico. Heavy barbed line is northeastward limit of Cordilleran foldbelt (according to Drewes, 1978). Baca-Eagar-Mogollon Rim gravel outcrop areas are also shown. Reference points: S=Socorro, M=Magdalena, D=Datil, Sp=Springerville, SL=Show Low, SC=Silver City, T=Tucson. Modified from Eardley (1962).

Mogollon Highland

The Mogollon Highland of southern Arizona and southwestern New Mexico forms the southwestern boundary of the basin and was the dominant contributor of detritus to the basin. The highland coincides with the segment of the Cordilleran foldbelt present in southern Arizona and New Mexico (Drewes, 1978). Early Tertiary thrusting probably created the relief in the highlands during Baca time. In the Little Hatchet Mountains of southwestern New Mexico, Loring and Loring (in prep.) have shown that the thrusting in that portion of the Mogollon Highland is Paleocene in age. According to Drewes (1978), the dominant style of deformation in the highland was one of imbricate thin-skinned thrusting and folding similar to that in those portions of the Cordilleran foldbelt present in southwestern Canada, near Salt Lake City and Las Vegas in the United States, and northern Mexico. Davis (1979), however, states that the early Tertiary deformation in southeastern Arizona is related to the formation of large basement uplifts in that area, similar to those of the classic Laramide Rocky Mountains to the north. The Mogollon Highland was often a positive area during Mesozoic time. It was an important source terrane for both the Triassic Chinle and Upper Jurassic Morrison Formations (Cooley and Davidson, 1963;

Dodge, 1973). Lithologies present in the highland include Precambrian quartzites, granites, and schists, and Paleozoic quartzites, sandstones and carbonate rocks (Dodge, 1973; Silver, 1978; Hayes, 1978).

Lucero Uplift

The northern boundary of the Baca-Eagar basin is defined by the Lucero, Zuni, and Defiance uplifts which are Laramide monoclinal flexures typical of the Colorado Plateau (Kelly, 1955). The Lucero uplift lies on the eastern margin of the Colorado Plateau and consists of broadly arched, westward-dipping strata except along its eastern flank which is marked by a complexly faulted and folded section of steeply east-dipping strata (Callender and Zilinski, 1976). Sedimentary rocks ranging in age from Pennsylvanian to Triassic comprise the majority of the exposures on the uplift. The structurally low area between the Lucero and Zuni uplifts is termed the Acoma sag (Kelly, 1951).

Zuni Uplift

The Zuni uplift trends northwesterly and is markedly asymmetric; the northeastern flank dips gently into the San Juan basin, while the southwestern flank (the Nutria

monocline) dips steeply toward the Baca-Eagar basin. Precambrian gneisses and schists are exposed in the center of the uplift. The majority of the remainder of the exposures on the uplift consist of sedimentary rocks of Permian to Triassic age. The structurally low area between the Zuni and Defiance uplifts is termed the Gallup sag. More than 8,000 ft (2462 m) of structural relief exists between the highest part of the Zuni uplift and the Gallup sag. The structural relief between the uplift and the deepest part of the San Juan basin to the north is more than 13,000 ft (4,000 m) (Kelly, 1955).

Defiance Uplift

The north-trending Defiance uplift is asymmetrical with its steep eastern flank facing the Gallup sag and the San Juan basin. The steep eastern boundary of the uplift is defined by the sinuous Defiance monocline. Structural relief between the highest part of the uplift and the Gallup sag is at least 8,000 ft (2462 m) (Kelley and Clinton, 1960). With the exception of a few small exposures of Precambrian quartzite, the majority of the rocks which crop out in the Defiance uplift are Permian to Triassic sedimentary rocks.

Sierra-Sandia Uplift

Eardley (1962) proposed the existence of two Laramide uplifts adjacent to the eastern boundary of the Colorado Plateau in New Mexico and termed them the Sandia and Sierra uplifts. The term Sierra-Sandia uplift will herein be used to denote both the Sierra and Sandia uplifts of Eardley (1962) and the intervening area between them. Data from Johnson (1978), Snyder (1971), and this study suggest that the area between the Sierra and Sandia uplifts in the Socorro vicinity was a Laramide positive area, as will be discussed in later sections in more detail. Evidence for this conclusion includes: (a) paleocurrent and paleoenvironmental data from the Baca outcrops east of the Rio Grande (between the Joyita Hills and Carthage) indicate the presence of southeastward to northward flow in an alluvial-fan environment (Johnson, 1978), thus suggesting a source area nearby to the west; (b) paleocurrents are generally southwest-directed in the Baca exposed in the Bear Mountains vicinity (Johnson, 1978; Snyder, 1971) and presumably represent flow off the western flank of the uplift; (c) the presence of a large, persistent, closed lacustrine system in the Bear-Gallinas Mountains area indicates the presence of a damming element to the east.

The generally west-dipping Paleozoic strata exposed in the Ladron, Lemitar, and Magdalena Mountains and Socorro Peak probably represent the western flank of the Sierra-Sandia uplift, although an appreciable component of this dip is surely related to rotation of fault blocks during rifting. The geometry of the northern portion of the uplift is problematical. Eardley (1962) depicts the Sandia uplift as encompassing both the Nacimiento uplift and the present-day Sandia uplift. Paleocurrent analysis of the Galisteo Formation, however, indicates that the vicinity of the present-day Sandia uplift may not have been a Laramide positive area (Gorham and Ingersoll, 1979). Drill-hole data in the western portion of the Albuquerque-Belen basin shows the presence of early Tertiary sediments (Foster, 1978), thus requiring the western boundary of the Sierra-Sandia uplift to lie to the east of that area. In this study, I will not attempt to resolve the controversy concerning the geometry of the Laramide uplifts in northern New Mexico. The uplift configurations depicted in Figure 10 in that area should be regarded as highly tentative.

Baca sediments derived from the Sierra-Sandia uplift are arkosic and contain abundant Precambrian granite and schist clasts. Only a few isolated exposures of Precambrian rocks are present along the Rio Grande rift near Socorro. Thus, the Precambrian detritus in the Baca was probably

largely derived from source terranes which have been subsequently downfaulted in the Rio Grande rift. This is analogous to the Laramide Tularosa uplift in southern New Mexico (Eardley, 1962; Kottlowski, 1967), in which the central portion of the uplift has collapsed to form a graben during late Tertiary regional extension.

The Sierra-Sandia uplift implies a Laramide compressional phase prior to late Tertiary extension along the Rio Grande rift. This early stage of compressive tectonism has been noted by Kelly and Clinton (1960, p. 55). They state:

...there is much evidence along the Rio Grande trough of an early tectonic compressional history. The structures of the Caballos Mountains (Kelly and Silver, 1952, p. 136-146) are clearly early Tertiary and compressional. Low-angle (15°) faults in which gneiss rests on Cambrian limestone are clearly displayed within a few hundred yards of the Rio Grande trough in the Fra Cristobal Range of Sierra County, New Mexico (Jacobs, 1957, p. 257). Thrusts and overturns have been mapped in many places in the Sandia and Manzano uplifts...

Thrusts of Laramide age have also been reported along the eastern margin of the rift in the vicinity of Socorro (Wilpolt and Wanek, 1951).

On the basis of trend, geographic location, the presence of thrust faults along its east flank, and evidence for large exposures of Precambrian rocks along its crest,

the Sierra-Sandia uplift probably represents a basement-cored anticlinal uplift similar in structural style to the classic Laramide Front Range uplifts of Colorado and Wyoming.

Morenci Uplift

The probable existence of a Laramide drainage divide along the southeastern margin of the Baca-Eagar basin which was subsequently obscured by thick accumulations of mid-Tertiary Datil-Mogollon volcanic rocks was pointed out to the writer by C. E. Chapin (1980, oral commun.). The presence of large amounts of Laramide volcanic and plutonic rocks in southwestern New Mexico and adjacent Arizona (Fig. 11) and the nearly complete lack of volcanic-derived detritus in the eastern portion of the Baca outcrop belt (see volcanic rock fragment section) implies the presence of an intervening uplift which prohibited the input of volcanic materials into the eastern part of the Baca-Eagar basin. The Morenci lineament (Chapin and others, 1978) provides a likely site along which a drainage divide may have developed.

Monoclinial flexures represent the dominant style of deformation on the Colorado Plateau during the Laramide, and Davis (1978) states that these monoclines were produced by

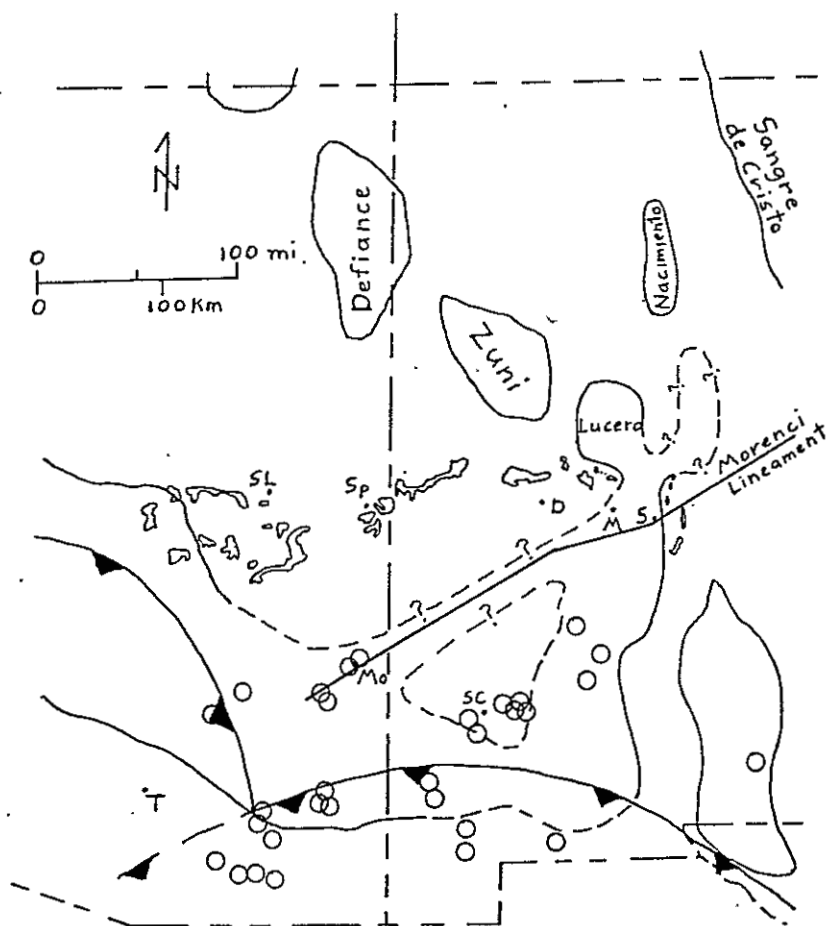


Figure 11. Location of Morenci lineament and distribution of Laramide plutons adjacent to the Baca-Eagar basin. Presumably the majority of these plutons (circles) were associated with coeval volcanic centers. Reference points same as Figure 10, except Mo=Morenci. Lineament and pluton data from Chapin and others (1978).

reactivation along basement fracture zones (lineaments) during early Tertiary compression. Thus, if a drainage divide was present in the vicinity of the Morenci lineament during Baca time, this so-called "Morenci uplift" was possibly monoclinical in nature. Davis (1978) recognized two sets of dominant trend directions ($N 20^{\circ} W$ and $N 55^{\circ} E$) of lineaments which controlled the development of Colorado-Plateau monoclinical flexures (Fig. 12). The orientation of the Morenci lineament is closely parallel to that of the northeast-trending set. Coalescing series of northeast-trending monoclines (e.g. Cow Springs, Organ Rock, and Comb Ridge monoclines) may be as much as about 175 km in length, which is approximately the length inferred for the Morenci uplift. The existence of a Morenci uplift would also explain the increased abundance of volcanic clasts in the Baca-Eagar gravels in the western portion of the outcrop belt (Johnson, 1978, p. 87-88); the Laramide volcanics in the vicinity of Morenci, Arizona, would not have been isolated by the drainage divide and could have easily supplied volcanic detritus to the western portion of the Baca-Eagar basin.

On the other hand, additional data indicating the existence of an uplift in the vicinity of the Morenci lineament is lacking. Residual Bouguer gravity maps of the Datil-Mogollon volcanic province do not suggest the presence

of a Laramide uplift in the area, but the gravimetric manifestation of such an uplift could easily have been masked by subsequent mid-Tertiary volcanism and plutonism. Colorado Plateau monoclinial flexures generally do not contain large exposures of Precambrian rocks. However, the occurrence of large amounts of metamorphic detritus in the study area (see provenance section) and elsewhere throughout the Baca-Eagar outcrop belt indicates that the Morenci uplift must have contained significant exposures of Precambrian terranes.

Plate Tectonics and the Development of the Laramide Foreland

Numerous theories concerning the origin and mechanics of Laramide foreland deformation have been proposed. In order to understand the relationship of the Baca-Eagar basin and associated uplifts to the overall Early Tertiary tectonic framework in western North America, I will attempt to, briefly describe the evolution of the Laramide foreland.

In Late Jurassic to Late Cretaceous time, prior to the inception of the Laramide orogeny, the locus of deformation in the foreland was along the Cordilleran foldbelt which extended without major interruption from

Alaska to Guatemala (Drewes, 1978) (Fig. 13). During this time, motion of the Farallon plate relative to the North American plate was east-northeastward at about 8 cm/yr (Coney, 1978). Deformation along the Cordilleran foldbelt continued throughout Laramide time in Mexico and Canada (Coney, 1976), but ceased in Late Cretaceous time in Nevada and Utah (Armstrong, 1968).

About 80 m.y. ago the relative plate motion between the North American and Farallon plates changed, resulting in northeastward motion of the Farallon plate with respect to the North American plate. The magnitude of relative plate convergence rates also changed, increasing to about 14 cm/yr (Coney, 1978) (Fig. 14). These changes created a strong northeast-southwest-directed compressive stress field in western North America and marked the beginning of the Laramide orogeny (Coney, 1976; 1978). Dickenson and Snyder (1978) suggest that the uplifts of the Laramide foreland formed in response to compression generated by a very shallowly dipping to subhorizontal subducted plate scraping along the bottom of the continental lithosphere in the western United States. This model seems to explain both how Laramide deformation took place so far inboard of the subduction zone and the largely amagmatic nature of the Laramide orogen. In Late Cretaceous to Paleocene time, the asymmetric basement-cored anticlinal uplifts of Colorado-

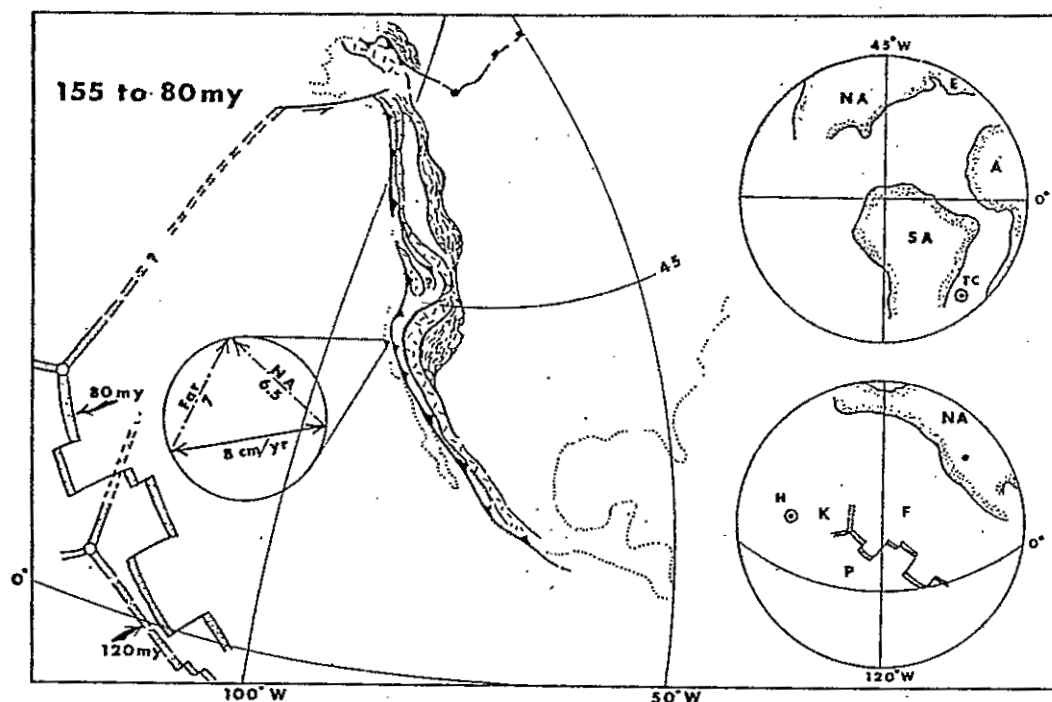


Figure 13. Map showing plate positions and relative motion vectors prior to Laramide orogeny. F=Farallon plate, K=Kula plate, P=Pacific plate, NA=North American plate. Vectors show motion of Farallon (Far) and North American (NA) plates relative to hot-spot frame of reference. Resultant shows direction and magnitude of plate convergence. Spreading centers shown by stippled areas between parallel lines, subduction zones by heavy barbed lines, thrust belts by light barbed lines, metamorphic core complexes by fine wavy lines, and arc terranes by short, dashed lines. Modified from Coney (1978).

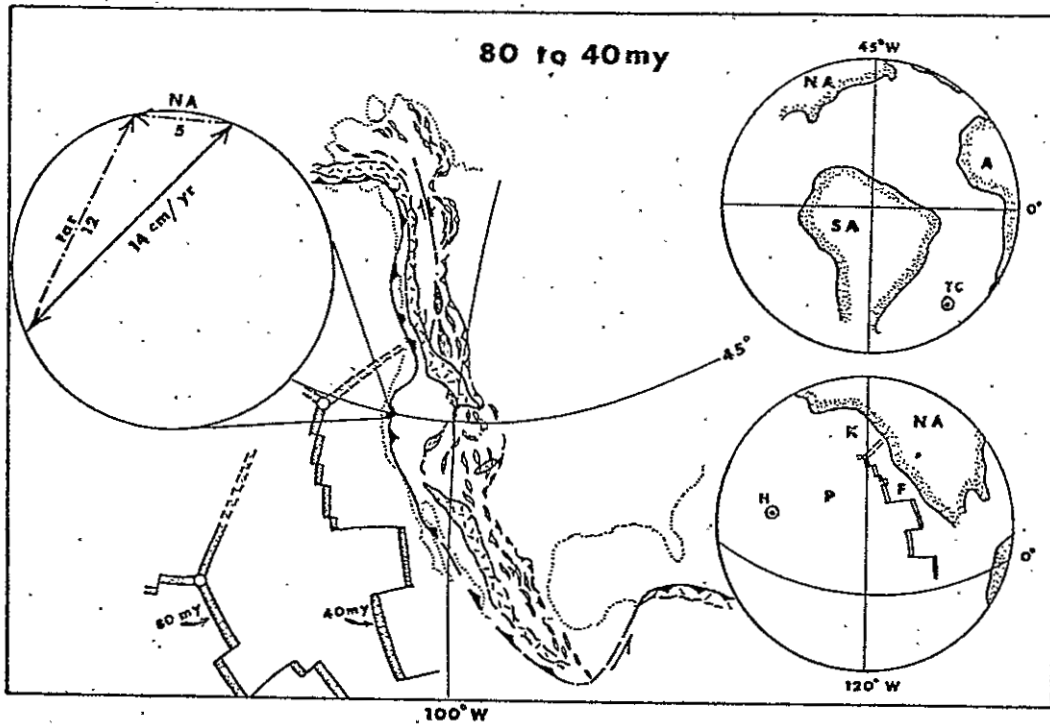


Figure 14. Map showing plate positions and relative motion vectors during Laramide orogeny. Uplifts shown by small, elongate, closed areas. Other symbols same as Figure 13. Modified from Coney (1978).

Wyoming and the monoclinial flexures of the Colorado Plateau began to form, creating large, often closed, intermontane basins between them. The Baca-Eagar basin probably also began to form during this period, but differed from the deeper, better-known Laramide basins to the north in that its southwestern boundary and dominant source of detritus was comprised by a segment of the Cordilleran foldbelt, the Mogollon Highland.

About 40 m.y. ago tectonic activity nearly synchronously ceased along the entire Cordillera, including the deformation in the Laramide Rocky Mountains and Colorado Plateau structural provinces (Fig. 15). This cessation of deformation coincides chronologically with a decrease in relative plate convergence rates along the west coast of North America (Coney, 1976). The tectonically quiescent period following the end of the Laramide orogeny resulted in the development of a widespread, late Eocene erosional surface of low relief in some areas of the Rocky Mountain foreland (Epis and Chapin, 1975). The next phase of the Cenozoic tectonic history of the western United States is represented by the widespread Oligocene calc-alkaline ignimbrite flare-up.

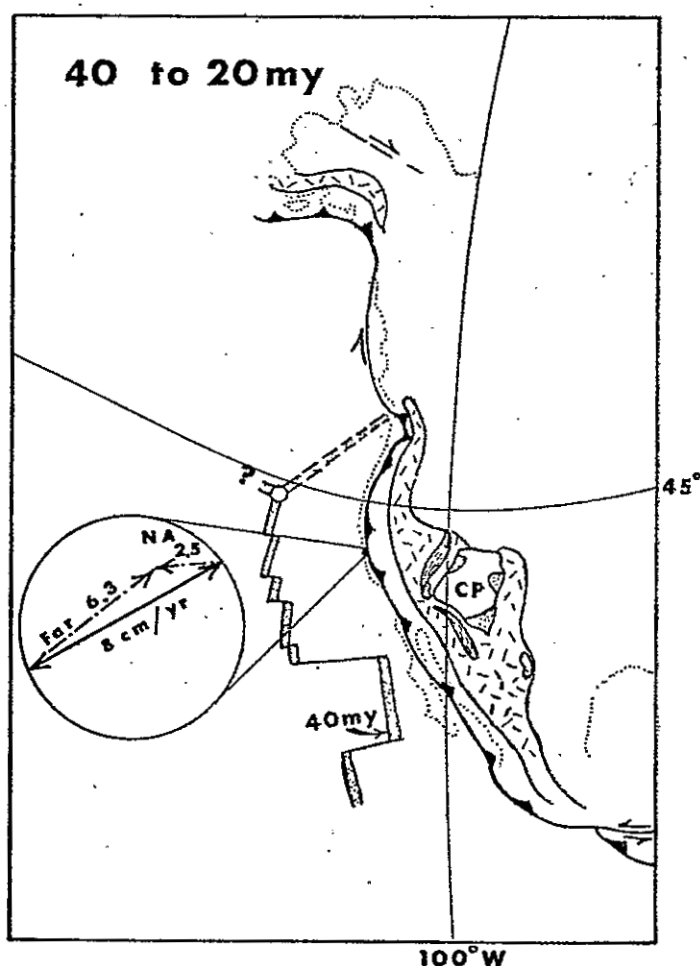


Figure 15. Map showing plate positions and relative motion vectors during post-Laramide, middle-Tertiary ignimbrite flare-up. CP= Colorado Plateau. Dotted areas are large caldera complexes. Other symbols same as Figure 11. From Coney (1978).

STRUCTURAL GEOLOGY

The study area is located in the transition zone between the Colorado Plateau to the north and the Rio Grande rift system to the southeast. Three episodes of structural development have modified the study area. A poorly defined monoclinial flexure of probable Laramide age is present in the southeastern portion of the area. North-trending normal faults and associated drag folds and mafic dikes are common in the eastern part of the area and were produced by Neogene extension. Epeirogenic uplift of the Colorado Plateau during Neogene time resulted in the southward tilting of strata in the region.

Laramide Folding

Monoclinial flexures typify the Laramide style of deformation of the Colorado Plateau. The presence of a poorly defined southeast-facing monocline in the southeastern part of the study area is indicated by a zone of steepened bedding and the abrupt termination of a plunging anticline (Fig. 16). Maximum structural relief along the monocline is about 250 ft (77 m). C. E. Chapin (oral commun., 1978) suggests that the structure may have resulted from draping of sedimentary strata over a vertical

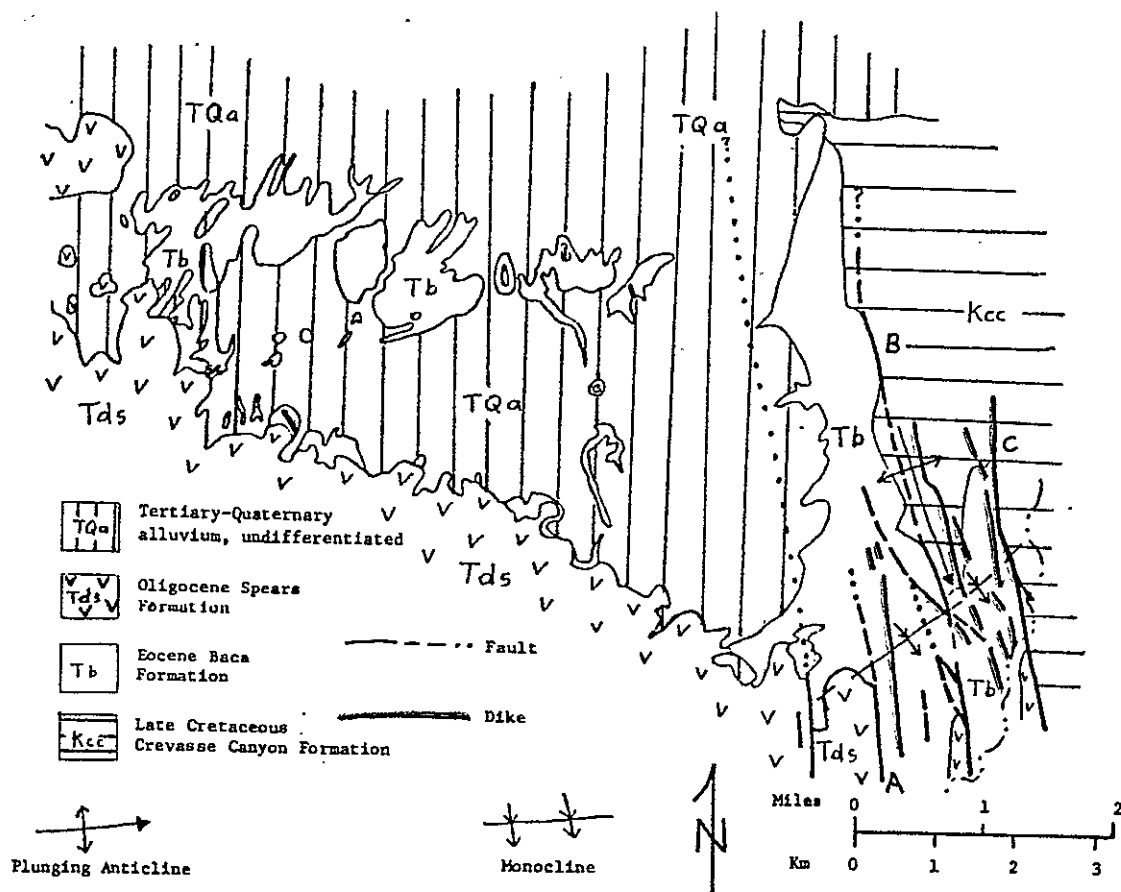


Figure 16. Structure index map of study area.

displacement in the crystalline basement along a northeast-trending lineament. A similar origin for monoclines on the Colorado Plateau has been proposed by Davis (1978). Paleocurrent data suggest that the monocline may have been active during Baca deposition, as will be discussed in a later section.

The monocline lies approximately on trend with the Tijeras lineament, which is well exposed in Tijeras Canyon near Albuquerque, New Mexico. Chapin and others (1979) describe several Tertiary features west of the Rio Grande which may be related to reactivation along the Tijeras lineament.

Early Rift Faults, Drag Folds, and Dikes

The Rio Grande rift consists of a series of essentially parallel, north-trending horsts and grabens formed by Neogene regional extension and extends about 600 mi (966 km) from near El Paso, Texas, to Leadville, Colorado.

Numerous north-trending normal faults are exposed in the eastern part of the study area (Fig. 15). In the Magdalena Mountains, similar faults may be as old as 32 m.y. (C. E. Chapin, 1979, oral commun.). Mafic dikes dated at

24-25 m.y. (C. E. Chapin, unpubl. dates) have been intruded along many of these faults.

Most of the faults dip steeply westward and are downthrown to the west. Fault-plane dip angles average about 75 degrees, and range from vertical to about 55 degrees. Rare slickensides indicate slip was generally vertical with little or no horizontal component. Vertical separation along the faults is generally less than a few tens of feet. Faults A, B, and C (Fig. 14), however, exhibit large displacements of as much as 750 ft (231 m), 350 ft (108 m), and 830 ft (255 m), respectively. All of the large-displacement faults dip steeply westward and exhibit down-to-the-west movement.

A large south-plunging asymmetrical anticline is present in the eastern part of the area. The steep limb faces eastward and the fold axis plunges southward at about five degrees, terminating abruptly against the southeast-facing monocline described previously. The configuration of the anticline corresponds to that of a fold produced by drag due to down-to-the-west movement along fault B. Local small-scale drag folds associated with normal faults are common throughout the study area.

Colorado Plateau Uplift

The Colorado Plateau is a broad, stable, relatively undeformed segment of the crust comprising about 150,000 mi² (388,500 km²) of northwestern New Mexico, northeastern Arizona, southeastern Utah, and southwestern Colorado. Locally, the generally flat-lying strata of the plateau are interrupted by large monoclinal flexures of Laramide age (Kelly, 1955; Davis, 1978).

The study area is located in a west-trending belt of gently south-dipping sedimentary rocks along the southern margin of the Colorado Plateau; this belt has been termed the Mogollon slope (Fitzsimmons, 1959). Except where modified by normal faulting and drag folding, strata within the study area dip from three to six degrees southward. Southward tilting resulted from the epeirogenic uplift of the Colorado Plateau which began in early Miocene time (Chapin and Seager, 1975). This tilting probably also produced the southward plunge of the anticline described previously. Similar southward tilting of pre-Miocene strata in the Bear Mountains vicinity was reported by Massingill (1979).

DEPOSITIONAL SYSTEMS

A depositional system is a genetically defined, three-dimensional, physical stratigraphic unit composed of a contiguous set of process-related sedimentary facies (Galloway, 1977). Depositional systems are the stratigraphic manifestation of major ancient geomorphic features, such as barrier islands, lakes, eolian dune fields, etc. Criteria utilized in discrimination of paleoenvironments include lithofacies geometry, lateral and vertical variation in grain size and sedimentary structures, nature of contacts between lithofacies, petrographic data, and fossils.

Two ancient depositional systems are present in the Baca Formation in the Gallinas Mountains vicinity. These are the lacustrine and braided alluvial-plain systems.

Braided Alluvial-Plain System

The importance of braided-stream-dominated depositional systems within the Baca-Eagar basin has been demonstrated by Johnson (1978), who described the depositional framework of the entire basin. In this study I will use the term "braided alluvial plain" instead of Johnson's "humid alluvial fan", although the sediments and depositional processes represented by both systems are

identical. I chose to abandon Johnson's terminology for the following reasons: (a) the adjective "humid", although intended to distinguish this system from its arid alluvial fan counterpart, connotes climatic conditions that were not present during Baca time in west-central New Mexico; (b) there is no evidence for a fan-shaped geometry for the braided-stream-dominated Baca-Eagar system. In contrast, this system probably consisted of a series of highly coalesced fans forming an extensive, low-gradient, piedmont slope or braided alluvial plain.

Johnson (1978) recognized proximal-, mid-, and distal-fan facies within the Baca-Eagar outcrop belt. Only the distal facies is present in the study area.

Distal Braided Alluvial-Plain Facies

Facies Characteristics. The distal braided alluvial plain facies comprises the entire middle sandstone unit and the basal 40 ft (13 m) of the lower red unit. Facies characteristics are summarized in Table 3. A typical vertical section (Fig. 17) shows a dominance of horizontally laminated, fine to coarse sandstone with minor lenses of conglomerate. Mudstones and claystones are rare, occurring primarily as thin, discontinuous layers within sandstones. Large-scale vertical textural trends are

Table 3

Distal Braided Alluvial-Plain Facies Characteristics

Lithology	Sedimentary Structures
<p>Moderate- to well-sorted, very coarse- to fine-grained sandstone with minor conglomerates and mudstones. Conglomerates occur as thin, discontinuous lenses within sandstones. Mudstones occur as isolated, thin layers within sand units. Sandstone/mudstone ratios are very high.</p>	<p>Dominantly horizontal laminations with subordinate trough crossbedding and minor tabular crossbedding. Vertical textural trends are generally lacking, but upward-fining sequences are sometimes observed. Channels are poorly developed and exhibit high width-to-depth ratios. Root mottling is locally abundant.</p>

generally lacking; however, upward-fining sequences as much as 6 ft (2 m) thick were occasionally observed. Channels are poorly defined and range in width up to 150 ft (46 m). Channel deposits exhibit high width/depth ratios (ranging between about 50:1 to 100:1) and abundant medium- to large-scale trough crossbeds as much as one meter thick. Foreset crossbedding is medium scale and occurs rarely. Root mottling and plant fragments are common. Contorted bedding and dewatering structures are sporadically abundant. Coloration of sandstones ranges from red to yellowish gray and is controlled by diagenesis, as will be discussed in a later section.

Depositional Processes. The prevalent horizontal laminations within distal braided alluvial-plain sandstones represent plane-bed transport and aggradation predominantly occurring during overbank flow in broad, flat interchannel areas during flood events. Similar horizontal laminations have been reported by McKee and others (1967) in the recent overbank flood deposits of ephemeral Bijou Creek, Colorado. Large-scale, upward-fining sequences were deposited predominantly in overbank areas in a regime of decreasing flow velocity during waning flood stages (McKee and others, 1967).

Channel deposits are characterized by an abundance of trough crossbeds, minor tabular crossbeds, and often contain thin conglomeratic lenses. Horizontal laminations, similar to those described above, are common. The trough crossbedding is the result of deposition by subaqueous sinuous-crested dunes which migrated down the channel during high-discharge periods. Similar intrachannel trough crossbedding has been described in the recent flood deposits of Bijou Creek, Colorado (McKee and others, 1967). Dunes were the dominant bedform within channels in recent flooding of sandy ephemeral streams in central Australia (Williams, 1971). Rare tabular crossbeds were produced by lateral accretion on foreset surfaces of transverse or linguoid bars during waning and low-flow stages. Such bars are common in channel areas of braided streams during low-flow stages (Williams and Rust, 1969; Harms and Fahnestock, 1965; Williams, 1971). Thin, discontinuous conglomerate lenses are sometimes present in the basal portions of trough cross-sets. These conglomerates represent channel-lag gravels which were deposited in scours on the lee side of migrating dunes. Similar recent pebble-floored hollows preceeding dune lobes have been described by Williams (1971).

Mudstones are rare within the distal braided alluvial-plain facies. Occurrences are limited to thin (generally less than a few centimeters thick), discontinuous layers within sandstone units. These layers were formed by settling of silt and clay within ponds in both channel and floodplain areas following flood events. These clay drapes were rarely preserved; they were usually reworked by subsequent high-discharge events and occur as claystone-clast lag gravels in superjacent sediments. Thin clay deposits formed in post-flood pools and cut-off channels have been described in central Australian braided streams by Williams (1971).

Braided streams of the distal braided alluvial-plain facies exhibited flashy discharge characteristics and may have been ephemeral. The abundance of overbank flood deposits and the scarcity of tabular crossbedding in this facies differs from perennial braided stream models (Smith, 1970; Kessler, 1971; Rust, 1972a; Cant and Walker, 1976; Costello and Walker, 1972). The ephemeral braided streams of central Australia (Williams, 1971) and Bijou Creek, Colorado (McKee and others, 1967) provide useful models for the braided streams of the distal braided alluvial-plain facies. Miall (1977) summarizes braided stream characteristics. Lack of eolian features and presence of common plant debris and root mottling may indicate vegetative

stabilization of sediments, although the nature of the vegetation is not known.

Braided Alluvial Plain Model. Johnson (1978) described an extensive braided-stream-dominated humid alluvial-fan system (renamed braided alluvial-plain system in this study) in the western portion of the Baca-Eagar basin, of which only the distal facies is present in the study area. The following discussion of the braided alluvial-plain system is drawn largely from Johnson (1978).

Two alluvial-plain models are commonly cited in the literature. The first is the familiar arid alluvial fan (Bull, 1972; Hooke, 1967), which is characterized by relatively small size, steep gradients, lack of systematic downstream decrease in grain size, and the presence of braided-stream, mudflow, sieve, and eolian deposits. The recent fans of the arid and semiarid southwestern United States are stereotypical arid alluvial fans.

In contrast, humid or tropical alluvial fans exhibit gentle, smooth gradients, large areal extents, systematic decreases in grain size downstream, and the dominance of braided-stream processes to the virtual exclusion of all others. The most commonly cited recent examples of these fans are the Scott proglacial braided outwash fan (humid alluvial fan) in Alaska (Boothroyd and Ashley, 1975) (Fig.

18), and the Kosi tropical fan in India (Gole and Chitale, 1966). Braided streams on these fans are perennial and do not exhibit the flashy discharge characteristics of arid alluvial fan ephemeral braided streams. The dominance of fluvial processes and the relatively uniform discharge characteristics of braided-outwash and tropical-fan braided streams distinguish these fans from arid alluvial fans. The sporadic supply of coarse, unsorted sediments by mudflows to all surfaces of arid alluvial fans prevents the development of the systematic downstream decrease in grain size characteristic of braided outwash and tropical fans, on which mudflow processes are rare or absent (J. C. Boothroyd, 1979, oral commun.). The relatively uniform flow conditions of braided-outwash and tropical-fan braided streams result in steady, long-term deposition, which favors the development of the large, low-gradient surfaces of these fans. Gradients on the Kosi tropical fan range between one and five feet per mile, and average about three feet per mile.

The Scott braided outwash fan (Boothroyd and Ashley, 1975) and the Kosi tropical fan (Gole and Chitale, 1966) both provide useful models for the Baca-Eagar braided alluvial-plain system, however, neither is entirely satisfactory (Johnson, 1978). Two important differences exist between the braided outwash model and the analogous

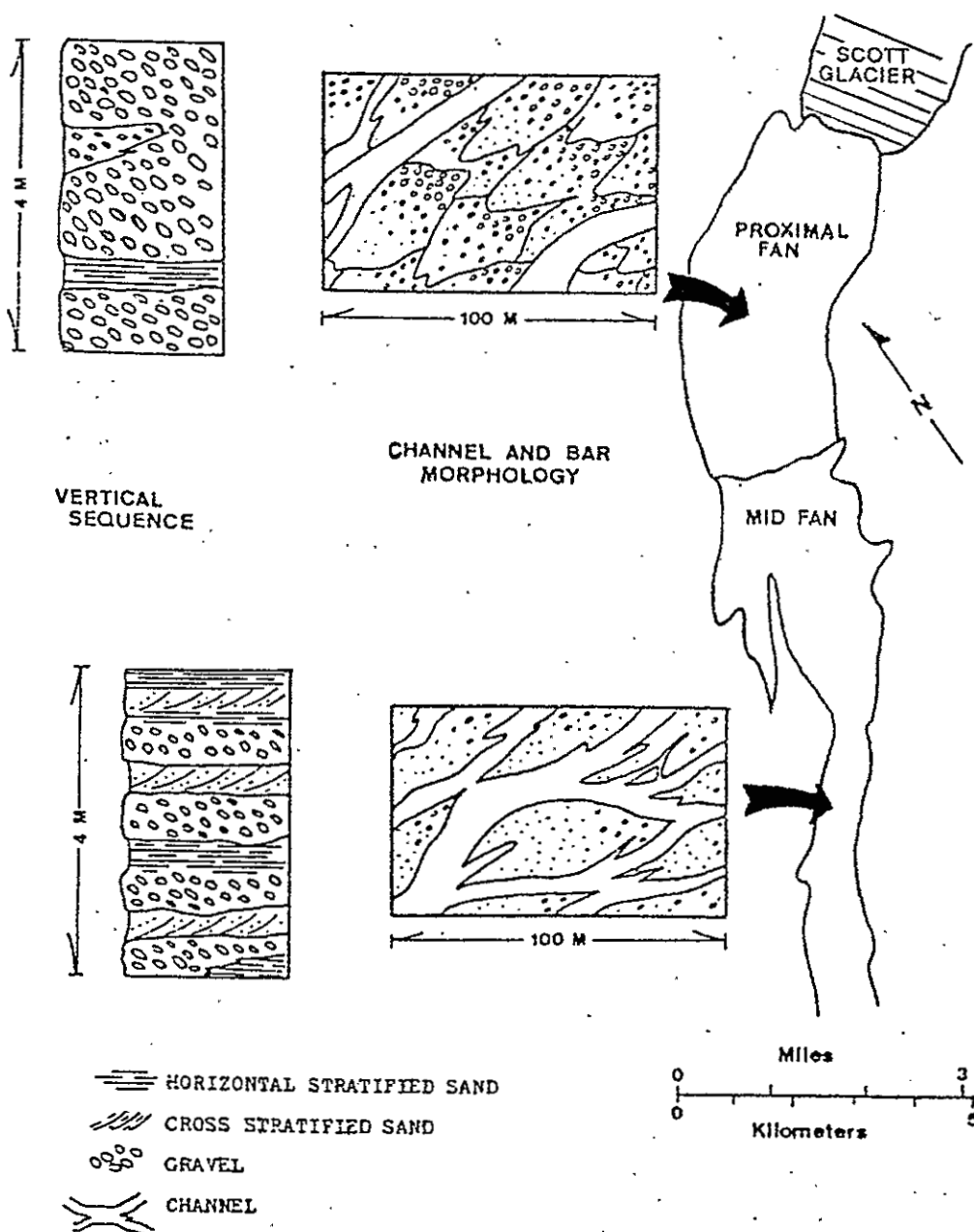


Figure 18. Map showing distribution of bar types and sedimentary structures in proximal and mid-fan facies of Scott glacial outwash fan, Alaska. From Johnson (1978), after Boothroyd and Ashley (1975).

system in the Baca and Eagar Formations. First, the length of proglacial braided outwash fans is only about five to ten miles (8 to 16 km), compared to a length of about 100 mi (160 km) for the Baca-Eagar braided alluvial-plain system. This size difference can probably be explained by the fact that the Scott braided outwash fan has only been active for a relatively short period (during Pleistocene and Recent time), while the Baca-Eagar braided alluvial plain was presumably active for several millions of years during the early Tertiary. Secondly, the braided streams of the Scott fan are perennial, while the Baca-Eagar braided streams show evidence of more flashy, perhaps even ephemeral, flow. The Kosi tropical fan is comparable in size with the Baca-Eagar braided alluvial-plain system, but contains more fine-grained sediments in its distal portions.

Lacustrine System

The lacustrine system is widespread throughout the Baca-Eagar basin. Lacustrine sedimentation took place in two general settings (Johnson, 1978): (a) in small, semipermanent lakes situated on fluvial-system floodplains; (b) in a large, shallow, persistent lake located in the Bear-Gallinas Mountains area.

Johnson (1978) recognized lacustrine fan-delta, fine-grained delta, and basinal facies within the Baca-Eagar lacustrine system. Only the lacustrine fine-grained delta and basinal facies are present in the Gallinas Mountains area. The lacustrine system comprises the entire upper red member and all of the lower red unit in the study area except the basal 40 ft (13m). In contrast to the braided alluvial-plain system, mudstones and claystones are a volumetrically important constituent of the lacustrine system; sandstone/mudstone ratios are about 1:1. Coloration is controlled by the diagenetic history of the sediment and ranges from red to yellowish gray.

Lacustrine Fine-grained Delta Facies

Facies Characteristics. Cyclical upward-coarsening sequences characterize vertical sequences in this facies (Fig. 19). Facies characteristics are summarized in Table 4. Individual cycles range in thickness from about 20 to 120 ft (6 to 35 m), and average about 30 ft (9 m) thick.

The basal portion of an idealized cycle consists of a laterally persistent calcareous mudstone or claystone intercalated with thinly bedded (generally less than 25 cm thick) very-fine to medium sandstones. Mudstone carbonate content, determined by weighing samples before and after

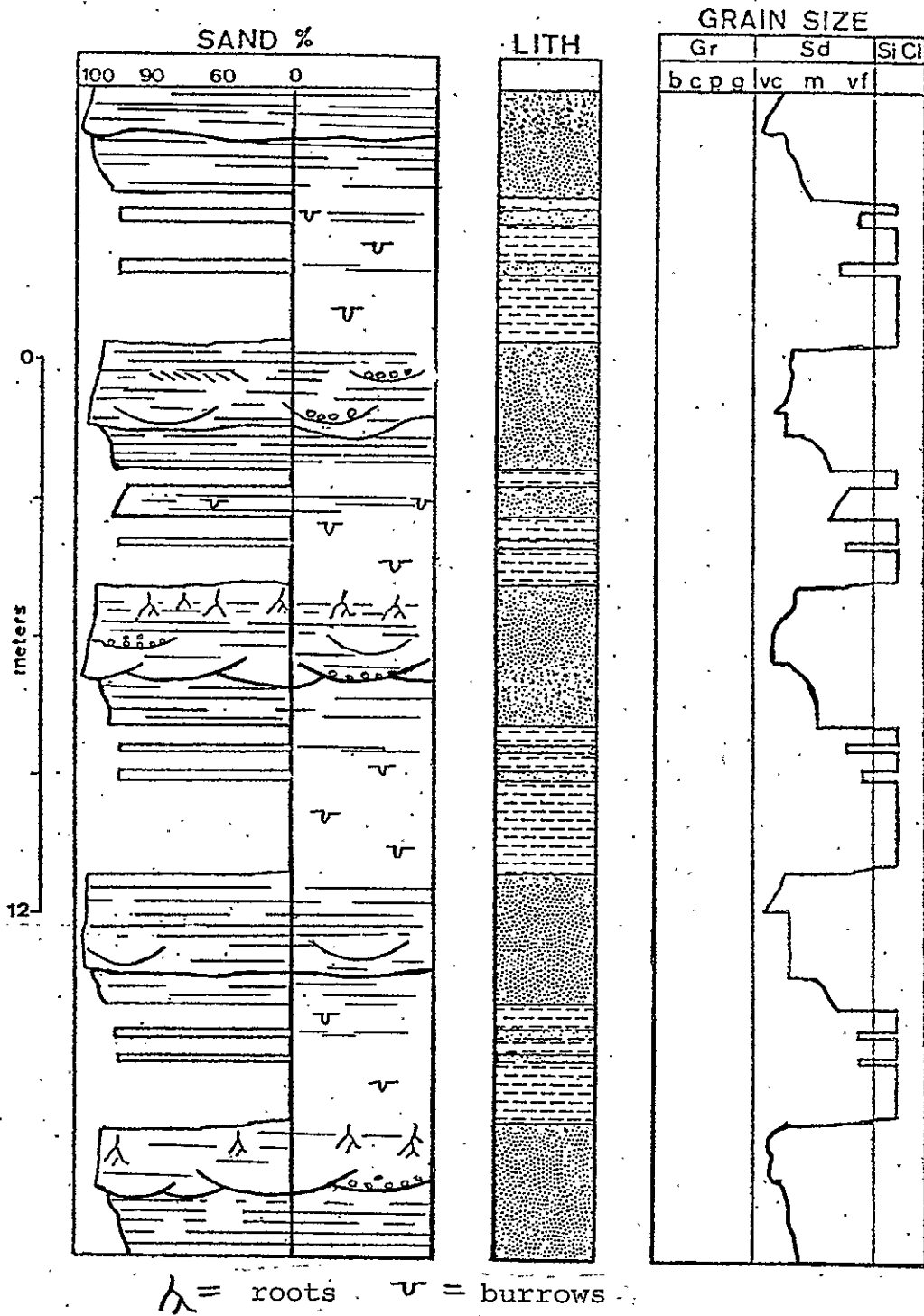


Figure 19. Typical vertical section of lacustrine fine-grained delta facies, showing upward-coarsening cycles. Modified from Johnson (1978).

Table 4

Lacustrine Fine-Grained Delta Facies Characteristics

Lithology	Sedimentary Structures
<p>Upward-coarsening sequences of mudstones and sandstones with minor conglomerates. Mudstones are generally highly calcareous. Sandstones are very fine to coarse grained and moderately to well sorted. Sandstone/mudstone ratios are about 1:1.</p>	<p>Mudstones: burrows and rare laminations. Sandstones: horizontal laminations, parting step lineations, ripple cross-lamination, occasional trough crossbeds, rare tabular crossbeds. Conglomerates form rare thin, discontinuous lenses in the upper parts of delta cycles. Large-scale, gently inclined foresets are sometimes present near the bases of cycles. Burrows and root mottling are locally abundant.</p>

acidization with cold, dilute hydrochloric acid, generally ranges between 10 and 15 percent by weight. Carbonate content decreases upward within deltaic cycles, as will be discussed in more detail in the diagenesis section. Mudstones rarely exhibit laminations and are usually structureless and homogeneous, with the exception of burrows. Burrowing in the mudstones is pervasive. In contrast to sandstones in the lower portions of deltaic cycles, mudstones do not exhibit well-defined burrows, but rather show a churned, curdled texture both megascopically and microscopically, which gives rise to the homogeneous nature of the mudstones.

Structures present within the thinly bedded sandstones intercalated with the above-described mudstones include horizontal laminations, current-ripple laminations, parting step lineation (McBride and Yeakel, 1963), occasional normal-graded beds, and burrows. Burrows (Fig. 20) are vertical, horizontal, and oblique, range in diameter from 1/4 to 2 in (1 to 5 cm), and sometimes exhibit knobby surface ornamentation and scoop-shaped backfill laminae (Johnson, 1978, p. 77). According to Johnson these burrows are similar to Scoyena sp., which are common in non-marine redbeds (Hantzschel, 1975), and are believed to have been formed by polychaete worms. Rare horizons of calcium-carbonate nodules and mudcracks were observed within the



Figure 20. Branching horizontal burrows (feeding traces?) in a red, lacustrine sandstone.

mudstones. The thinly bedded sandstones in the lower portions of cycles are often inclined (Fig. 21), forming large-scale foresets with dip angles ranging up to 15 degrees in rare instances. Dip angles are more commonly only a few degrees (Fig. 22), and are often so gently inclined that the angularity is not readily apparent in a solitary exposure.

The above-described units are transitionally overlain by a horizontal and current-ripple-laminated, laterally continuous, fine to coarse sandstone which averages about 5 ft (1.5 m) in thickness. Orientation of current-ripple cross laminations usually indicate a direction of flow at high angles to that shown by other paleocurrent indicators within the same deltaic cycle. The well-sorted, nearly homogeneous nature of these sandstones gives rise to a quasi-spheroidal weathering habit (Fig. 22). Coloration of this and superjacent sandstones within a given cycle may be red or yellowish gray, whereas coloration of previously described subjacent intercalated mudstones and sandstones is almost always red.

Moving upsection, the next and uppermost part of an ideal cycle will sometimes exhibit large, symmetrical, channel-shaped units which have erosional bases. Channels may be as much as 50 ft (15 m) wide and 15 ft (5 m) deep (Fig. 23), but are generally much smaller. Intrachannel



Figure 21. Baca fine-grained delta deposit exhibiting unusually steeply inclined prodelta foreset beds.



Figure 22. Gently inclined prodelta foreset beds overlain by quasi-spheroidally weathering delta front deposits. Hammer handle points in direction of delta progradation.

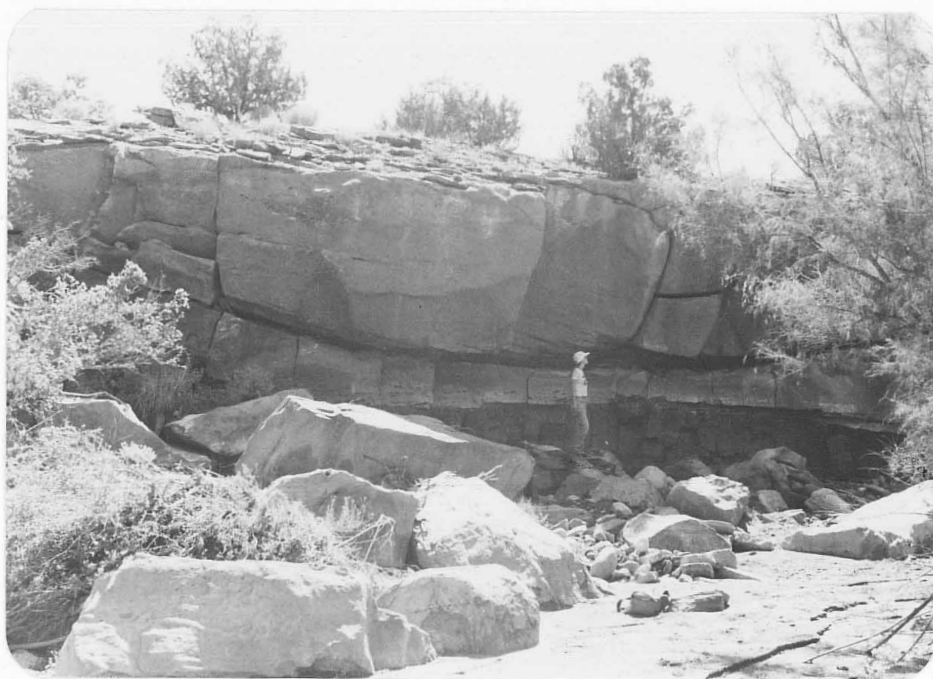


Figure 23. Exceptionally large deltaic distributary-channel deposit. Note the low width-to-depth ratio (less than 10:1) and the highly symmetrical nature, which are characteristic of distributary channel deposits in marine deltas.

sedimentary structures include medium-scale trough crossbedding and plane beds. Where symmetrical channel-shaped units are not present, the base of the upper part of each cycle is represented by an irregular, low-relief, erosional surface. The remainder of the upper portion of the cycle is composed of fine- to coarse-grained sandstones with minor conglomerates and mudstones exactly similar to the rocks of the distal braided alluvial-plain facies.

Depositional Processes. The cyclical sediments of the fine-grained delta facies record alternate deltaic progradation and abandonment in a shallow lake. Geometry of lithofacies and vertical and lateral sequences of textures and sedimentary structures are similar to those found in lobate high-constructive marine deltas (Fisher and others, 1969). Depositional processes are inferred to be the same as in these marine deltas (Johnson, 1978).

The lower intercalated mudstones and thinly bedded sandstones were deposited in a prodelta and distal delta-front environment. Silt and clay were deposited by settling from suspension. The thin sandstone beds are frontal-splay deposits, probably representing prodelta turbidites. Normal graded beds, a typical feature of turbidites, are occasionally seen in these sandstones. Turbidites in lacustrine environments have been described by

many workers, including Normark and Dickson (1976), Theakstone (1976), and Grover and Howard (1938).

The laterally continuous, quasi-spheroidally weathering, horizontally laminated and rippled sandstones are delta-front deposits. These sandstones were deposited in channel-mouth bars or in longshore-current-redistributed bars. The primary processes on the delta front were plane-bed aggradation and ripple migration. The large divergence between paleocurrent directions shown by delta-front ripples and that of other indicators within a given deltaic cycle suggest that ripple migration direction was predominantly controlled by longshore currents.

The large, symmetrical, channel-shaped sandstones sometimes present in the upper part of deltaic cycles are distributary-channel deposits. Sedimentary structures indicate that plane beds and subaqueous dunes were the dominant bedforms within distributary channels. Vegetative stabilization of delta-platform braided stream channels near the lake allowed for the development of large, symmetrical, relatively low width-to-depth-ratio distributary channels. Deltaic deposits which lack distributary channels indicate non-stabilization of delta-platform stream channels, as is common in classic "Gilbert-type" delta or fan-delta deposits (Gilbert, 1885; Theakstone, 1976). The remainder of the upper deltaic cycle is composed of delta-platform sandstones

and minor conglomerates deposited by braided-stream processes identical to those of the distal braided alluvial-plain facies. These sediments represent the braided-stream-dominated subaerial portion of the delta, and are analogous to the topset beds of classic Gilbert-type deltas.

Basinal Facies

Facies Characteristics. When present, the lacustrine basinal facies occurs directly beneath the above-described delta facies and consists of generally structureless mudstones and claystones with sparse, thin interbeds of very fine sandstone and siltstone. Evidence of burrowing is abundant. Facies characteristics are summarized in Table 5. The basinal facies is identical to the lower prodelta portion of the fine-grained delta facies with the exception that the sand and silt interbeds of the basinal facies are never inclined and are generally thinner and less abundant than those of the delta facies. The boundary between the two facies is arbitrary.

Depositional Processes. Basinal depositional processes are exactly the same as those of the lower prodeltaic portion of the fine-grained delta facies, and

Table 5

Lacustrine Basinal Facies Characteristics

Lithology	Sedimentary Structures
<p>Dominantly mudstones with sparse, thin interbeds of sandstones and siltstones. Mudstones are usually highly calcareous. Sandstones and siltstones are poorly to well sorted and are usually calcareous.</p>	<p>Mudstones: burrows and rare horizontal laminations. Sandstones and siltstones: horizontal laminations, ripple laminations, burrows, and parting step lineation.</p>

include settling of silt and clay from suspension, deposition of silt and sand by turbidity currents, and homogenization of mudstones and claystones by burrowing. The thin, sparse nature of the sand and silt interbeds indicates deposition far from nearshore sources of coarse sediments.

General Characteristics of the Lacustrine System

The laterally persistent nature of the delta front and delta platform sandstones and the general lack of destructional-phase features indicate that Baca fine-grained deltas were mainly high constructive lobate (Fisher and others, 1969), which suggests progradation into relatively shallow water. The other variety of high-constructive delta is the elongate or birdsfoot delta, which is characterized by laterally discontinuous bar-finger sands which result from progradation into deeper water. Water depth, as indicated by the thickness of prodelta mudstones and prodelta foreset beds, was generally less than 20 ft (6 m). During deposition of the upper red unit, however, water depth may have been considerably deeper, as attested by the large thicknesses of mudstones in that unit.

Baca deltaic and basinal sediments in the Gallinas Mountains area show evidence of deposition in a closed lacustrine basin. Evidence includes: (a) high concentrations of early (pre-compaction), phreatic, authigenic calcite in basinal and lower-delta mudstones and sandstones (see diagenesis section); and (b) rarity of lacustrine megafauna. Only a few scattered ostracods were observed. The climate in west-central New Mexico during Baca time was probably semiarid (see paleoclimate section). Langbein (1961) states that closed lakes are found exclusively in arid and semiarid regions. Closed lakes usually exhibit widely fluctuating water levels (Langbein, 1961). Rare caliches and mudcracked horizons in Baca basinal and prodelta sediments are indicative of lake-level low stands. The presence of the fluvially dominated middle sandstone unit between the predominantly lacustrine upper and lower red units indicates a large-scale regression, which was probably caused by a drastic drop in lake level due to a climatic change (see depositional history section).

Steeply inclined Gilbert-type foresets are rare in the fine-grained delta facies. Factors contributing to the development of foresets include: (a) homopycnal flow (inflow density approximately equal to lake-water density) which causes three-dimensional mixing and an abrupt decrease in current velocity, resulting in rapid deposition of

sediment (Bates, 1953); (b) deltaic progradation into deep water (McGowen, 1970; Axelsson, 1967; Hjulstrom, 1952); and (c) transport of coarse bedload sediments, of which Gilbert-type foresets are composed, to the distributary mouth (Smith, 1975; Axelsson, 1967). The conditions listed above were rarely present during deposition of the Baca deltas in the Gallinas Mountains area. Water depths were shallow and Baca sediments in the study area were rarely coarser than coarse sand. The closed nature of the lake implies that lake waters were more dense (due to salinity) than inflowing river water, producing hypopycnal flow and plane jet formation (Bates, 1953). Lack of three-dimensional mixing causes the plane jet to maintain its velocity over a relatively long distance basinward, resulting in deposition of sediments over a considerable distance from the distributary mouth. This leads to the development of a gently sloping prodelta surface, which produces the typical shallowly inclined prodelta foresets seen in the fine-grained delta facies. The Gilbert-type deltas in the Baca Canyon area (Johnson, 1978) probably formed in response to possible deeper-water conditions and the input of coarse, conglomeratic sediments derived from the nearby Sierra-Sandia uplift.

Thin, destructional-phase shoreface sequences produced by reworking of upper-delta sediments by waves and longshore currents following deltaic abandonment and subsidence (Fisher and others, 1969) are rarely seen. The paucity of destructional-phase shoreface sequences suggests relatively low-energy conditions within the lake basin. Attenuation of wave energy resulting from shallow water depths may explain the rarity of destructional-phase features.

The large, shallow lake system present during Baca time in the Bear-Gallinas Mountains area would tend to be polymictic (frequent overturn) since surface mixing due to eddy diffusion would be expected to penetrate at least several tens of feet (Johnson, 1978). Evidence of abundant burrowing of basinal and prodelta sediments indicates that lake-bottom sediments were oxygenated, supporting a polymictic regime. Preservation of laminations in lake-bottom sediments is usually restricted to oligomictic and meromictic (permanently stratified) lakes, in which lack of oxygen inhibits the activities of burrowing organisms. Johnson (1978, p. 85) states that the shallow, polymictic nature of the Baca lacustrine system resulted in oxygenated lake-bottom waters which may be responsible for the almost complete lack of reduced (gray and green) Baca lacustrine sediments. Lake bottom sediments in shallow, frequent-

overturn, Lake Chad, Africa, are dark yellowish brown (Mothersill, 1975), which probably indicates the presence of limonite and, thus, positive-Eh conditions. Upon burial of less than 60 cm, however, the bottom sediments of Lake Chad assume a dark greenish-gray coloration, probably indicative of reduced iron and negative-Eh conditions. This change from an oxygenating to a reducing regime is probably due to removal, during burial, of bottom sediments from the presence of oxygenated lake waters. Isolation of bottom sediments from oxygenated lake waters would allow for the uptake of free oxygen in the interstitial waters through decomposition of organic material by aerobic bacteria, which would lead to negative-Eh conditions. The majority of the coloration of the Baca sediments (in both lacustrine and fluvial facies) in the study area appears to be due to intrastratal solution of iron-bearing minerals, precipitation of hydrated iron oxides, and the subsequent dehydration of these oxides, which results in the development of hematite pigment. Thus, the Baca sediments did not necessarily contain any iron-oxide colorants upon deposition; in fact, there is some evidence to suggest that the lacustrine sediments were reducing and contained iron sulfides which later provided iron for red coloration, as will be discussed in the diagenesis section.

Several other lines of evidence exist which support a lacustrine interpretation for large parts of the Baca Formation in the Bear-Gallinas Mountains area. These include: (a) the presence of rare oolites and ostracods and common intraclasts which were observed in thin sections from many parts of the Baca in the study area, as will be discussed in the sandstone petrology section. (b) In his work on the palynology of the Baca Formation in the Bear Mountains vicinity, Chaiffetz (1979) stated that the predominantly pink-gray Baca sediments (i.e. the lower and upper red units, which I interpret to be dominantly lacustrine) yielded only a few poorly preserved pollen grains and the fresh-water alga, Pediastrum. However, a greenish-gray shale sample from a thin mudstone in the fluvially dominated middle sandstone unit (I was present during sampling) produced spores and pollen from a wide variety of upland flora, including conifers. Chaiffetz (1979) further states that the presence of Pediastrum "...perhaps requires some standing fresh-water bodies in the region at that time".

Lacustrine Model

The limited exposures of the Baca lacustrine system make comparison to modern and ancient analogues difficult. Exposures in the study area and the Baca Canyon area consist only of marginal lacustrine deposits. Paleocurrent directions in the study area (see sediment dispersal patterns section) are generally northeast directed, indicating that the location of the basin center was in that direction. The nature of the basin-center deposits are not known due to erosional stripping following late Tertiary uplift of the Colorado Plateau. Any model of the Baca lacustrine system must take into account the following characteristics: (a) shallow water depth; (b) fluctuating lake levels; (c) rarity of lacustrine megafauna; and (d) high concentrations of early authigenic calcite cements in marginal lacustrine sediments.

Surdam and Wolfbauer (1975) have proposed a closed-basin, playa-lake model for Eocene Lake Gosiute in Wyoming which adequately fits most of the characteristics of the Baca lacustrine system. Lake Gosiute was a large, shallow, closed lake which exhibited widely fluctuating lake levels and crude, concentric zonation of both chemical and detrital facies (Fig. 24). The marginal facies of Lake Gosiute is characterized by calcareous sandstones and siltstones

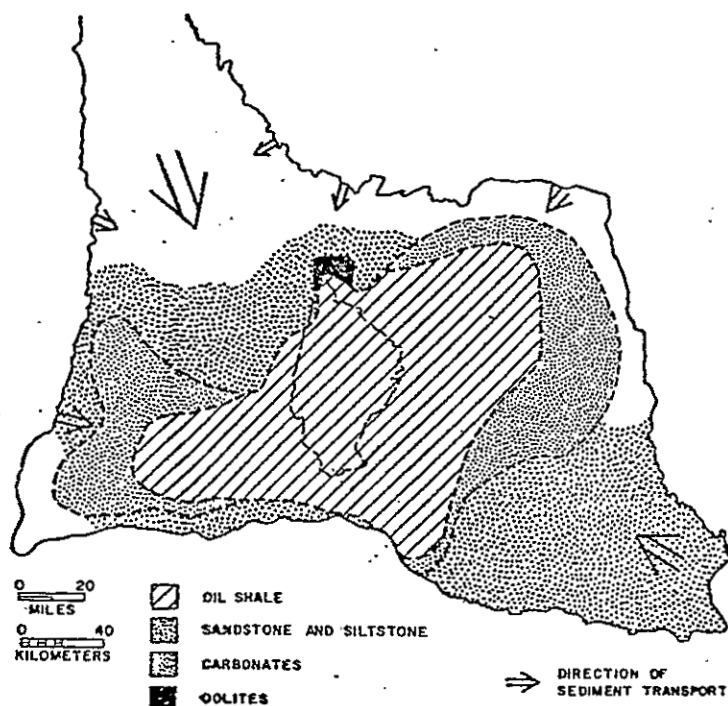


Figure 24. Map showing crude, concentric zonation of facies in Eocene Lake Gosiute, Wyoming, during a high stand (Tipton Shale time). Marginal facies is composed of calcareous sandstones and siltstones, somewhat similar to the lacustrine system rocks in the study area. Surdam and Wolfbauer (1975).

(Surdam and Wolfbauer, 1975, p. 339) somewhat similar to Baca marginal lacustrine rocks. Megafaunal diversity in Lake Gosiute was greater than that of the Baca Formation lacustrine system, and included ostracods, molluscs, algal reefs, and fish. The more restricted assemblage of the Baca lacustrine system may be due to: (a) lack of exposure of potentially more fossiliferous basin-center deposits; (b) higher salinity resulting from higher evaporation rates in the more southerly Baca lacustrine system.

Deep Springs Lake in Inyo County, California (Jones, 1965), exhibits quasi-concentric zonation of facies similar to that of ancient Lake Gosiute (Surdam and Wolfbauer, 1975), and may represent a modern analogue of the Baca lacustrine system in the Bear-Gallinas Mountains area. Marginal sediments of Deep Springs Lake contain high concentrations of authigenic carbonate minerals. Certain aspects of Lake Chad, Africa, (Mothersill, 1975) are similar to those inferred for the Baca lacustrine system. These include: (a) polymictic regime; (b) closed nature of the lake; and (c) shallow water depth (less than 5 m).

DEPOSITIONAL RECONSTRUCTION

Sediment Dispersal Patterns

Paleocurrent indicators were used to delineate sediment dispersal patterns in the study area. Two general types of paleocurrent indicators, unidirectional and bidirectional, were utilized. Unidirectional indicators include imbricated pebbles and trough-crossbed axes. Rust (1972b) has documented the relationship between flow direction and imbricated pebble orientation in modern streams. The coincidence of the azimuths of trough-crossbed axes with flow direction has been demonstrated by Dott, (1973), High and Picard, (1974), and Meckel (1967). Unidirectional paleocurrent indicators occur in the braided-stream-dominated delta-platform portion of the fine-grained lacustrine delta facies and the distal braided alluvial-plain facies.

Parting step lineations (McBride and Yeakel, 1963) (Fig. 25) constitute the bidirectional indicators and, due to their abundance and ease of measurement, were the dominant paleocurrent indicator utilized in this study. Stokes (1947) has documented that parting-step lineation trend is parallel to current flow. Due to its bidirectional nature, parting-step lineation data must be used in

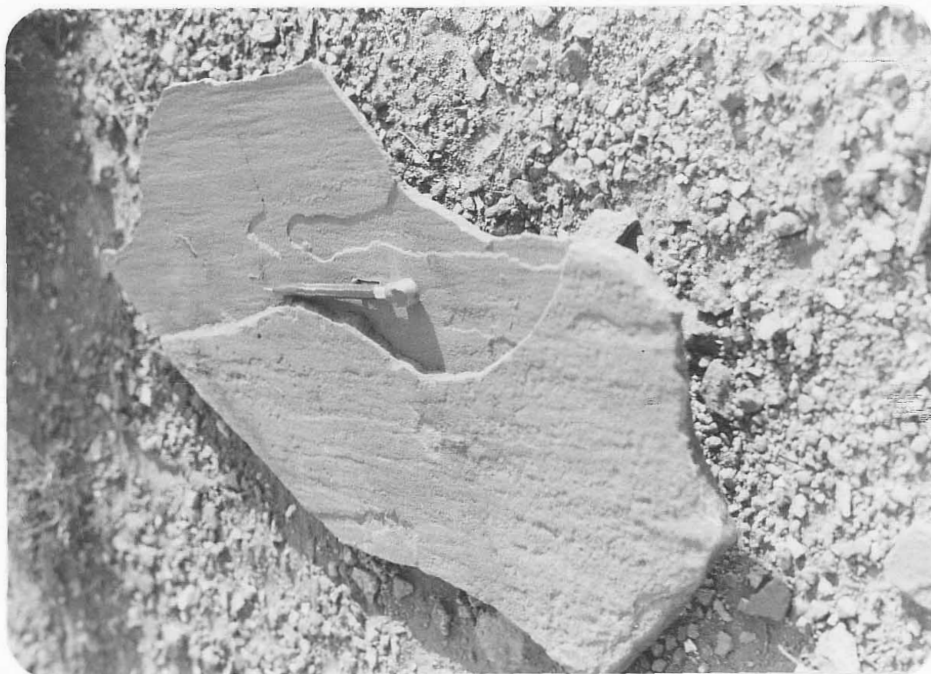


Figure 25. Well-developed parting-step lineation in a fine-grained Baca sandstone. Paleoflow was parallel to trend of mechanical pencil.

conjunction with unidirectional data in order to determine the true transport vector. Parting-step lineations are sometimes seen in braided-stream deposits in the delta-platform portion of the fine-grained lacustrine delta facies and the distal braided alluvial-plain facies. They are very commonly observed in thin, prodelta frontal-splay sandstones. As discussed previously, these sandstones probably represent deltaic turbidity-current deposits. Parting-step lineation within turbidites has been described by Crowell (1955).

Paleocurrent directions vary in a somewhat systematic manner from the western to eastern portions of the study area. In the western part of the study area, paleocurrents were generally northeastward directed (Fig. 26 a, b), whereas, in the eastern part of the area, paleocurrent directions trend generally east-southeastward (Fig. 26 c; d). This divergence of paleoflow may have been caused by activity along the previously described northeast-trending monoclinial flexure present in the southeastern portion of the area. Downwarping of the southeastern side of the monocline during Baca time may have created a topographically low area which may be responsible for the deflection of paleocurrents to the east-southeast in the eastern portion of the study area. If this hypothesis is true, then the "regional" paleocurrent direction in the

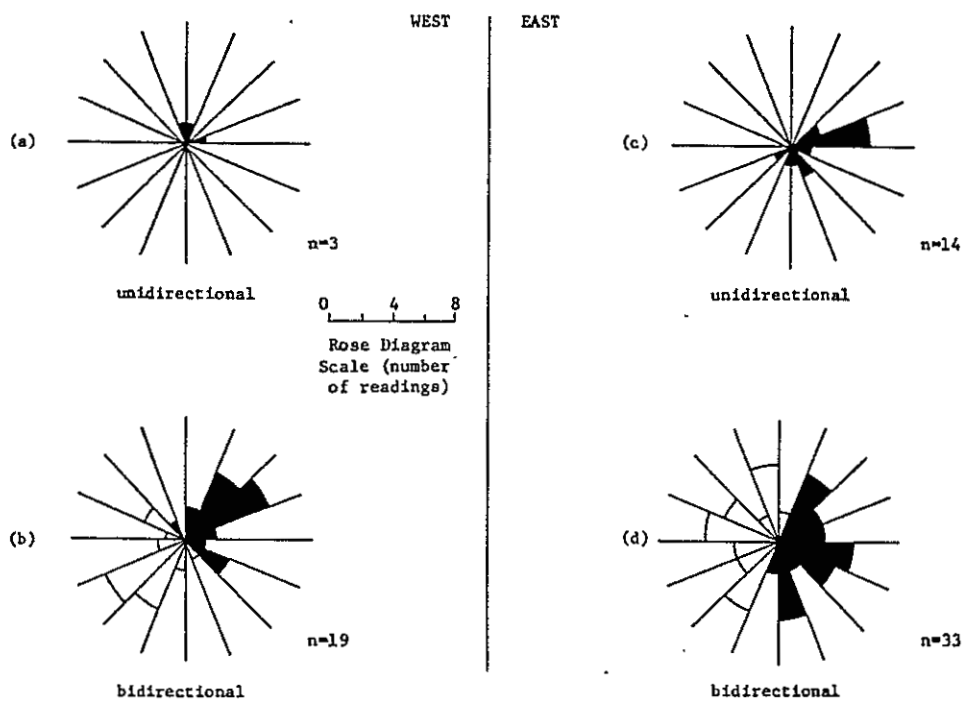


Figure 26. Comparison of paleocurrent data in western (a,b) and eastern (c,d) portions of study area. The significant portions of the bidirectional rose diagrams (shaded) were determined by comparison with associated unidirectional data. The study area was arbitrarily divided along the line between Indian Spring Canyon and Indian Mesa quadrangles.

Gallinas Mountains area was probably northeastward, as represented by the paleocurrent indicators in the western portion of the area which were farther away from, and presumably unaffected by, the monocline. Baca sediments in the study area were probably derived mainly from the Morenci uplift to the southwest, although detrital input by tributaries draining the western flank of that portion of the Sierra-Sandia uplift which lies to the south of the area may have also been important.

Depositional History

The rocks of the Baca Formation in the study area record the alternate prevalence of distal braided alluvial plain and lacustrine environments of deposition. The alternation of these two environments reflect large-scale fluctuations of water level in a large, shallow lake present during Baca time in the Bear-Gallinas Mountains vicinity.

Baca sedimentation in the study area was initiated by braided-stream deposition of sands and minor gravels predominantly derived from the southwest on a low-relief erosional surface developed on the Late Cretaceous Crevasse Canyon Formation. Braided-stream sedimentation in the lower Baca is represented by the distal braided alluvial-plain facies which comprises the basal 40 ft (13 m) of the lower

red unit (Fig. 27).

The initial interval of braided-stream sedimentation was followed by a prolonged period of marginal lacustrine sedimentation, as is represented by the cyclical deposits of the fine-grained delta and lacustrine basinal facies, which comprise the remaining 283 ft (86 m) of the lower red unit. These lacustrine deposits indicate a large-scale southwestward transgression of the shoreline of a lake whose center was to the northeast (as suggested by paleocurrent data), which resulted in onlap of lacustrine sediments over older braided stream deposits. Local, small-scale regressive-transgressive sequences within this initial transgressive phase of Baca sedimentation are recorded by cyclical deltaic progradation, abandonment, and subsidence.

The initial period of lacustrine sedimentation was followed by a return to a braided-stream-dominated regime, as represented by the sediments of the distal braided alluvial-plain facies which comprise the entire middle sandstone unit. The return to fluvially dominated processes indicates a large-scale regression of the lake shoreline to the northeast.

The final phase of Baca sedimentation in the study area is represented by the dominantly lacustrine sediments of the upper red unit. These sediments indicate a second major, widespread shoreline transgression coupled with minor

the locus of lacustrine sedimentation due to tectonism within the basin; (b) increased erosion caused by tectonic activity in the source area, with resultant large-scale regression due to progradation of alluvial aprons basinward; (c) climatic fluctuations with resultant large-scale transgressive and regressive phases. The relative importance of each of the above-listed hypotheses is difficult to determine. However, one line of evidence suggests that climatic changes were a major cause of the lake-level fluctuations. The lacustrine mudstones in the study area, with the exception of the prodelta mudstone of the basal deltaic cycle in the upper red unit, are highly calcareous and indicative of probable saline, closed-lake conditions. The essentially non-calcareous nature of the basal mudstone of the upper red unit (2 percent calcite by weight as compared with 10-15 percent in other mudstones) implies a temporary change to more fresh-water conditions during the beginning of the second transgressive phase. If the transgression was due to a change to a wetter climate, the low-saline characteristics could be easily explained by the introduction of large amounts of fresh water to the lake. Neither of the tectonic alternatives can explain the non-calcareous nature of the basal mudstone of the upper red unit. Large-scale lake-level fluctuations in contemporaneous Eocene Lake Gosiute, Wyoming, have been attributed to

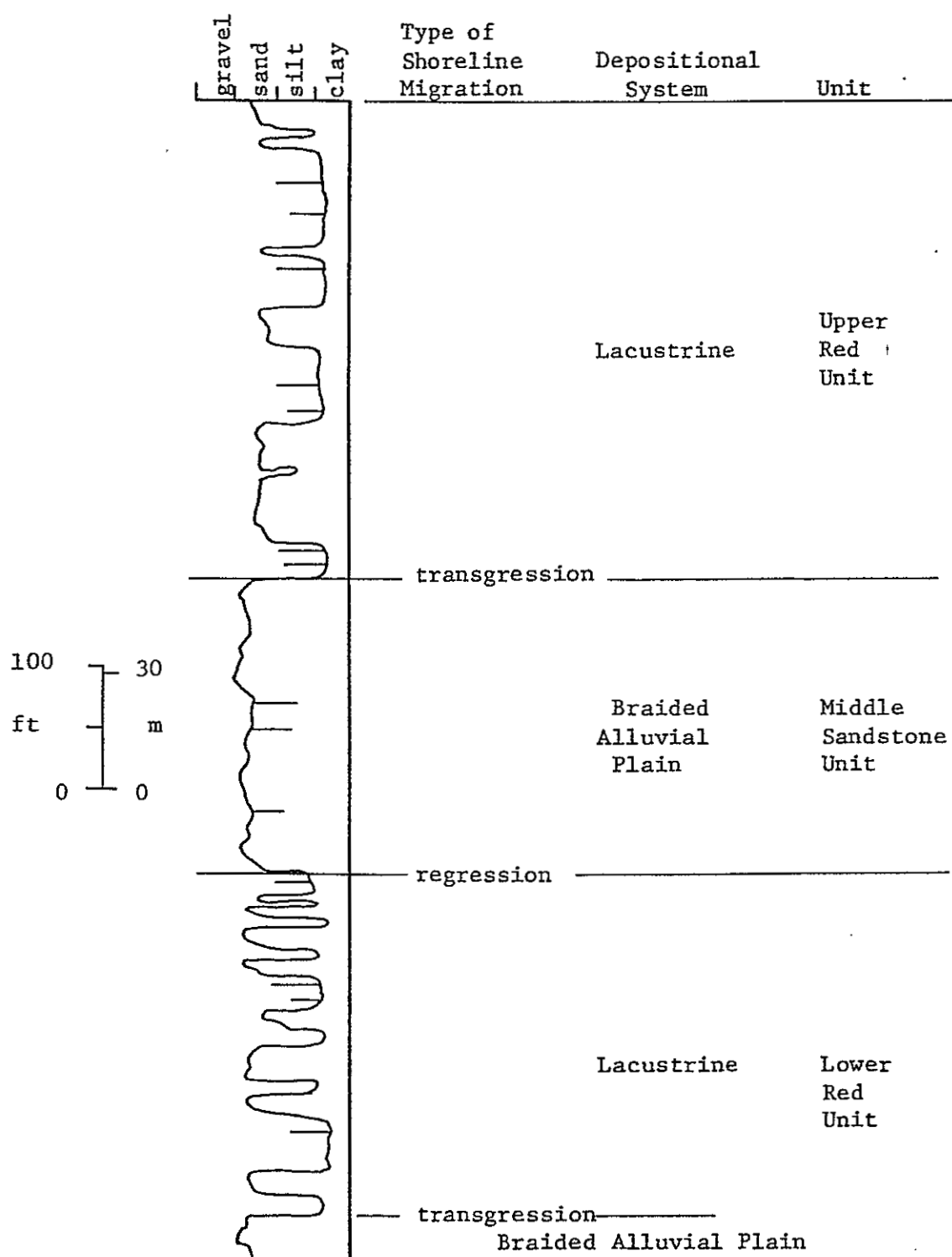


Figure 27. Generalized Baca stratigraphic section in the study area showing relationships between shoreline migrations, depositional systems, and informal units.

deltaic regressive sequences, similar to those of the first transgressive phase. Water depths during the second transgressive phase may have been deeper than those of the first, as shown by the large thicknesses of basinal and prodelta mudstones in the upper red unit. Lacustrine conditions continued to prevail in some parts of the study area during deposition of the lowermost Spears Formation, as attested by the occurrence of deltaic deposits in the basal portion of that unit in some areas (basal Spears deltaic deposits are well exposed in SW 1/4 and NW 1/4, SW 1/4, sec. 24, T.1N., R.6W.).

Examination by the writer of the Baca stratigraphic section in Baca Canyon revealed a similar, although coarser-grained, vertical sequence of facies to that seen in the study area, indicating that the transgressions and regressions recorded in the study area were not just local features, but were manifested throughout the lake basin. The Baca lacustrine system in the Bear-Gallinas Mountains vicinity may have been initiated in response to creation of the Laramide Sierra-Sandia uplift which acted as a damming element across the generally eastward-dipping regional paleoslope.

Three possible explanations exist for the large-scale transgressions and regressions recorded in the Baca sediments in the study area. These are: (a) shifting of

climatic changes by Surdam and Wolfbauer (1975). It is interesting to note that the relative thicknesses, sequence of occurrence, and number of transgressive and regressive phases in Eocene Lake Gosiute (Surdam and Wolfbauer, 1975) is very similar to those in the large lacustrine system present during Baca time in the Bear-Gallinas Mountains vicinity (Fig. 28). Although climatic fluctuations generally affect large regions, not enough data is available to determine possible relationships between the transgressive and regressive phases of Lake Gosiute and the Baca lacustrine system.

The existence of deltaic deposits in the basal Spears Formation in some parts of the study area indicates that the lake persisted for a short time during the beginning of Oligocene volcanism. The cause of the final demise of the lake is not known. Likely possibilities include climatic change and rapid infilling of the lake with volcanoclastic sediments.

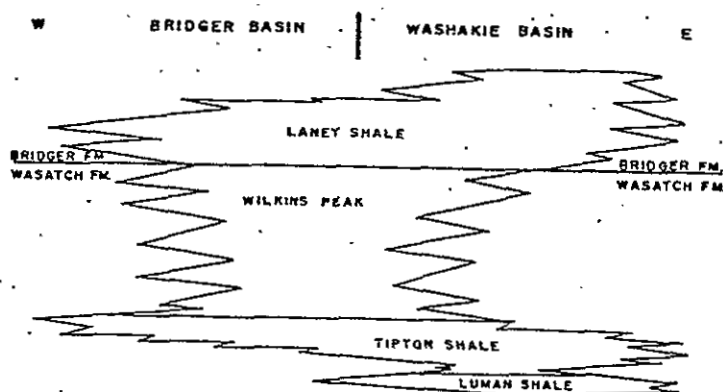


Figure 28. Generalized stratigraphy of the Green River Formation in Bridger and Washakie basins of Wyoming, showing alternation of high stands (Tipton and Laney Shales) and low stands (Luman Shale, Wilkins Peak) in Eocene Lake Gosiute. From Surdam and Wolfbauer (1975).

PETROLOGY

Conglomerate Petrology

Conglomerates are scarce but widespread throughout the study area. They occur primarily as thin, discontinuous lenses within sandstones of the distal braided alluvial-plain facies and in the upper portions of lacustrine deltaic cycles. Clast size averages about 1.6 in (4 cm), and ranges up to as much as 5 in (12.5 cm).

Clast Composition

Pebble counts from 15 localities within the study area were utilized to determine the clast composition of the Baca conglomerates. Lithologies present in the conglomerates are highly variable and consist predominantly of metaquartzite, limestone, and chert. Many other lithologies, however, are also present and often are important constituents in some areas. Silicified wood fragments are locally abundant in the middle sandstone and upper red units. Pebble composition data is summarized in Table 6. A ternary plot of pebble compositions is presented in Figure 29.

Table 6

Summary of Pebble Composition Data

Lithology	Range (%)	Average (%)	Color	Remarks
metaquartzite	0-90	44.2	red, black, pink, gray, white, multi- colored	Usually well rounded and subequant.
limestone	0-85	29.4	medium to dark gray	Dominantly micrite. Sometimes contains a few crinoid stem fragments or septarian cracks.
chert	0-65	10.4	dark gray to black	-
granite	0-75	6.2	grayish-pink	Contains abundant pink orthoclase. Usually present in small amounts. High concentrations (75%) only seen at one locality.
sandstone and siltstone	0-40	5.6	gray, pink, red	Some may be reworked Baca sediments.
schist	0-20	1.6	medium to dark gray	Contains abundant biotite.

Summary of Pebble Composition Data (cont'd)

Lithology	Range(%)	Average(%)	Color	Remarks
mudstone	0-25	1.6	red	Probable reworked Baca mudstones
andesite(?)	0-10	0.8	purplish to medium gray	Probably derived from pre-Laramide volcanics.

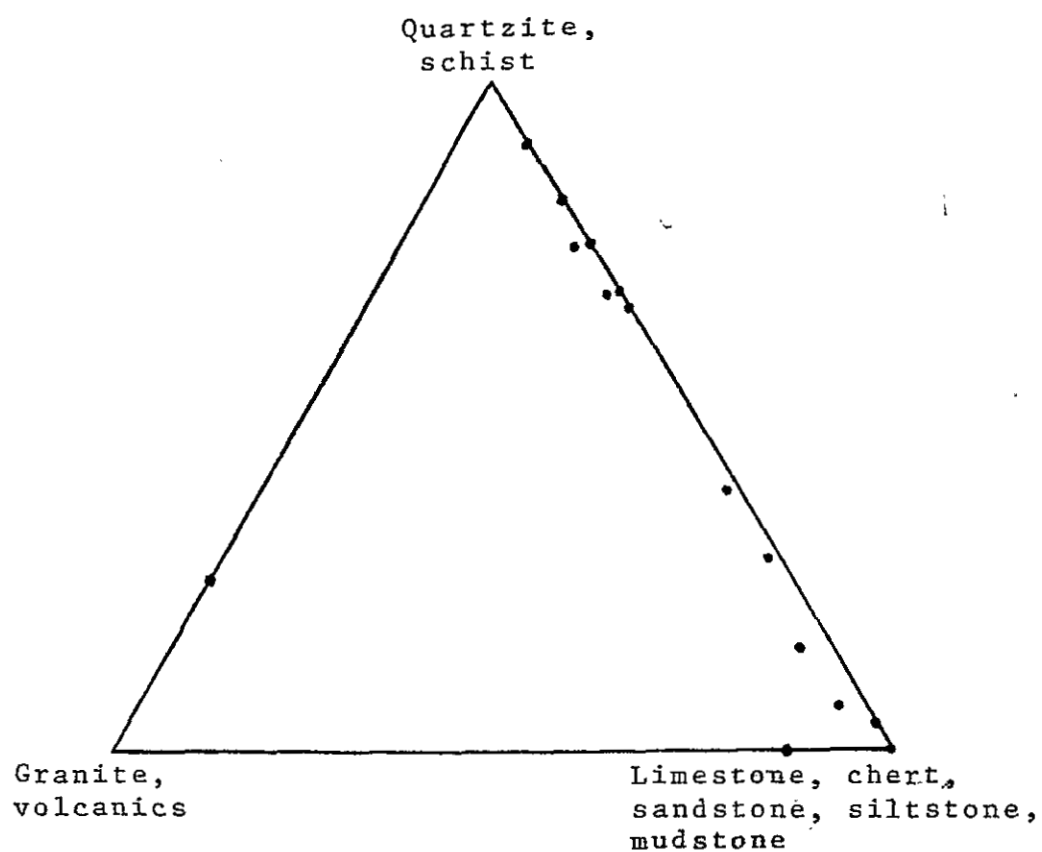


Figure 29. Ternary plot of Baca pebble compositions. Data from 15 pebble counts within the study area.

Baca conglomerate clasts are lithologically similar to rocks exposed in that portion of the Sierra-Sandia uplift now represented by the Magdalena Mountains. The variable nature of the clast compositions in Baca conglomerates suggests derivation from nearby sources. Some of the carbonate clasts exhibit fragile, platy shapes, which imply short distances of transport, and, thus, were probably either derived from a Paleozoic limestone source in the nearby Sierra-Sandia or Morenci uplifts or from an intraformational source. Limestones of lacustrine origin have been reported in the lower red unit of the Baca Formation in the Bear Mountains vicinity (Massingill, 1979, p. 100).

Clast Morphology

Baca conglomerate clasts from within the study area are usually highly spherical. Thirty-eight approximately equal-sized (2-3 cm in length) internally isotropic clasts from two localities within the study area were measured by the writer and 33 clasts from one location were measured by members of R. L. Folk's Geo 391 Sediments and Sedimentary Rocks class and plotted on a sphericity-form diagram (Fig. 30). Most points plotted in the compact platy, compact bladed, and compact elongated fields, with a few points

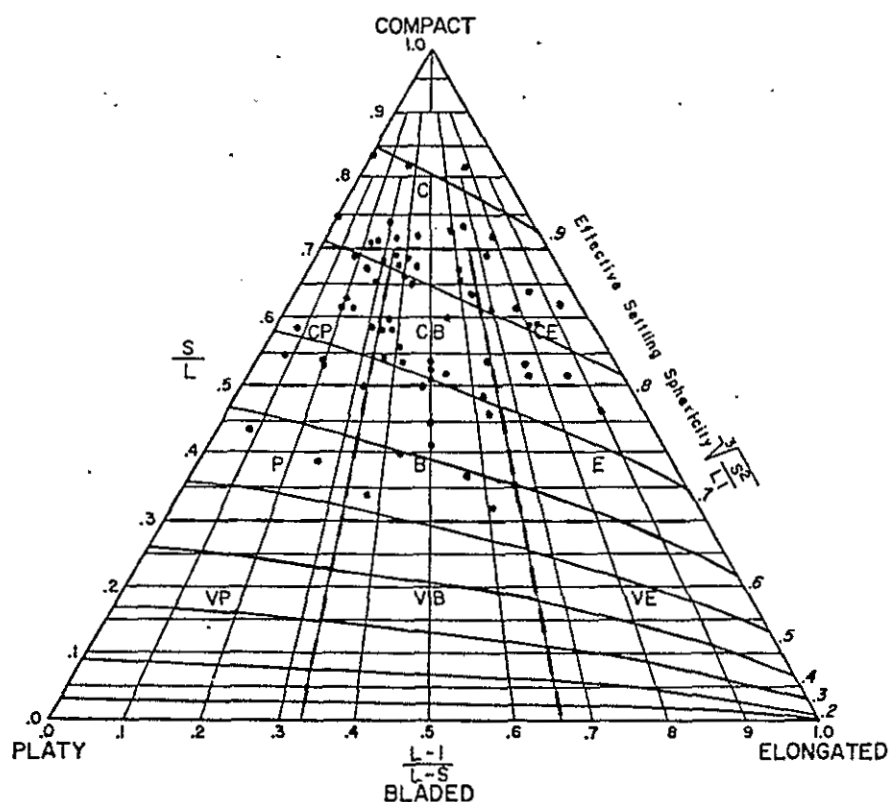


Figure 30. Sphericity-form diagram showing shapes of 71 Băca pebbles. Average maximum projection sphericity is 0.754. L=long diameter, I=intermediate diameter, S=short diameter. Sphericity-form diagram from Folk (1974).

falling in the compact, bladed, and platy fields. Average maximum projection sphericity $((S^2/LI)^{1/3})$ (Sneed and Folk, 1958) for the samples was 0.754. According to Folk (1978, oral commun.), the mean maximum projection sphericity is usually less than 0.66 for beach pebbles, between 0.66 and 0.75 for non-braided-stream fluvial pebbles, and greater than 0.75 for braided-stream pebbles. As described previously, the primary mode of transport of the Baca sediments in the study area (and, presumably, upstream of the study area) was by braided streams. The 0.754 value obtained for the Baca pebbles thus marginally supports Folk's hypothesis.

Dobkins and Folk (1970) state that the low-sphericity, platy form of Tahiti-Nui beach pebbles is caused by sliding back and forth due to the effects of swash and backwash. The high sphericity of braided stream pebbles may reflect the flashy discharge characteristics typical of most braided streams. High-discharge events, common in braided streams, would tend to transport pebbles in a turbulent, chaotic manner. This would result in nearly equal distribution of abrasive action to all surfaces of the pebbles, thus favoring the development of nearly equant clasts. Non-braided fluvial systems, on the other hand, typically exhibit more uniform discharge characteristics, which would favor transport of pebbles by rolling along

their short and intermediate axes. Such rolling would preferentially abrade the short and intermediate axes of the pebbles, resulting in a moderate-sphericity, bladed or elongate form typical of non-braided fluvial clasts.

According to the visual-comparison roundness scale of Powers (1953), Baca pebbles are generally rounded to well rounded. Fine-grained, well-indurated pebble types (e.g. metaquartzite, chert, micrite) tend to be more rounded than the coarser-grained or less well-indurated lithologies. Although metaquartzite clasts similar to those in the Baca are present in several Mesozoic units in west-central New Mexico, such as the Triassic Chinle Formation (Givens, 1957), and in several Precambrian units in southern Arizona (J. MacMillan, 1980, oral commun.), the well-rounded nature of the Baca clasts does not necessarily imply that these pebbles are multicycle. In fact, the well-rounded nature of the obviously first-cycle cobbles and boulders of the proximal braided alluvial-plain facies exposed along the Mogollon Rim implies that many of the well-rounded Baca pebbles are probably first cycle.

Baca pebbles in the study area often exhibit small, crescentic percussion marks on their surfaces. These surface features are indicative of high-velocity impacts (Folk, 1974, p. 12), which probably occurred during transport in braided streams.

Sandstone Petrology

Twenty-six thin sections of Baca sandstones from the study area were examined and 200 random points from each thin section were counted. Thin section data is presented in Appendix B. Sieve-equivalent grain size was calculated from thin-section data using Harrell and Eriksson's (1979) linear regression formula, as follows: (sieve grain size in phi units) = $0.227 + 0.973(\text{thin-section grain size in phi units})$. Sieve-equivalent grain size for the sandstone thin sections examined ranges from 0.6ϕ (coarse sand) to 3.1ϕ (very fine sand), with most samples falling in the medium and fine sand categories. Sandstone sorting values ranged from very poorly to well sorted, and averaged moderately to moderately well sorted. Most sandstones were texturally mature or submature, however, two samples contained greater than five percent detrital clay matrix (illite) and were classified as immature (Folk, 1951). According to Powers' (1953) visual-comparison roundness scale, most grains examined fell into the subangular and subrounded categories. A small population of rounded to well-rounded quartz grains were observed, however, and probably represent multicycle grains.

According to Folk's (1974) mineralogic sandstone classification, most of the Baca sandstones examined petrographically are sublitharenites, feldspathic litharenites, or lithic arkoses (Fig. 31). Only one sample plotted in either the subarkose or litharenite portions of the triangle diagram. Contrary to the interpretations of previous workers (Givens, 1957; Tonking, 1957), none of the Baca sandstones from the study area which were examined in thin section could be classified as "true" arkoses (as defined by Folk, 1974). Average feldspar content of these sandstones is 14.3 percent of the framework grains. In the Baca Canyon area, however, Baca Formation sandstones are very feldspathic, probably due to derivation from the nearby Sierra-Sandia uplift in which Precambrian granites are common.

Quartz (47-84%, average 66% of framework grains)

Quartz is the volumetrically most important detrital mineral of the Baca sandstones within the study area. In this study, I have assigned quartz types to two genetic categories: common quartz and metamorphic quartz. These two genetic categories reflect only the probable ultimate source rock type and are not meant to imply that no quartz has been reworked from older sedimentary rocks. Within

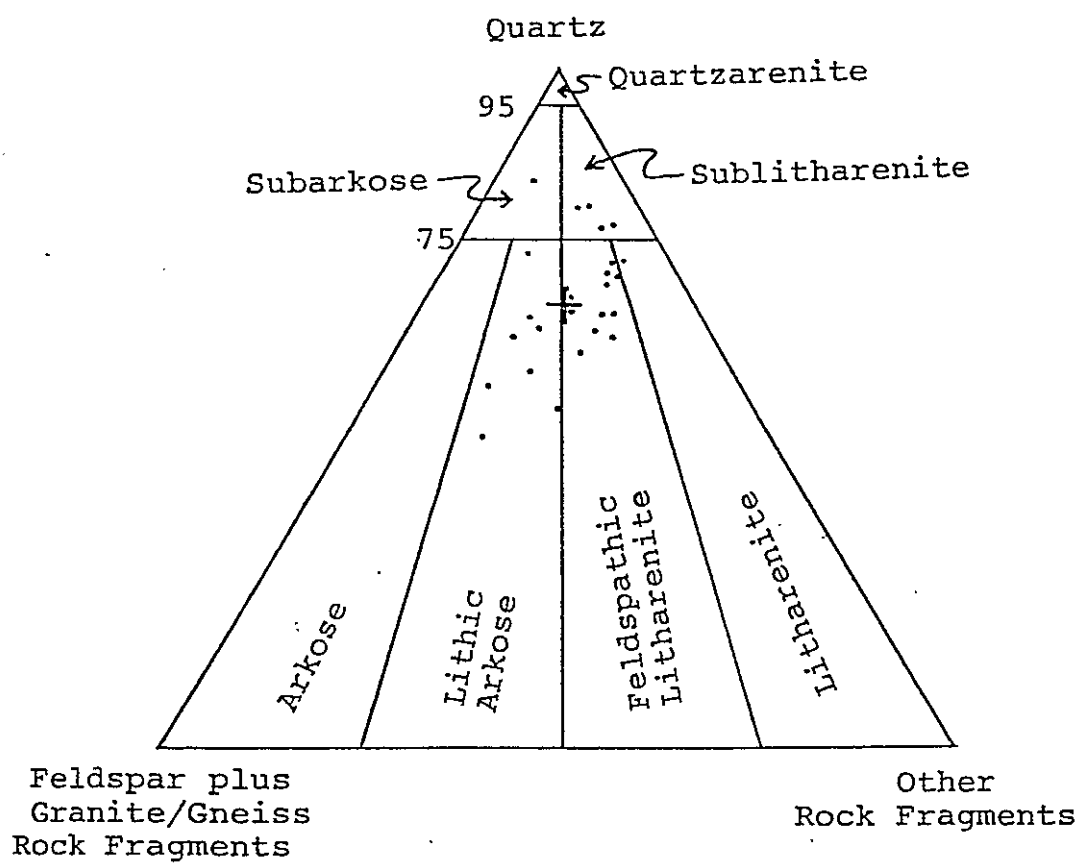


Figure 31. Classification of Baca sandstones based on data from 26 thin sections. Cross shows average composition. After Folk (1974).

these two general categories, several empirical quartz types (Folk, 1974) and genetic quartz types (Krynine, 1946) can be delineated.

Common Quartz (12-59%, average 37% of framework grains; average 55% of total quartz). Monocrystalline quartz grains which showed straight to slightly undulose extinction (extinction shadow sweeps across grains with stage rotation of five degrees or less) were classified in this category. Grains are usually subequant and xenomorphic. A small percentage of the common quartz grains (generally less than five percent) exhibit probable reworked quartz overgrowths or are anomalously well rounded, which is most likely indicative of derivation from older sedimentary sources. Common quartz grains often exhibit a few vacuoles which are randomly distributed throughout the grain and probably formed during crystallization. More rarely, vacuoles occur in linear zones within grains and may represent healing of incipient fractures. Microlites (mineral inclusions) were occasionally observed. Minute, hair-like rutile inclusions were present in a few grains.

Common quartz is most often derived from plutonic or gneissic source rocks and, less commonly, from recrystallized igneous veins and metamorphic rocks (Folk, 1974).

Metamorphic Quartz (13-51%, average 30% of framework grains; average 45% of total quartz) Monocrystalline quartz grains in which the extinction shadow sweeps the grain with greater than five degrees rotation of the stage (strongly undulose extinction) and polycrystalline (composite) quartz grains were placed in this category. Individual crystals in polycrystalline grains usually exhibit strongly undulose extinction, however, a small percentage of these grains are composed of crystals with straight to slightly undulose extinction. According to Krynine's (1946) genetic classification of quartz types, Baca metamorphic quartz is predominantly composed of stretched metamorphic quartz (Fig. 32), with minor amounts (generally less than a few percent) of schistose (Fig. 33) and recrystallized metamorphic quartz (Fig. 34).

The relative abundance of the various metamorphic quartz types is, in part, a function of grain size; polycrystalline, highly undulose quartz is usually more common in the coarser grain sizes, whereas monocrystalline, strongly undulose grains tend to be more prevalent in the finer-grained sandstones. Thus, due to the effects of the wide range in grain size of the Baca sandstones examined petrographically, no attempt was made to tabulate exact percentages of the various metamorphic quartz types. Indeed, even the relative abundances of metamorphic and

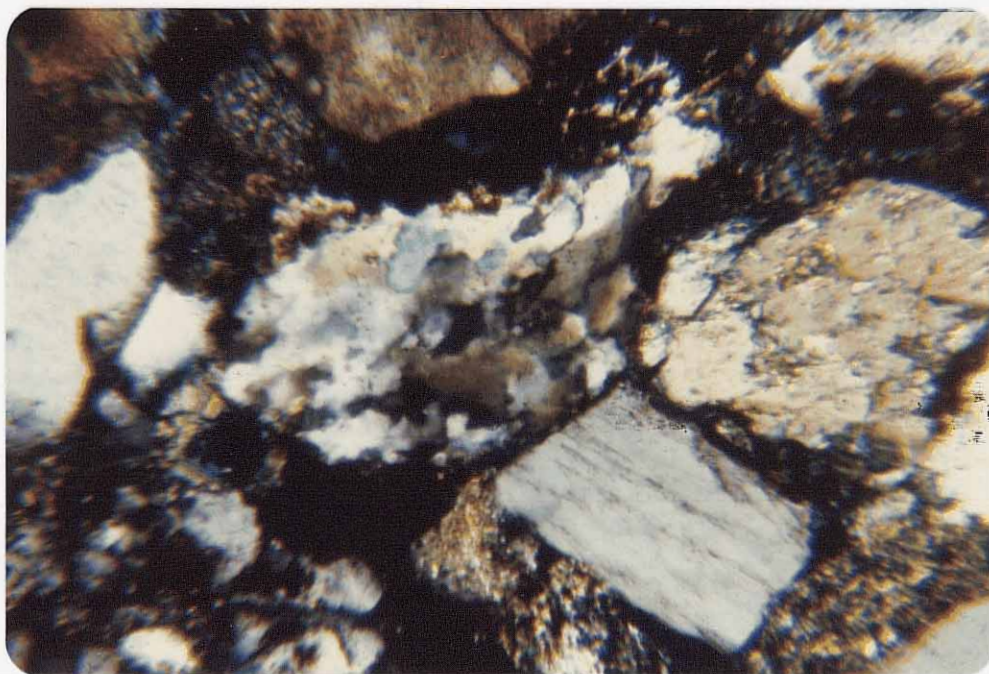


Figure 32. Stretched metamorphic quartz grain. Sample 68, crossed nicols, field width=0.75 mm.

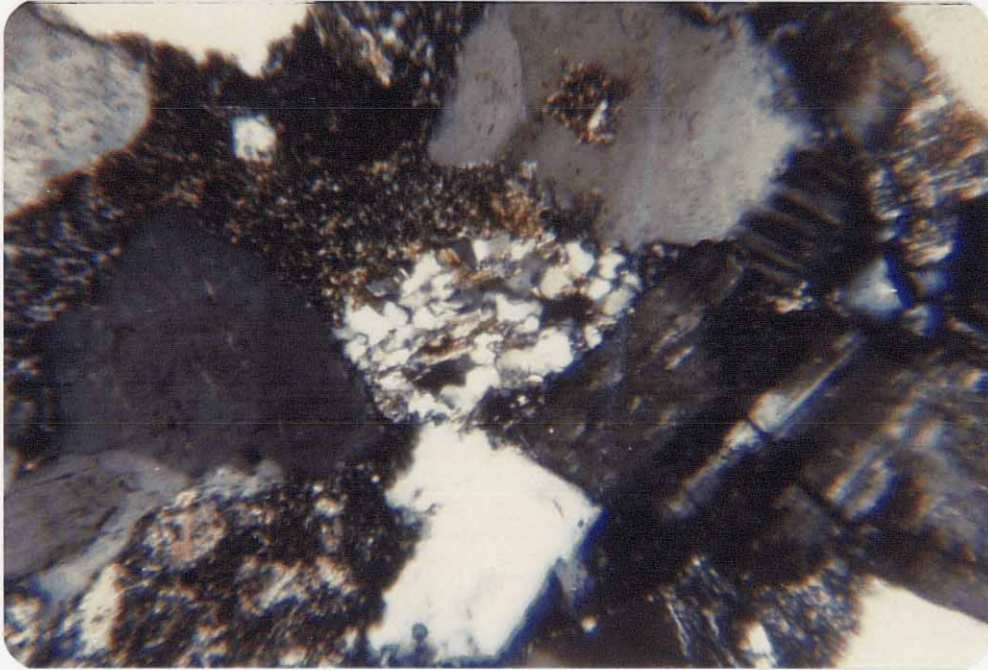


Figure 33. Schistose metamorphic quartz grain. Note minor amounts of parallel oriented muscovite and elongated quartz crystallites. Sample C, crossed nicols, field width=0.75 mm.

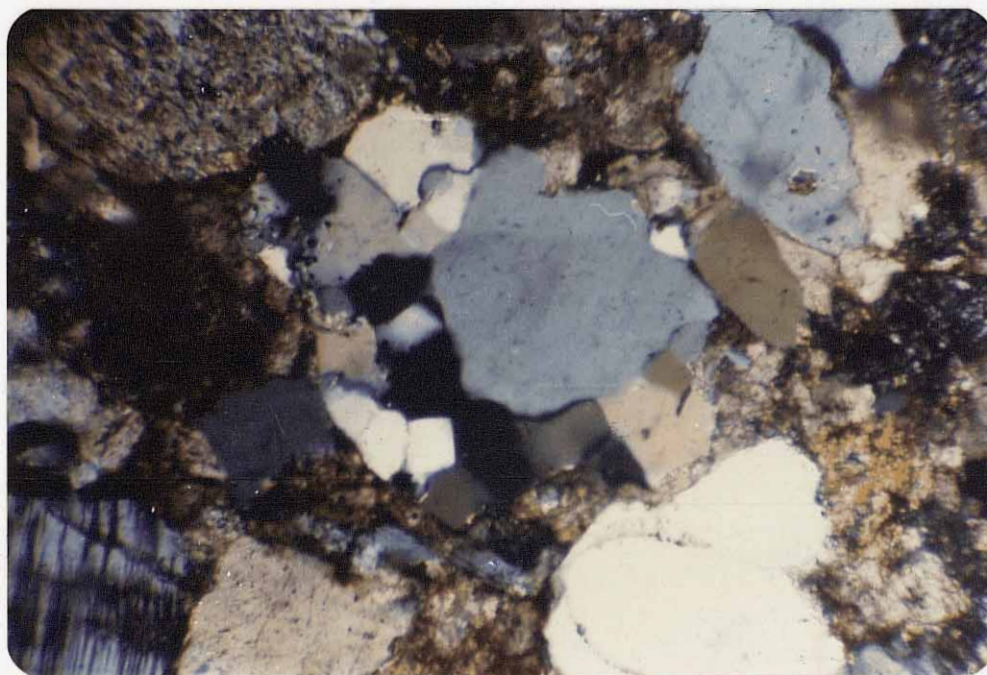


Figure 34. Recrystallized metamorphic quartz grain. Note equant shape of and simple boundaries between crystallites. Sample 32, crossed nicols, field width=0.75 mm.

common quartz is somewhat dependent on grain size. Figure 35 indicates a vague trend towards higher metamorphic/total quartz ratios with increasing grain size. The diminished abundance of metamorphic quartz in the finer grain sizes is due to the fact that increasingly strained crystal lattices are necessary to produce strongly undulose extinction with decreasing grain size and that polycrystalline quartz grains are less common in the finer sandstones.

Metamorphic quartz grains are generally subequant and xenomorphic. They often contain a few randomly dispersed vacuoles and sometimes exhibit minute inclusions of muscovite. Quartz grains containing large, aligned muscovite crystals were classified as metamorphic rock fragments.

According to Folk (1974), monocrystalline, highly undulose quartz is most commonly derived from stretched metamorphic and gneissic sources, but also may occur in some strained granites. Polycrystalline grains showing strongly undulose extinction are probably the most reliable quartz-type indicator of a metamorphic source area, and are derived primarily from gneisses and stretched metamorphic rocks. Polycrystalline grains exhibiting straight to slightly undulose extinction are most commonly derived from schists and recrystallized metamorphic rocks, but may, to a small extent, be derived from granites (Folk, 1974). Based on his

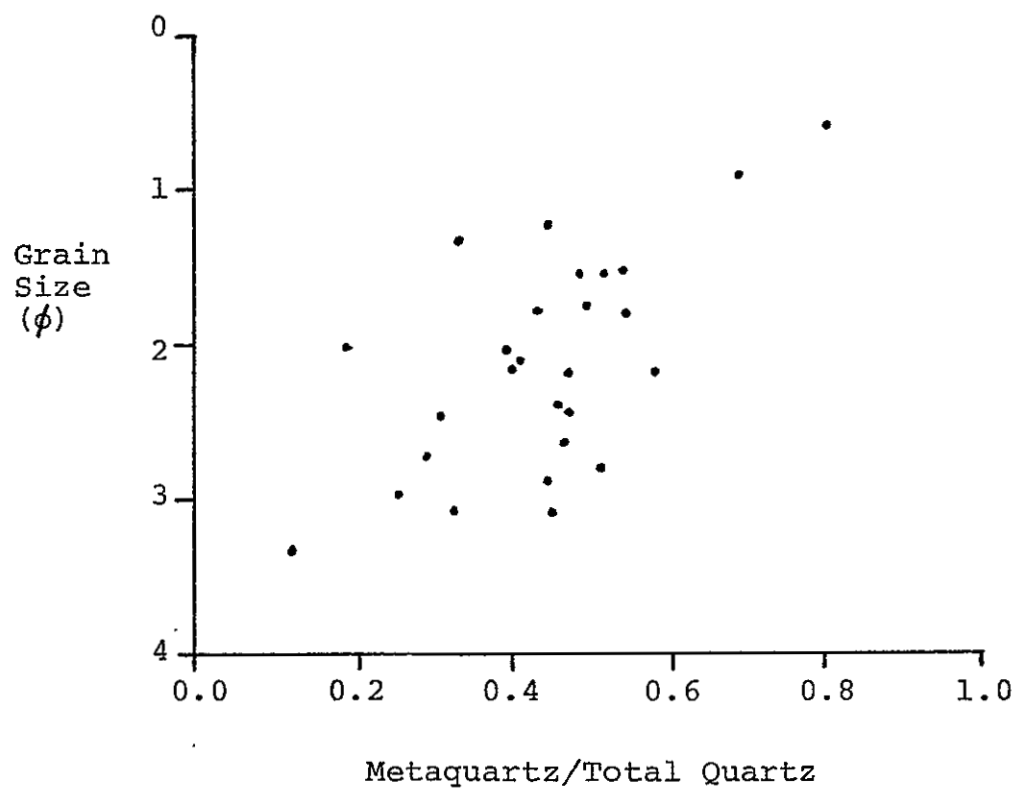


Figure 35. Plot of grain size vs. metaquartz/common quartz for 27 Baca sandstones, showing tendency towards increasing abundances of metaquartz with increasing grain size.

study of quartz from sediments with known source areas, Blatt (1967) states that monocrystalline, strongly undulose quartz grains and polycrystalline grains composed of less than five crystal units are not useful in distinguishing between plutonic and metamorphic source areas. In a similar study, however, Basu and others (1975) found that both degree of polycrystallinity and type of extinction was useful in discriminating source rock types. The abundance of metaquartzite pebbles in the study area implies that a large portion of the quartz in the Baca sandstones was probably derived from a similar lithology. The metamorphic/total quartz ratio appears to increase in the basal portion of the section (Fig. 36).

Feldspar (6-30%, average 14% of framework grains)

Three types of feldspars are present in the Baca sandstones in the study area. These are, in order of decreasing abundance, orthoclase, microcline, and plagioclase. Alteration types include vacuolization, sericitization, cavernous dissolution (Fig. 37), and minor calcitization (Fig. 38). Vacuolization is the most common type of alteration seen in Baca feldspars, and may be produced by surface weathering, hydrothermal alteration, or as inclusions trapped within the crystallizing feldspar.

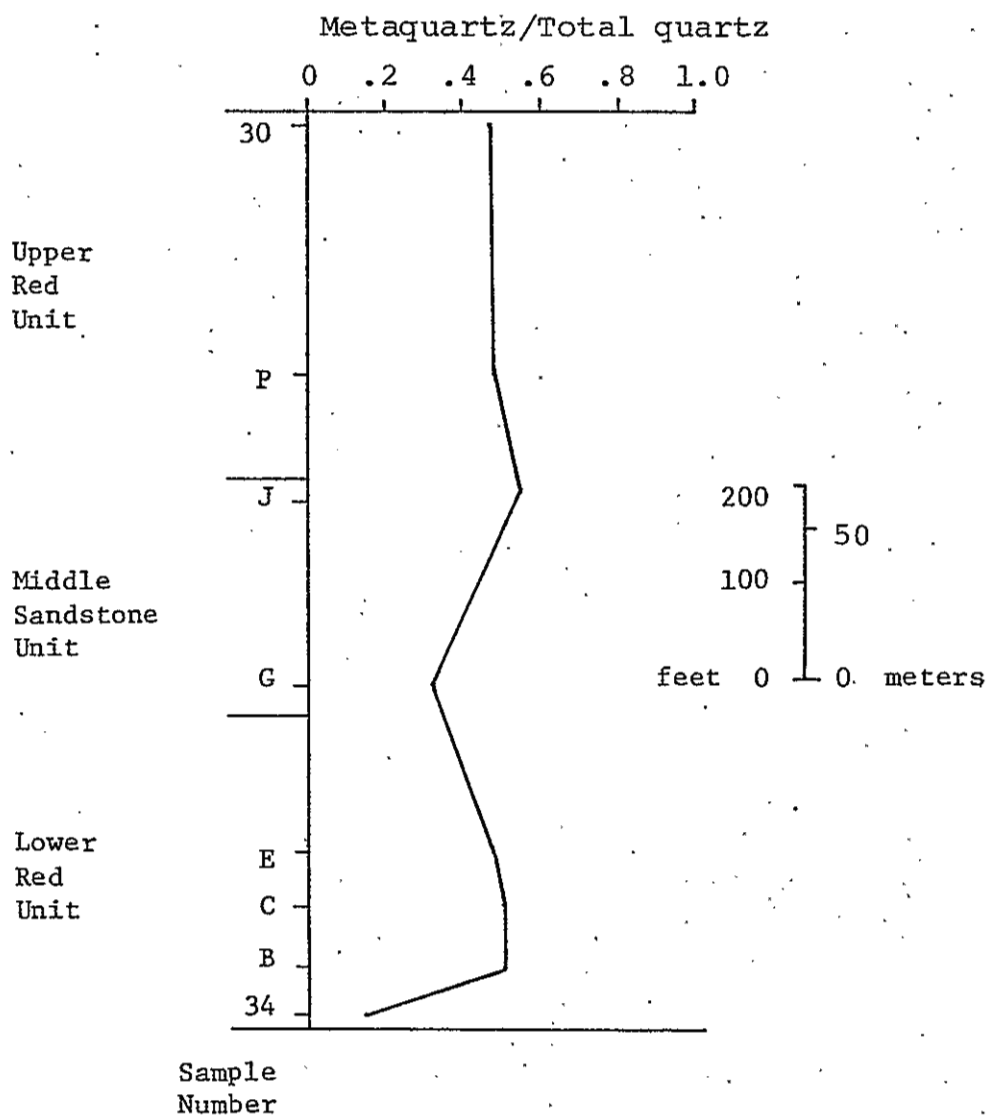


Figure 36. Plot of metaquartz/total quartz ratios as a function of stratigraphic position. Mean grain size ranges between 1.6 and 2.9 ϕ .

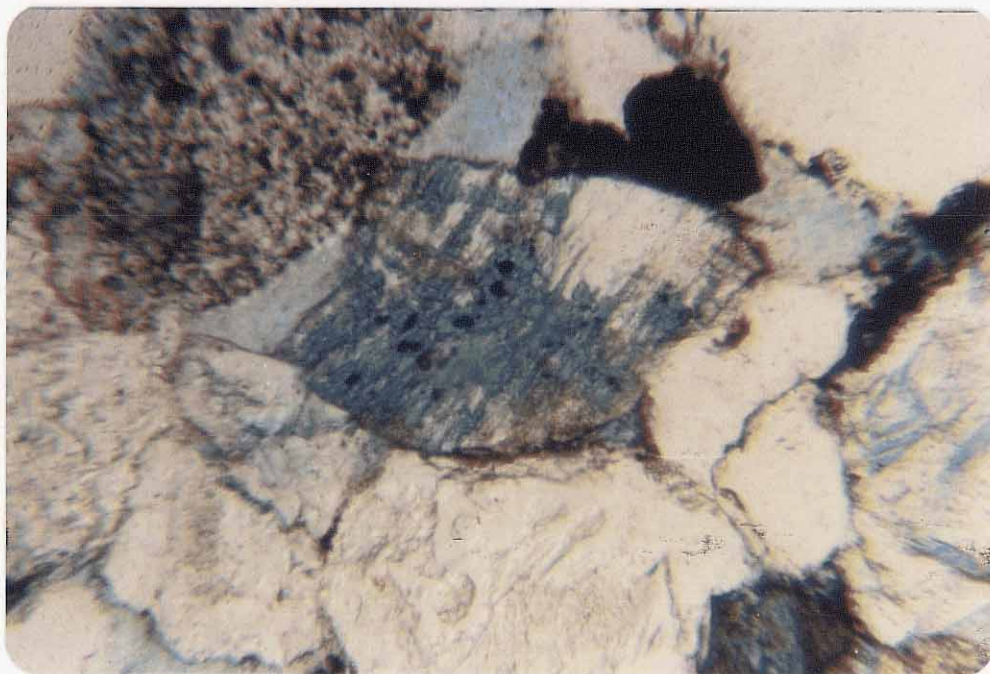


Figure 37. Cavernous dissolution in an orthoclase grain from a fluvial sandstone (sample 48). Secondary porosity within the grain appears blue, due to impregnation of sample with colored epoxy. Plane light, field width=0.75 mm.

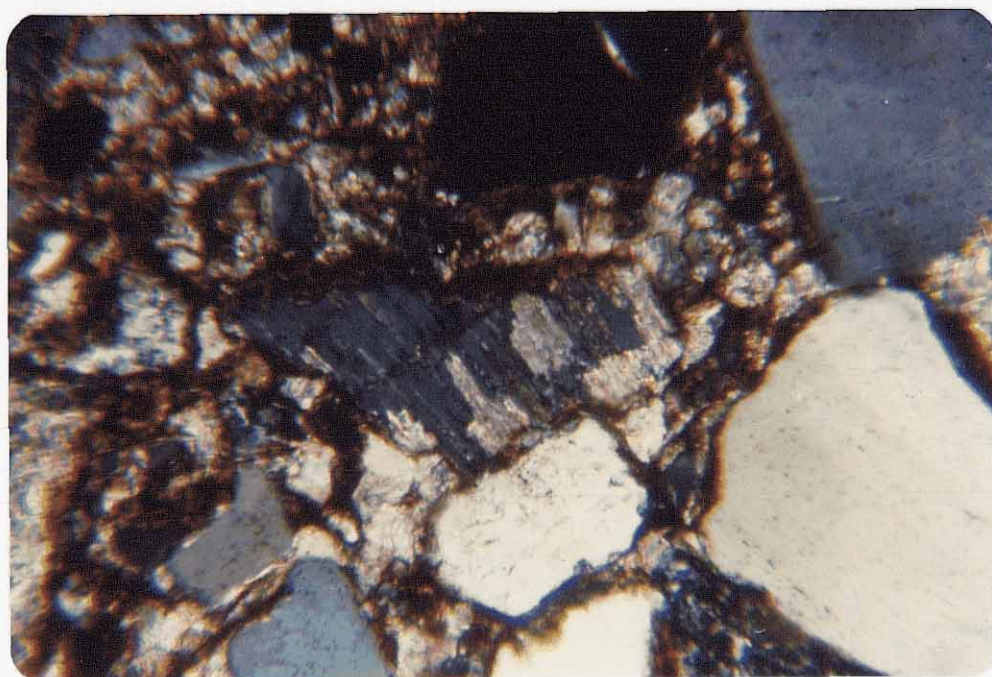


Figure 38. Orthoclase grain being replaced by calcite.
Sample 34, crossed nicols, field width=0.75 mm.

Sericitization is most often the product of hydrothermal alteration, although it may also form under arid or semiarid weathering conditions (Folk, 1974, p. 84). Calcitization takes place through replacement of feldspar by calcite in an alkaline environment. Dissolution porosity within feldspars can form in an acidic environment in soils (Begle, 1978) or in the subsurface, or by decalcitization of calcitized feldspars (Jonas and McBride, 1977). Extent of alteration ranges from unaltered (fresh) to extremely altered, occasionally making recognition of the feldspar type impossible. Degree of alteration is, in part, a function of feldspar composition. Plagioclase is generally the most altered, followed by orthoclase and microcline, which is the least altered. This is consistent with most reports on the relative stabilities of these three feldspar types (Folk, 1974, p. 84).

Alteration of feldspars can take place in several different settings: (a) by deuteric or hydrothermal processes in the source area; (b) in source-area soil zones; (c) in soil zones in the depositional basin; (d) by reaction with groundwaters after burial; and (e) in modern soil zones. One line of evidence suggests that, with the exception of minor vacuolization and sericitization which probably occurred within the source area, the majority of the alteration of Baca feldspars took place post-

depositionally, due to interaction with groundwaters migrating through permeable sandstones. The thin sandstones which represent frontal-splay deposits in the lower portion of deltaic cycles exhibit noncompacted textures and are tightly cemented with fine-grained sparry calcite, and thus indicate cementation within the lacustrine environment or following very shallow burial (see diagenesis section). This very early and complete cementation enables us to view the feldspars and other components of these sandstones as they appeared when they were deposited; the very low permeability inherent from the tightly cemented nature of these sandstones protected the feldspars from the effects of later-diagenetic groundwaters. Feldspars within these sandstones are generally fresh, but sometimes exhibit minor vacuolization and/or sericitization. The abundance of fresh feldspars in the early-cemented Baca sandstones can be explained by erosion, transportation, and deposition in an arid or semiarid climate and/or rapid erosion and burial which would protect feldspars from prolonged exposure to weathering processes (Folk, 1974). However, the intermittent nature of transport implied by the possibly ephemeral Baca braided streams suggests long residence times for sediments within the near-surface fluvial environment, and thus favors the preservation of feldspars by a dry climate.

On the other hand, the sandstones of the upper, non-lacustrine portions of deltaic cycles and of the distal braided alluvial-plain facies were incompletely cemented, which resulted in moderate to high porosities and permeabilities and, thus, favored the utilization of these sandstones as aquifers. Feldspars within these permeable sandstones are almost invariably more altered than those in the previously described tightly cemented sandstones. Degree of alteration ranges from slight to extreme. Alteration types include vacuolization, sericitization, calcitization, and cavernous dissolution. Cavernous dissolution, which produces secondary porosity, is almost entirely restricted to feldspars in the permeable upper-deltaic and fluvial sandstones (see diagenesis section). Feldspars exhibiting secondary porosity occur in the majority of these sandstones.

Feldspars observed in thin section are elongate to subequant, and range in roundness from angular to subrounded. Feldspar content increases upwards in the basal portion of the Baca stratigraphic section, and remains relatively constant throughout the remainder of the section (Fig. 39).

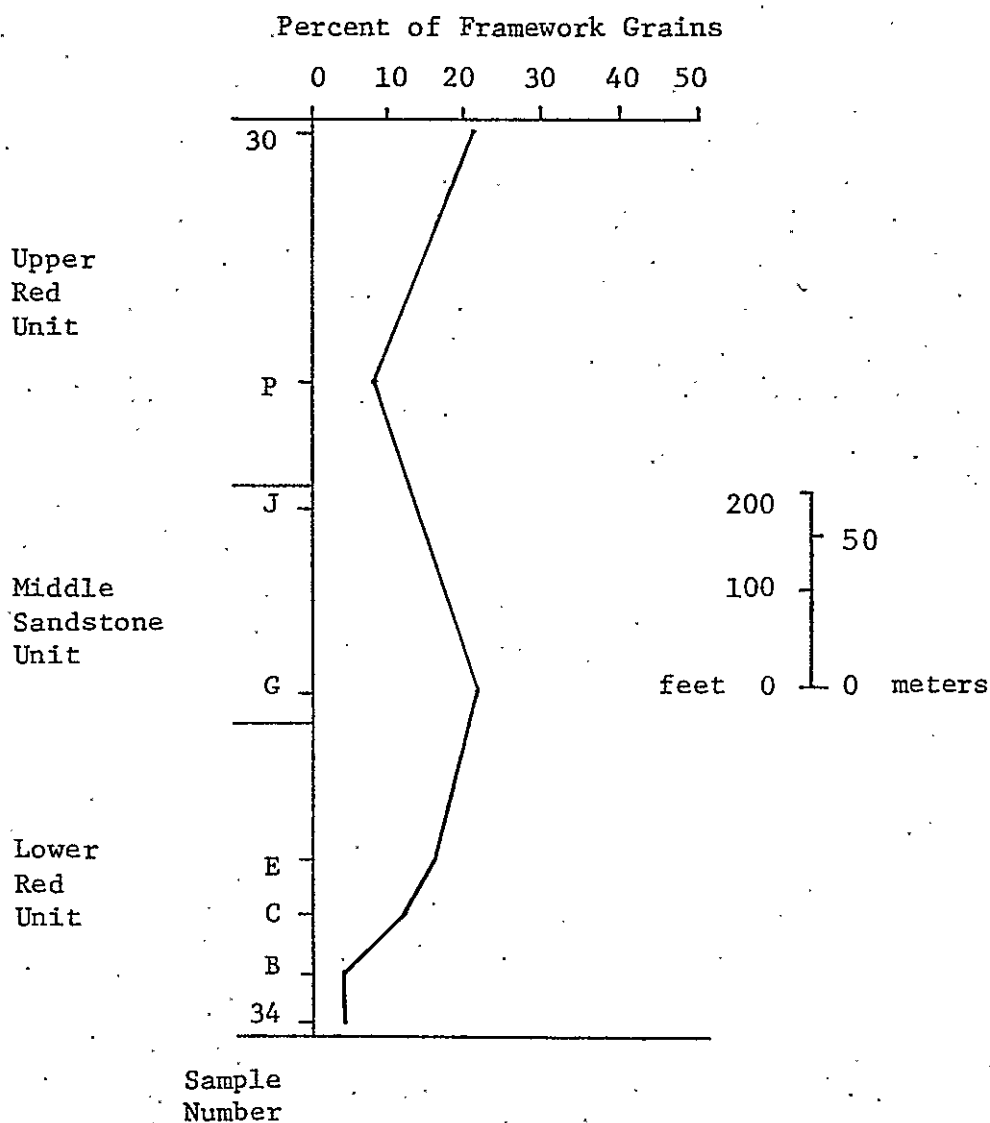


Figure 39. Plot of feldspar abundance as a function of stratigraphic position. Mean grain size of samples ranges between 1.6 and 2.9 ϕ .

Orthoclase (4-23%, average 11% of framework grains; average 74% of total feldspar). Orthoclase is the most abundant feldspar in the Baca sandstones which were examined in thin section. All untwinned feldspars were classified as orthoclase, thus small amounts of untwinned plagioclase and microcline may have been included in this category. Due to its availability, orthoclase is the most common feldspar in terrigenous sandstones, despite the fact that microcline is generally more resistant to alteration (Folk, 1974). Granites and gneisses are the primary source rocks for orthoclase.

Microcline (0-10%, average 3% of framework grains; average 21% of total feldspar). Microcline was present in all except one of the sandstone thin sections examined. Despite its relatively high stability, microcline is always less abundant than orthoclase, even in highly altered Baca sandstones. Microcline is dominantly derived from plutonic, pegmatite, and gneissic source rocks (Folk, 1974).

Plagioclase (0-3%, average 1% of framework grains; average 5% of total feldspar). Plagioclase is present in about half of the sandstones which were examined petrographically. It is evenly distributed throughout the Baca stratigraphic section, which suggests that the plagioclase

was not derived from contemporaneous, sporadic supply of airborne volcanic ejecta by Eocene volcanic centers to the south. Instead, it was probably derived from older volcanic and/or plutonic rocks exposed in the source area. The widespread occurrence of minor amounts of volcanic rock fragments throughout the Baca stratigraphic section suggests a largely volcanic source for the plagioclase.

Rock Fragments (8-29%, average 20% of framework grains)

Rock fragments present in the Baca sandstones include (in order of decreasing abundance) metamorphic, chert, mudstone, granite/gneiss, volcanic, carbonate, siltstone and sandstone rock fragments. Most rock-fragment varieties decrease in abundance with decreasing sandstone grain size.

Metamorphic Rock Fragments (2-20%, average 10% of framework grains). Two major types of metamorphic rock fragments were observed. The first, and most common, consists of strongly undulose, often composite, quartz which contains numerous aligned muscovite crystals (Fig. 40). Fragments of this type were probably derived from Precambrian micaceous metaquartzites in the source area. The major other type of metamorphic rock fragment is



Figure 40. Quartzose metamorphic rock fragment. Note abundant inclusions of muscovite. Sample 48, crossed nicols, field width=0.75 mm.

composed of aligned illite and fine-grained muscovite crystals interspersed with small amounts of silt-sized quartz (Fig. 41). These rock fragments often show evidence of ductile deformation by adjacent framework grains during compaction. Fragments of this type were derived from low-rank, metamorphic rocks, such as argillites and phyllites. Argillaceous metamorphic rock fragments were distinguished from mudstone rock fragments by the more coarsely crystalline and generally better-oriented nature of their argillaceous and micaceous components, and by the lack of red coloration that is characteristic of most Baca mudstone fragments.

Metamorphic rock fragments from the Baca Formation in the study area were derived predominantly from micaceous metaquartzites and, to a lesser extent, from phyllites and argillites. However, due to the effects of abrasion during transport on the soft, low-rank metamorphic rock fragments, the contribution of detritus by argillites and phyllites to the Baca-Eagar basin was probably much larger than would be assumed by examination of the sandstones in the study area. The abundance of metamorphic rock fragments increases upward through the basal portion of the Baca stratigraphic section, and remains relatively constant throughout the remainder of the section (Fig. 42).

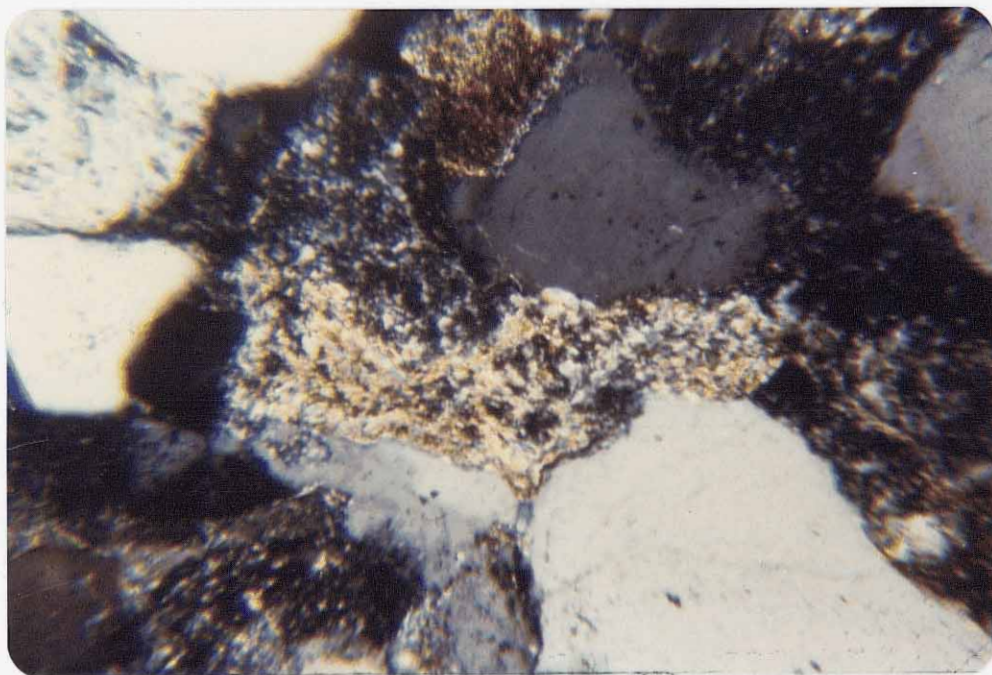


Figure 41. Argillaceous metamorphic rock fragment which has been ductilely deformed by adjacent grains during compaction. Sample C, crossed nicols, field width=0.75 mm.

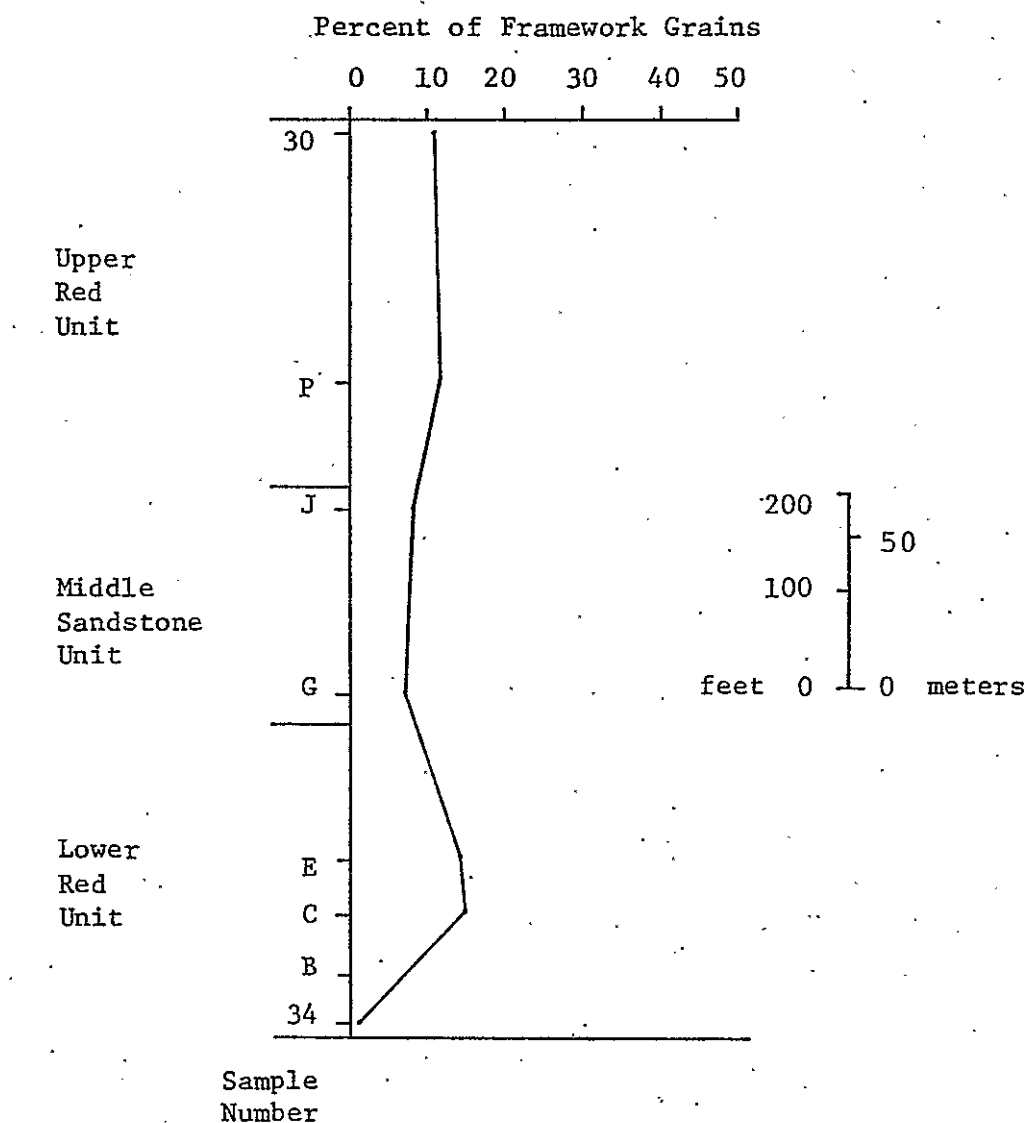


Figure 42. Plot of abundance of metamorphic rock fragments as a function of stratigraphic position. Mean grain size ranges between 1.6 and 2.9 ϕ .

Chert (1-17%, average 4% of framework grains).

Chert (Fig. 43) is a relatively minor constituent of the Baca sandstones in the study area, but it was present in every thin section that was examined. Grains consisting of microcrystalline quartz averaging less than 20 microns in diameter were classified as chert; finely crystalline quartz grains whose average crystal diameter was greater than 20 microns were counted as metamorphic quartz. There appears to be a gradation between chert and finely crystalline metamorphic quartz in the sandstones studied, which may indicate that some of the metamorphic quartz was derived from meta-cherts. Chert is always of sedimentary origin (Folk, 1974), but may be primary (e.g. derived from a silicified limestone) or reworked from an older sandstone. Detrital chalcedony was also present in the Baca sandstones in trace amounts. Approximately half of this chalcedony is length-slow, which is indicative of formation in an alkaline, sulfate-rich environment (Folk and Pittman, 1971). Chert abundance decreases upwards in the basal portion of the Baca stratigraphic section in the study area, and remains relatively constant throughout the remainder of the section (Fig. 44).

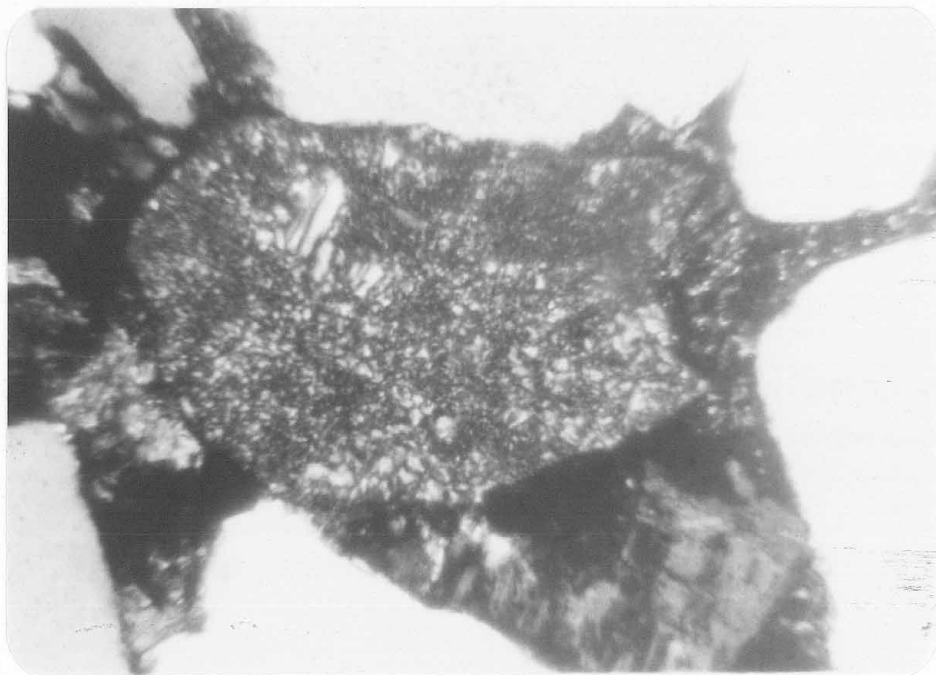


Figure 43. Chert grain. Sample A, crossed nicols, field width=0.75 mm.

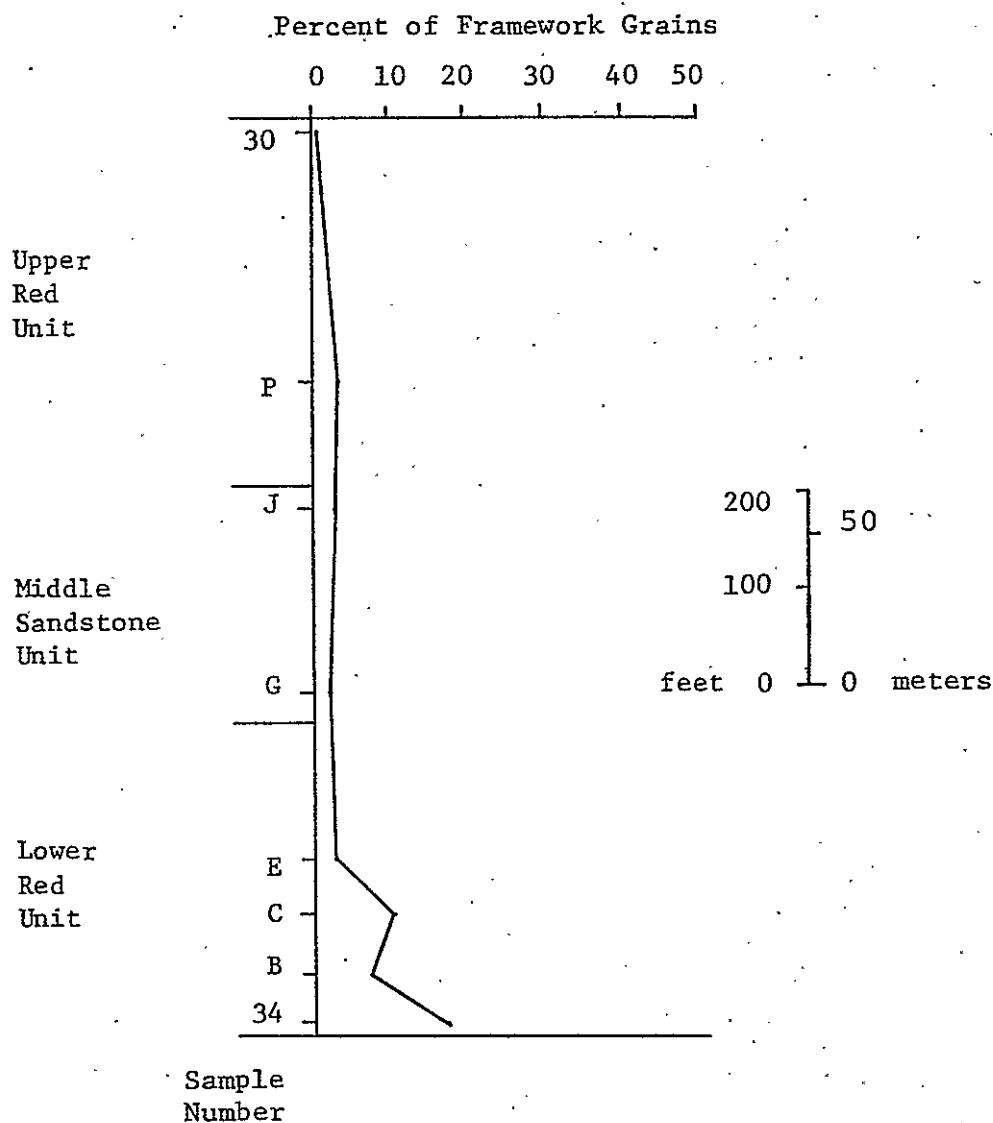


Figure 44. Plot of chert abundance as a function of stratigraphic position. Mean grain size ranges between 1.6 and 2.9 ϕ .

Granite and Gneiss Rock Fragments (0-7%, average 1% of framework grains). These rock fragments consist of varying proportions of feldspar and quartz. Feldspar types include orthoclase and microcline. Quartz may exhibit straight to strongly undulose extinction. The majority of the granite/gneiss rock fragments consist predominantly of one mineral, such as a grain containing a large crystal of orthoclase and a smaller one of quartz. Types and occurrence of alteration within component feldspar crystals are exactly the same as those described previously for feldspar grains.

The relative importance of contributions from granitic versus gneissic sources is difficult to determine. The occurrence of minor amounts of granite pebbles in the Baca imply that at least some of the granite/gneiss rock fragments were derived from a granitic source. Granite/gneiss rock fragments and the remainder of the rock fragments which will be subsequently discussed are present in such small quantities that I do not feel it would be meaningful to make any statements concerning vertical trends in their abundance.

Volcanic Rock Fragments (0-6%, average 1% of framework grains). Volcanic rock fragments are a widespread, but minor, component of the Baca sandstones in

the study area. They occurred in about one-half of the thin sections examined. Grains counted as volcanic rock fragments range in appearance from dark, aphanitic grains containing lath-shaped plagioclase crystals (Fig. 45) to grains which are similar to, and often difficult to distinguish from, chert (see Folk, 1974, p. 81). The chert-like rock fragments were probably derived from silicified volcanic rocks (R. L. Folk, 1979, oral commun.), however, the classification of many of these grains is equivocal.

The presence of only minor amounts of volcanic-derived detritus in the Baca sediments in the study area has some important implications concerning the geometry of the southeastern margin of the Baca-Eagar basin (C. E. Chapin, 1980, oral commun.). During the Laramide, the area adjacent to this portion of the basin was the site of widespread volcanism and plutonism. The fact that only small amounts of volcanic material were incorporated into the Baca sediments in the eastern part of the outcrop belt implies the existence of a drainage divide (herein termed the Morenci uplift; see tectonic framework section) basinward of the Laramide volcanic centers in southwestern New Mexico. The non-peaked stratigraphic distribution of volcanic rock fragments in the Baca suggests that these fragments were derived from older volcanic rocks (Precambrian?) in the

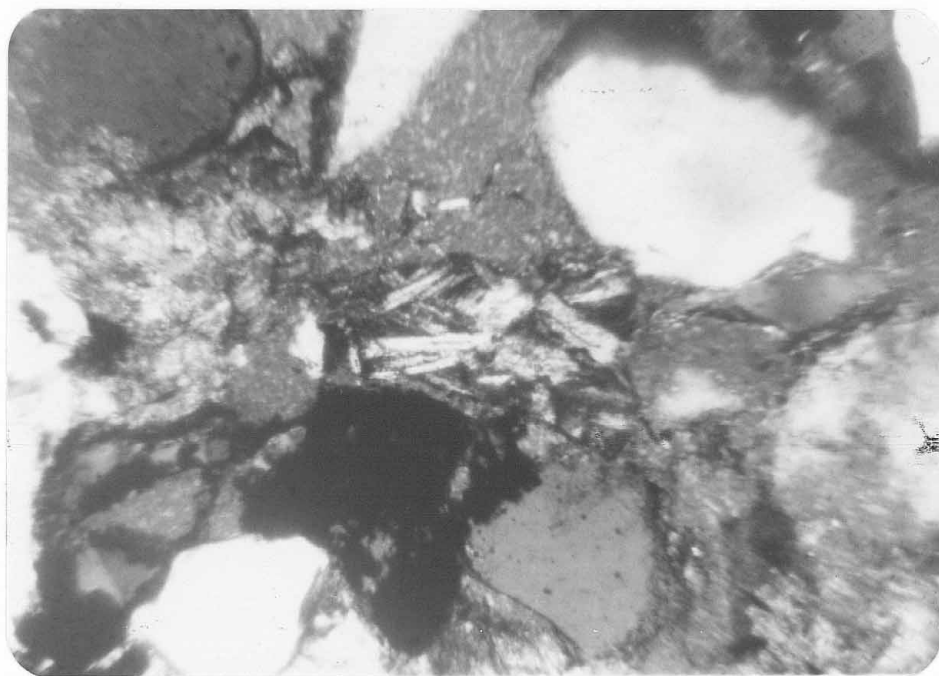


Figure 45. Volcanic rock fragment showing lath-like plagioclase crystals in dark, aphanitic ground-mass. Sample 45, crossed nicols, field width = 0.75 mm.

source area, and not by sporadic airborne supply to the basin by Eocene volcanic centers to the south. Cameron and Blatt (1971) show that felsic-silicic volcanic rock fragments can endure several hundred miles of braided-stream transport without a significant reduction in their abundance, which implies that abrasion during transport cannot account for the nearly complete lack of volcanic detritus in the eastern portion of the basin. Thus, the small percentage of volcanic rock fragments in the Baca sandstones in the study area suggests that volcanic rocks were a relatively minor lithology in the source area during Laramide time.

Mudstone Rock Fragments (0-5%, average 2% of framework grains). Mudstone rock fragments occur in about one-half of the thin sections examined. They are usually red (due to hematite pigmentation) and may contain significant amounts of quartz and feldspar silt. When not masked by red coloration, the component clays generally show yellowish birefringence and an index higher than balsam, which is characteristic of illite (Folk, 1974, p. 91). Some mudstone rock fragments exhibit evidence of ductile squashing by adjacent grains during compaction.

The red coloration of the mudstone rock fragments indicates derivation from a redbed source, such as the Permian Abo Formation or the Triassic Chinle Formation, or penecontemporaneous reworking of Baca mudstones. The soft, easily abraded nature of these fragments suggests short distances of transport and, thus, favors derivation from intraformational sources.

Sandstone and Siltstone Rock Fragments (0-2% of framework grains). These rock fragments are generally present in trace amounts and were observed in about one-fourth of the thin sections examined. A complete gradation in size of component detrital grains exists between both types of these rock fragments. Sandstone and siltstone rock fragments are highly quartzose but may contain minor amounts of orthoclase. Grains within these fragments are tightly cemented with syntaxial quartz; the original detrital grains are sometimes vacuolized, which facilitates distinguishing between grains and cement. Sandstone and siltstone rock fragments were derived from older sedimentary rocks in the source area. The highly quartzose, silica-cemented nature of these rock fragments precludes the possibility of an intraformational source.

Carbonate Rock Fragments (0-8%, average 1% of framework grains). Carbonate rock fragments were present in about one-third of the sandstone thin sections examined. They often are stained red by hematite and are dominantly composed of well-sorted, subequant sparry calcite crystals averaging about 10-15 microns in diameter. Carbonate rock fragments are more abundant in lower-delta sandstones than elsewhere. This, in addition to the fact that the calcite in these fragments closely resembles the early-diagenetic lacustrine carbonate cements (see diagenesis section), suggests that many of the carbonate rock fragments were penecontemporaneously derived from within the lacustrine basin, and therefore are more properly termed "intraclasts" (Folk, 1974, p. 160). The presence of probable Paleozoic limestone pebbles in the Baca, however, implies that these carbonate rock fragments were, in part, derived from older limestones exposed in the source area.

The presence of trace amounts of oolites (Fig. 46) was noted in several of the thin sections. The oolites average about 0.3 mm in diameter. They are usually complete and show little or no effects of abrasion during transport, which indicates that the oolites were locally derived. The sporadic occurrence of oolites in both deltaic and fluvial sandstones implies that the oolites were not formed in situ, but were probably derived intraformationally and transported

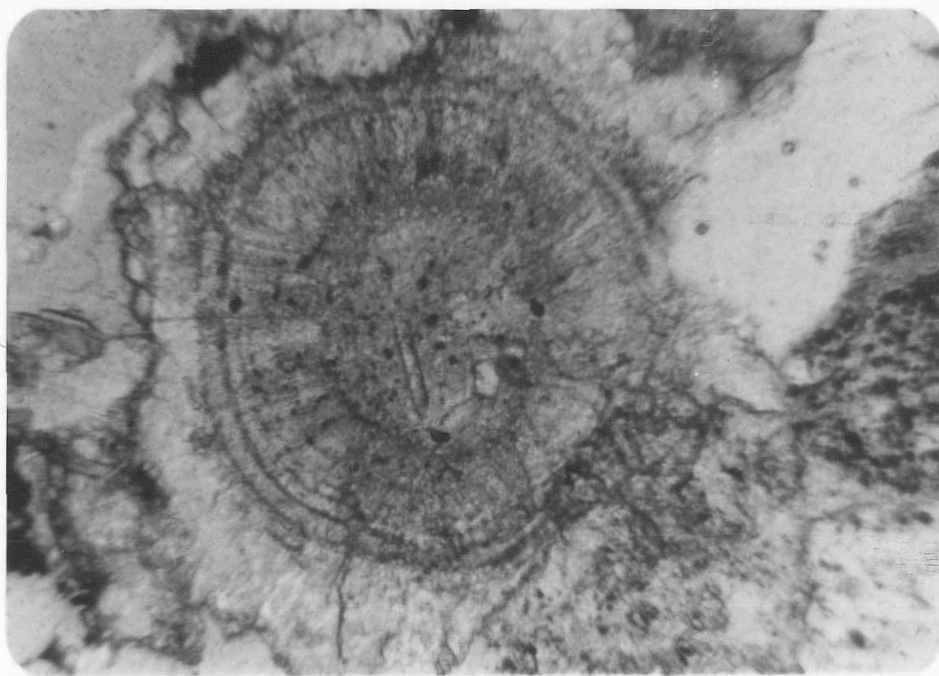


Figure 46. Well-developed oolite in an upper-delta sandstone. Note both concentric and radial structures. Sample 73, plane light, field width=0.75 mm.

a short distance prior to deposition. Oolites form in current- or wave-agitated, carbonate-rich environments, and have been noted in modern lakes, such as the Great Salt Lake, Utah (Sandberg, 1975), and in ancient lake deposits (Swirydczuk and others, 1979). The composition of oolites can be initially either calcite or aragonite, however, aragonite inverts relatively rapidly to calcite. Assereto and Folk (1976) state that square-ended rays in pisolites indicate an initial aragonitic composition. No square-ended rays were seen in the few oolites which were available for petrographic examination, but, due to the lack of sufficient quantities of oolites which could be inspected, I do not feel that an initial aragonitic composition can be ruled out.

Heavy Minerals (trace)

Heavy minerals were generally present in trace amounts (<1%) within the Baca sandstone thin sections, although abundances of as much as several percent were occasionally observed within placers. Petrographic examination of six heavy-mineral grain mounts revealed the presence of the following species (in order of decreasing abundance): magnetite/ilmenite/specular hematite, leucoxene, zircon, garnet, apatite, biotite, and muscovite.

Magnetite, ilmenite, and specular hematite were not differentiated. The majority of the heavy minerals range in size from 0.1 to 0.2 mm.

The relative abundance of several of the heavy mineral species (magnetite, ilmenite, specular hematite, and leucoxene) appears to be a function of the degree and type of alteration of their host sandstone. Magnetite, ilmenite, and specular hematite are the most abundant types of heavy minerals present in the relatively little-altered, red Baca sandstones, usually comprising about 90 percent of the heavy mineral fraction (Fig. 47). However, the yellow to gray Baca sandstones, which show evidence for the passage of negative-Eh groundwaters (see diagenesis section), contain little or none of these minerals. Instead, the yellow to gray sandstones contain abundant leucoxene (which is present only in minor amounts in the red sandstones) (Fig. 48), which was presumably produced as an alteration product of ilmenite. A heavy-mineral suite from one yellow-sandstone sample (54) showed subequal proportions of magnetite/ilmenite/specular hematite and leucoxene. This incomplete removal of magnetite/ilmenite/specular hematite indicates a lesser degree of negative-Eh alteration of the host sandstone, which probably took place by either the passage of a smaller volume of reducing groundwater through the rock, or by interaction with more mildly reducing



Figure 47. Typical heavy-mineral grain mount from a red Baca sandstone (sample 48). Note dominance of magnetite/ilmenite/specular hematite. White grains are leucoxene. Field width=0.8 mm.

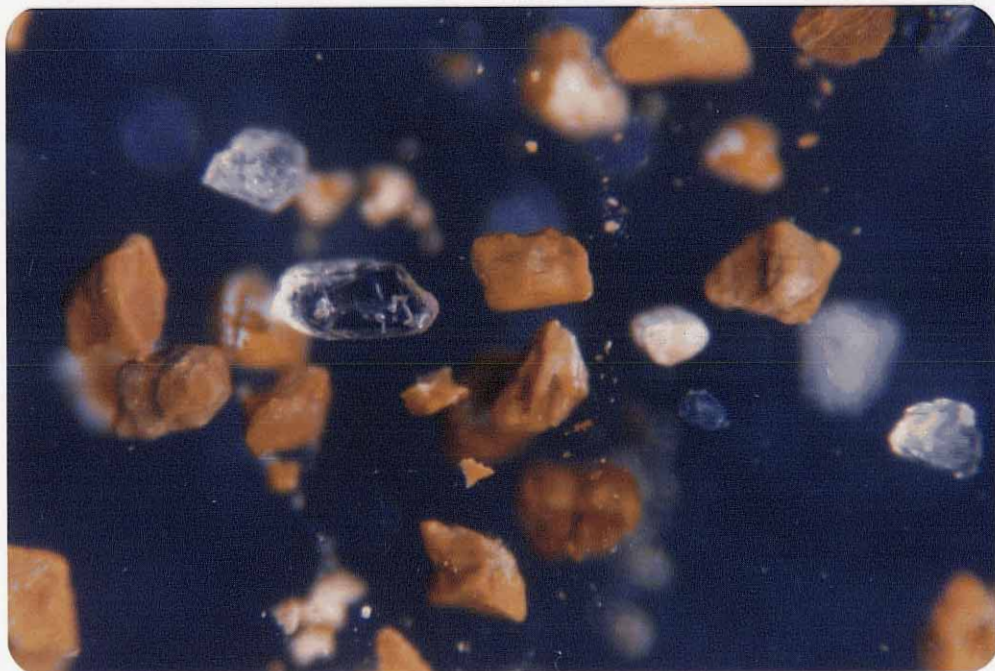


Figure 48. Typical heavy-mineral suite from a yellow Baca sandstone (sample 56), showing dominance of limonite-stained leucoxene grains. Note sub-hedral zircon grain. Field width=0.8 mm.

groundwaters. The common occurrence of abundant magnetite and ilmenite in red sediments and the near or complete absence of these minerals in non-red areas within, or intercalated with, redbeds was noted by Miller and Folk (1955), who conclude that the lack of magnetite and ilmenite in the non-red portions of redbed sequences is due to their removal by dissolution in a reducing environment. In summary, the heavy-mineral suite of the red Baca sandstones is dominated by magnetite/ilmenite/specular hematite, whereas that in the yellow to gray sandstones are generally dominated by leucoxene.

Compared with the above-described minerals, the volumetric importance of the remaining heavy minerals is minor. Zircon was present in all of the heavy-mineral grain mounts. It exhibits extreme relief, usually clear to slightly pinkish color, and ranges from well rounded to euhedral in shape. Mica types include biotite and muscovite. Flakes of both varieties usually show ragged, abraded edges, but a few of the biotite grains exhibited hexagonal outlines (Fig. 49). Euhedral biotite is most commonly derived from volcanic rocks (Folk, 1974, p. 88). Apatite grains are usually clear, exhibit low relief, and range from subhedral to euhedral in shape. Garnets are clear to pink in color, commonly exhibit well-developed conchoidal fractures, and are most often anhedral to

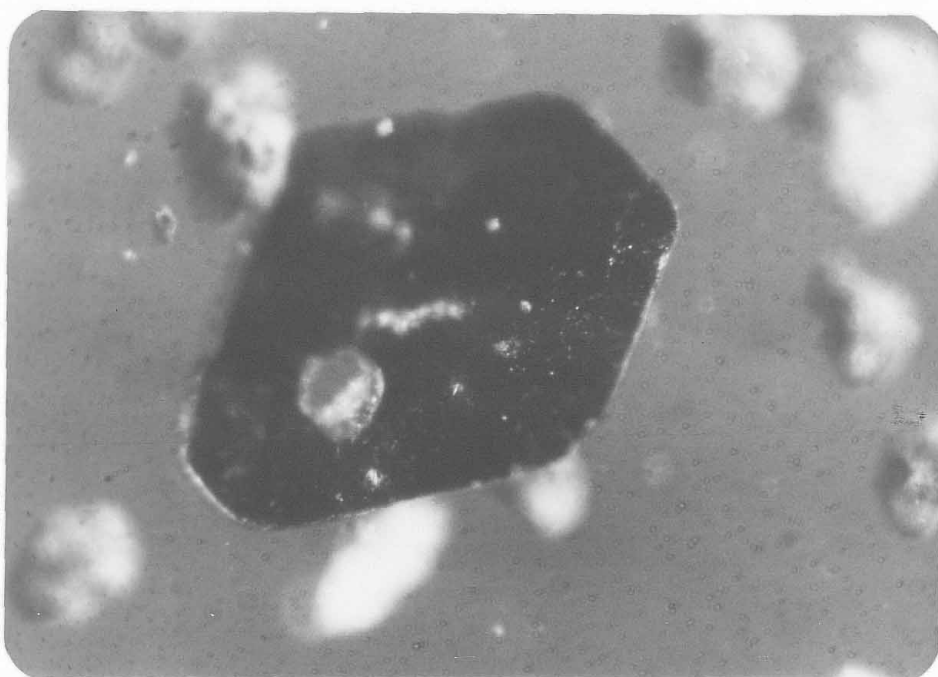


Figure 49. Hexagonal biotite observed in a heavy-mineral grain mount from sample 48. Width of field = 0.75 mm.

subhedral in shape. Garnets from one of the kaolinite-cemented sandstone samples (51) exhibit crystallographically controlled, etched surfaces. Both precipitation of authigenic kaolinite and the dissolution of garnet take place in an acidic environment, as will be further discussed in the diagenesis section.

Mudstone Petrology

Baca mudstones in the study area are generally red in color, devoid of sedimentary structures except occasional poorly developed burrows, and commonly contain appreciable amounts of silt. Mudstones dominantly occur in the basinal lacustrine facies and in the lower prodelta portion of fine-grained lacustrine deltas; their occurrence in the distal braided alluvial plain facies and the upper portion of lacustrine deltas is rare and limited to thin, discontinuous mud-drape deposits. Prodelta and basinal mudstones, except for those in the lowermost portion of the upper red unit, are generally highly calcareous. Calcite content, as determined by weighing crushed samples before and after acidization with cold, dilute hydrochloric acid, ranges between 10 and 15 percent by weight, with the exception of the basal mudstone in the upper red unit, which contains about two percent calcite. The thin mudstones

which represent mud-drape deposits are usually noncalcareous. The red coloration, typical of most Baca mudstones, was probably produced diagenetically, as will be discussed in a later section.

Six thin sections of Baca mudstones from the study area were examined. Most contained appreciable (as much as 30 percent) quartz and feldspar silt. All lacustrine mudstone thin sections exhibited, to varying degrees, a churned and disrupted texture (Fig. 50) which was probably produced by bioturbation. This explains the general lack of sedimentary structures in the Baca mudstones and suggests that the lake-bottom muds were oxygenated, which supports a polymictic regime for the Baca lacustrine system. Carbonates within lacustrine mudstones usually occur as homogeneously distributed, small (10-15 micron), subequant crystals of calcite spar. This calcite is similar in appearance to that observed in the loosely packed, tightly cemented frontal-splay sandstones which are intercalated with the lacustrine mudstones. These cements formed very early in the diagenetic history of the Baca lacustrine sediments, and will be further discussed in the diagenesis section. Another mode of occurrence of calcite was observed in one lacustrine-mudstone thin section (sample 8). This sample contained large void spaces (as much as 1.5 mm in diameter) which were subsequently filled with large crystals

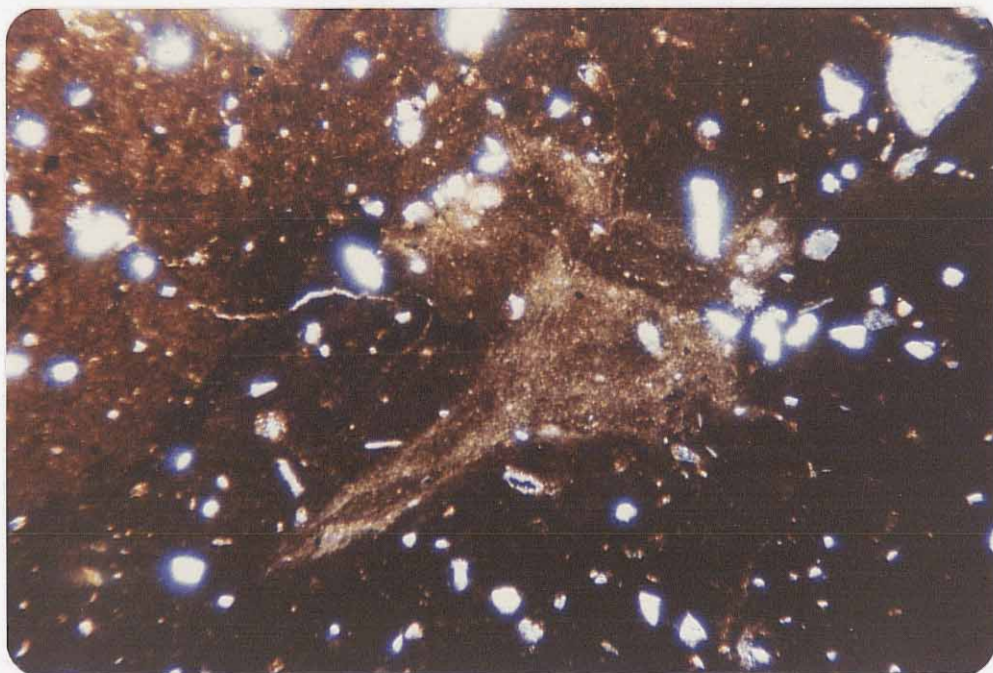


Figure 50. Churned, disrupted texture typical of Baculacean lacustrine mudstones, which was probably produced by intense bioturbation. Sample F, crossed nicols, field width=3.0 mm.

of sparry calcite (Fig. 51). Many of these void spaces are filled with a single, large crystal of spar. These features are reminiscent of "bird's-eye structures" in limestones (Folk, 1959). The presence of large, spar-filled voids implies very early cementation (prior to compaction) of the mudstone; cementation must have occurred in the lacustrine environment or upon very shallow burial. Similar features have been reported by Van Houten (1962) in the red lacustrine mudstones of the Upper Triassic Lockatong Formation of west-central New Jersey and adjacent Pennsylvania.

When not masked by hematite stain, the clays in the Baca mudstones from the study area generally exhibit yellowish birefringence and have an index greater than balsam, which is characteristic of illite (Folk, 1974, p. 91). X-ray diffraction data for the clay-size fraction of six Baca mudstone samples indicates the presence of illite with minor amounts of montmorillonite and kaolinite. Similar compositions for Baca clays in the Gallinas Mountains area have been reported by Johnson (1978, p. 99). Argillaceous Precambrian rocks exposed in that portion of the Sierra-Sandia uplift now comprised by the Magdalena Mountains (Sumner, 1980) and were probably a major contributor of illite to the Baca lacustrine system in the Bear-Gallinas Mountains vicinity. See Johnson (1978) for

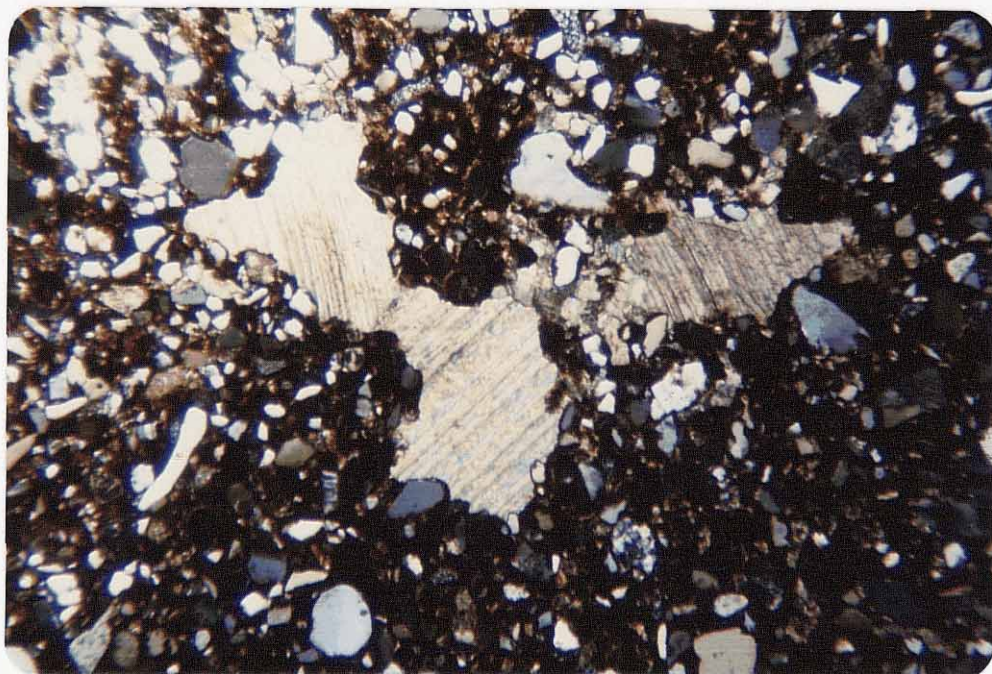


Figure 51. Large, spar-filled void spaces in a sandy lacustrine mudstone (sample 8), which are indicative of very early, pre-compactional cementation. Crossed nicols, field width= 3.0 mm.

more information concerning the distribution of clay types throughout the Baca-Eagar outcrop belt.

PROVENANCE

The occurrence of large amounts of metamorphic- and igneous-derived detritus in both Baca conglomerates (metaquartzite, granite, schist) and sandstones (metamorphic quartz, orthoclase, microcline, metamorphic rock fragments, granite and gneiss rock fragments) indicates that a large portion, possibly the majority, of the Baca sediments in the study area were supplied by a Precambrian source terrane, although some was undoubtedly derived from older sedimentary rocks containing Precambrian detritus. The red coloration of the majority of the Baca sediments and the abundance of detrital ilmenite and magnetite in these sediments indicate that much of the Baca detritus was not recycled from older sediments but must have been derived from a metamorphic or igneous source (Miller and Folk, 1955). Minor occurrences of plagioclase, volcanic rock fragments, and euhedral biotite imply that volcanic rocks made small contributions to the Baca sediments. The presence of significant amounts of detritus derived from sedimentary rocks in both the Baca conglomerates (chert, limestone, sandstone, siltstone, mudstone) and sandstones (chert, carbonate rock fragments, sandstone, siltstone, and mudstone rock fragments) indicate both extraformational and intraformational sedimentary sources.

There is much evidence to suggest the progressive "unroofing" of a Precambrian plutonic and metamorphic source area during Baca time. The upward increase in feldspar, metamorphic rock fragments, and metamorphic/total quartz ratios within the basal portion of the Baca stratigraphic section, and the coincident decrease in the abundance of chert upward through the same interval (Fig. 52), strongly suggests the diminishing importance of older sedimentary sources during early Baca time. I can envision no mechanism, whether pre- or post-depositional, which can explain the observed upsection changes in mineralogy of the Baca sandstones except for increasing contributions by Precambrian plutonic and metamorphic terranes, at the expense of sedimentary sources, during basal Baca sedimentation in the study area. Interestingly, point counts made by the writer on five thin sections from G.L. Massingill's (1979) Baca Formation measured section near the Bear Mountains show similar upsection changes (Fig. 53). However, due to the greater variability in thin-section grain size and the utilization of only five thin sections from the Bear Mountains stratigraphic section, I feel that the data in Figure 53 should be interpreted somewhat cautiously.

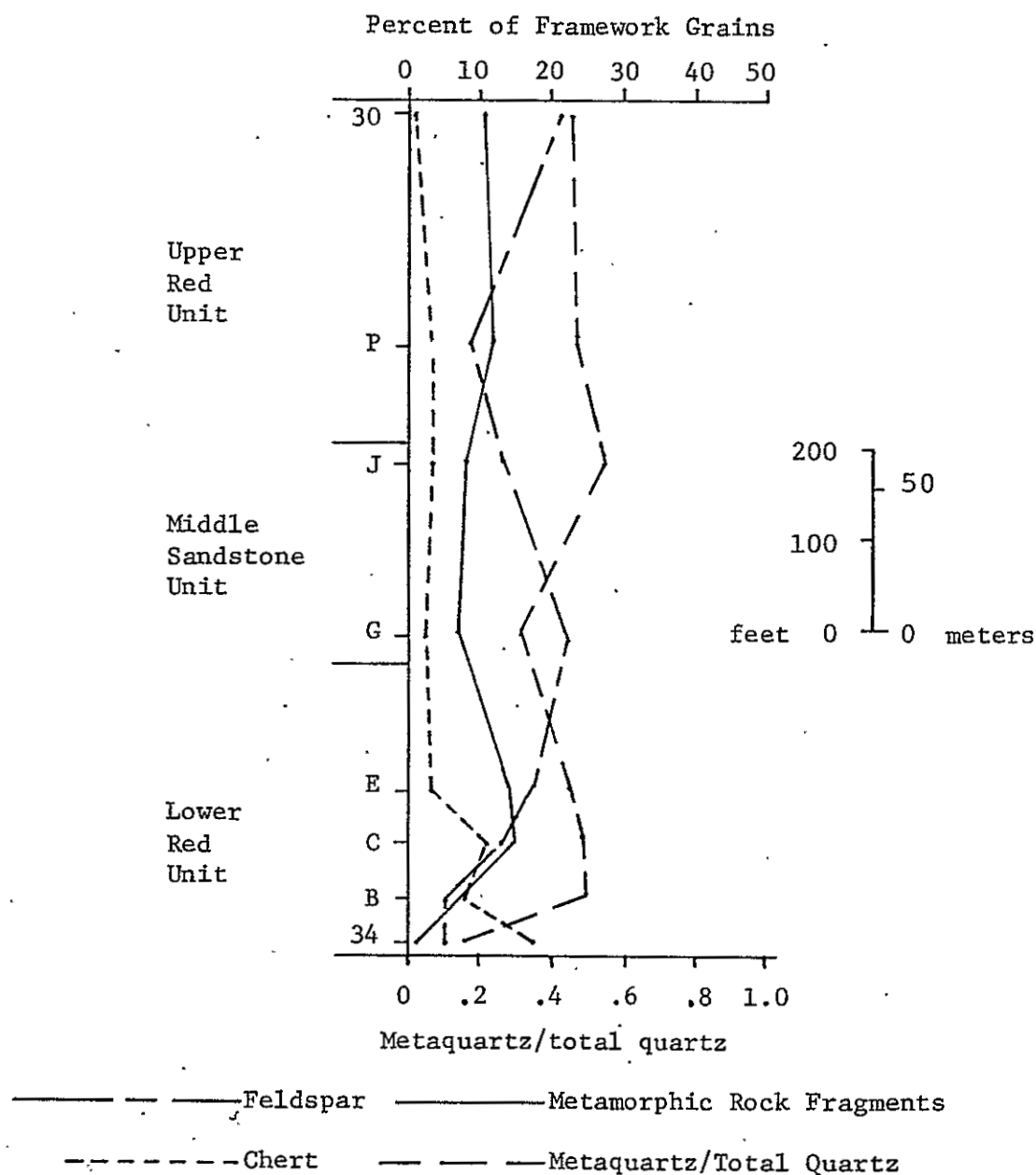


Figure 52. Plot of metaquartz/total quartz ratios and abundances of feldspar, chert, and metamorphic rock fragments within Baca sandstones as a function of stratigraphic position. Samples were taken from a section measured by the writer in the study area. Mean grain size of the sandstones ranges between 1.6 and 2.9 ϕ .

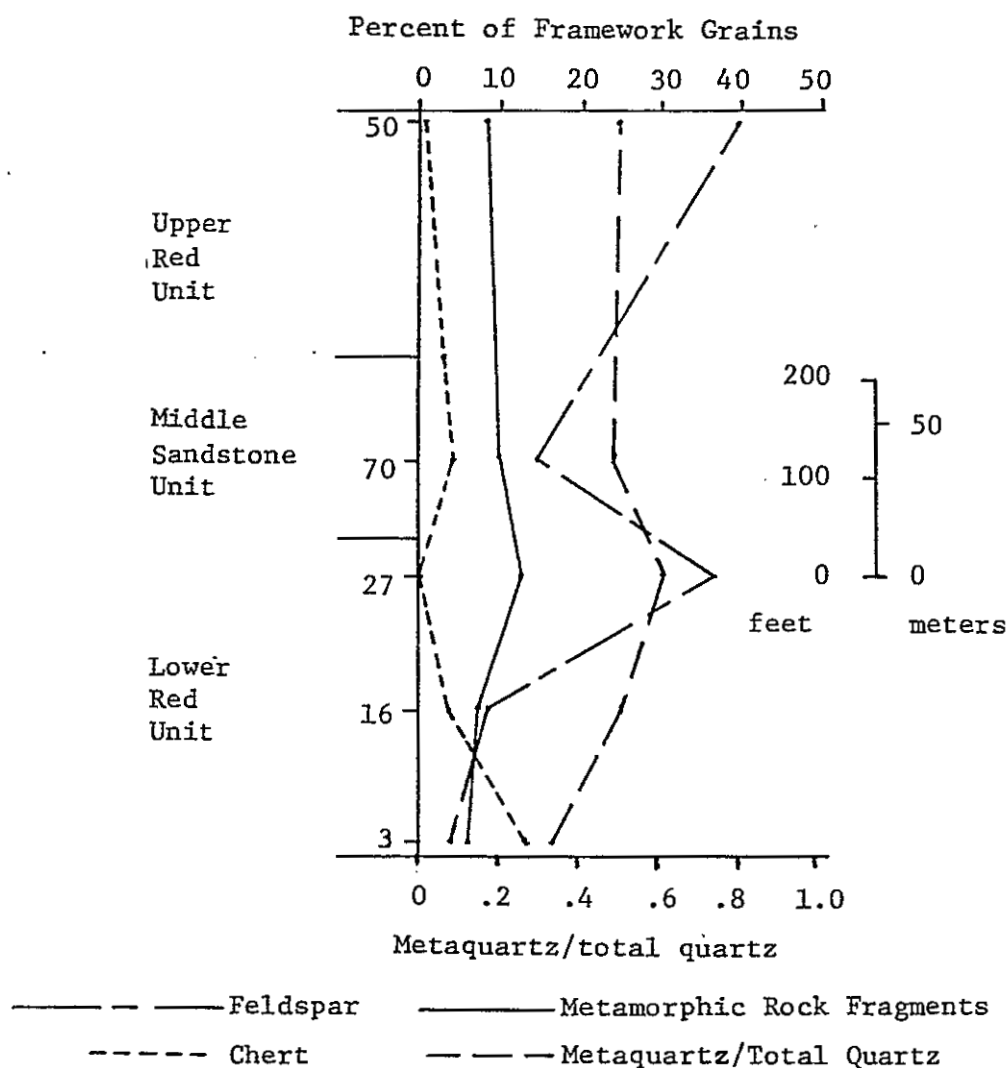


Figure 53. Plot of metaquartz/total quartz ratios and abundances of feldspar, chert, and metamorphic rock fragments within Baca sandstones as a function of stratigraphic position. Samples were taken from Massingill's (1979) measured section in the Bear Mountains vicinity. Mean grain size varies widely, therefore caution is advised in the interpretation of this data.

DIAGENESIS

Cements

Four types of cements occur within the Baca sedimentary rocks in the study area. These are (in order of decreasing abundance) calcite, kaolinite, quartz, and dolomite.

Calcite (0-48%, mean 18%, median 12% of bulk rock volume)

Authigenic calcite is the most abundant and earliest cementing agent in the Baca sediments in the study area. There are three modes of occurrence of calcite in the thin sections: finely crystalline spar which is associated with lacustrine prodelta and basinal sediments, large, blocky, pore-filling calcite crystals dominantly occurring in upper-delta and braided alluvial-plain sandstones, and caliche. Caliches are scarce, but widespread, within the Baca. They occur as thin, laterally persistent, often nodular horizons within both lacustrine and non-lacustrine sediments. Caliches within lacustrine rocks presumably represent soils which developed during lake-level low stands. A laterally continuous zone of rhizoconcretions (calichified root tubes) (Fig. 54) is present in the basal



Figure 54. Well-developed calichified paleosol showing numerous tube-shaped rhizoconcretions.

portion of the lower red unit in the eastern portion of the study area. In thin section, caliche characteristically exhibits a wide range of crystal sizes and morphologies. Crystal size ranges from micrite (<4 microns) to blocky, equant crystals of spar as much as 60 microns in diameter (Fig. 55). Detrital grains within caliches are often surrounded by horrendly oriented blades of spar. Clay-coated grains, typical of soil zones, are common. Caliches are produced in the B-horizon of alkaline soils in arid and semiarid climates (Goudie, 1973). The widely varying calcite crystal size in the caliches reflect the fluctuating vadose-zone chemical environment. Incipient caliches have formed in the archaeological site at Tel Yinam, Israel, within the last 1,300 years (R. L. Folk, 1979, oral commun.). Caliches produced in lacustrine mudstones during lake-level low stands, however, may have formed over a considerably shorter period of time, due to the initial highly calcareous nature of these sediments.

Large crystals of blocky, pore-filling spar are a common cement type in the sandstones of the distal braided alluvial-plain facies and the upper, non-lacustrine portions of deltas. Occurrence of this type of cement within lower-delta and lacustrine basinal sediments is limited to minor, spar-filled void spaces within lacustrine mudstones, as has been previously described in the mudstone petrology

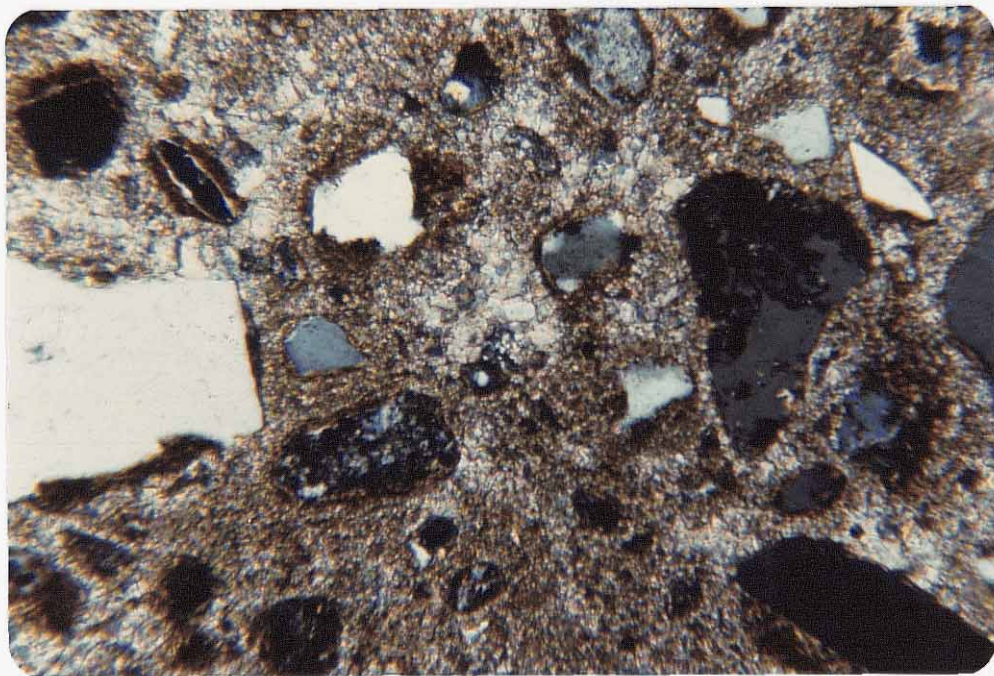


Figure 55. Baca caliche as seen in thin section. Note wide range in calcite crystal sizes and the presence of numerous grains which exhibit hematitic clay cutans. Sample 34, crossed nicols, field width=0.8 mm.

section. The spar crystals are moderately well sorted with respect to size (Fig. 56); the mean grain size ranges between about 80 and 250 microns. Poikilotopic calcite cements were occasionally observed. Coarsely crystalline calcite sometimes partially replaces feldspar in non-lacustrine sandstones (see feldspar section). In thin section, coarsely crystalline spar cements generally exhibit patchy distribution. Sand grains within spar-cemented patches are typically loosely packed, indicating that these areas were cemented early (prior to compaction) in the diagenetic history of the sediment. The patchy, incomplete nature of the early calcite cementation within upper-delta and distal braided alluvial-plain sandstones resulted in relatively high porosities and permeabilities within these sandstones and favored their utilization as aquifers by later-diagenetic groundwaters.

Several parallel-oriented, brown, cigar-shaped concretions as much as 6 inches (15 cm) in diameter were observed within sandstones of the middle sandstone unit at NW 1/4, SW 1/4, NW 1/4, Sec. 6, T.1N., R.6W. Sand grains within these concretions exhibit very loose packing, and are tightly and completely cemented with coarse sparry calcite which is morphologically identical to that described above (Fig. 57). The reasons for the parallel orientation, the cigar-like shape, and the tightly cemented nature of these

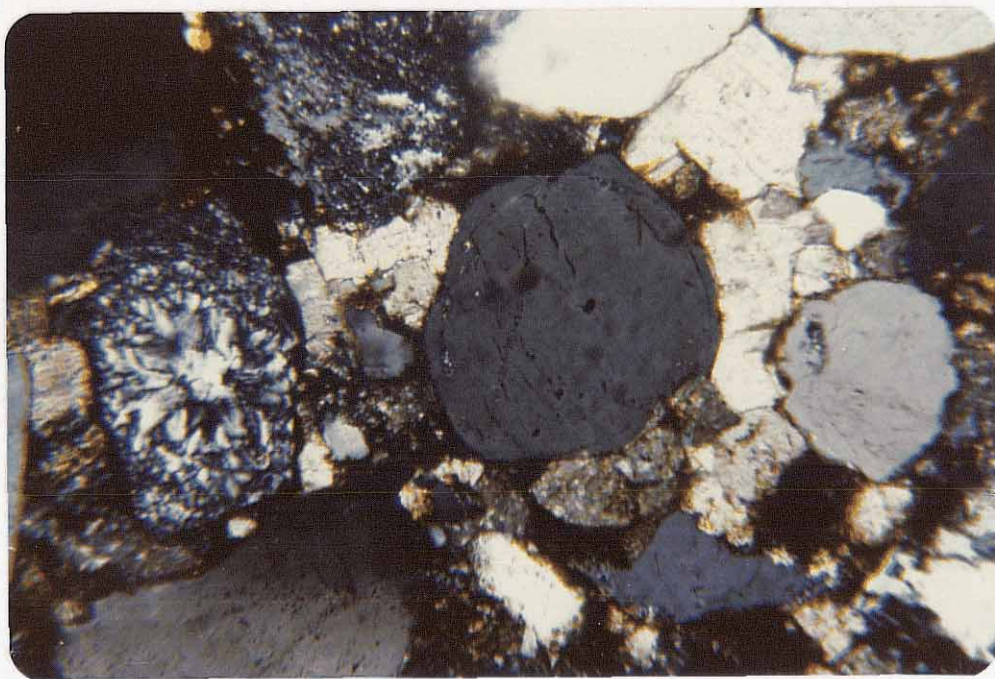


Figure 56. Coarsely crystalline spar cement in an upper-delta sandstone (sample C). Crossed nicols, field width=0.8 mm.

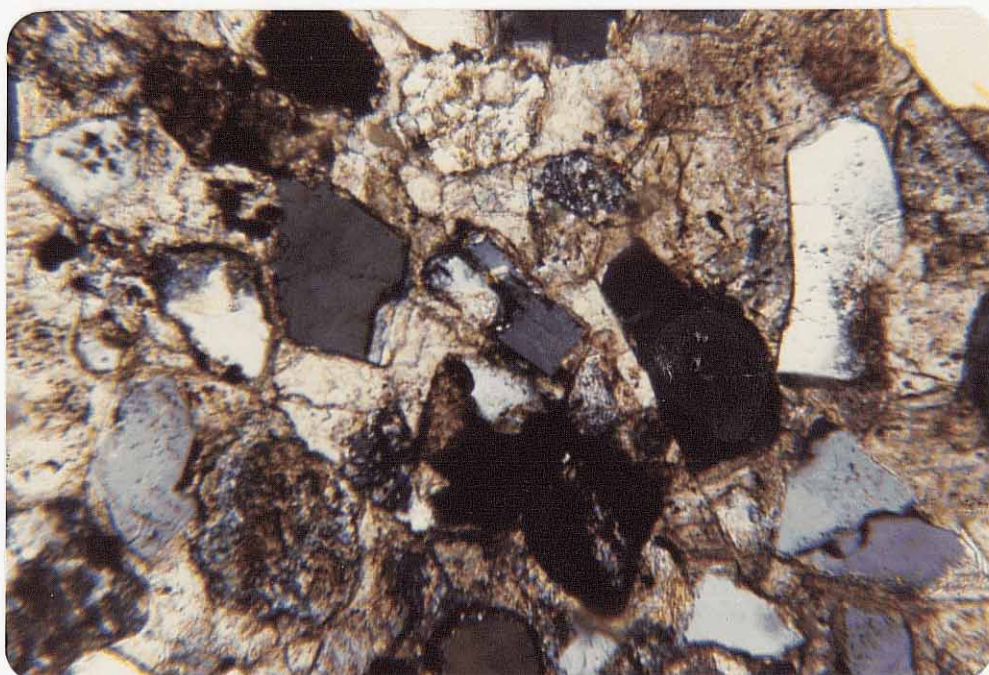


Figure 57. Coarsely crystalline sparry calcite cement in cigar-shaped sandstone concretion (sample 49). Loosely packed fabric is indicative of very early cementation (prior to compaction). Crossed nicols, field width=0.8 mm.

concretions are not known.

The moderately well-sorted nature of the coarsely crystalline spar implies cementation took place under relatively uniform, stable geochemical conditions. This, and the lack of characteristic vadose-cement indicators such as gravitationally oriented and meniscate cements (Dunham, 1971), shows that cementation occurred below the water table. The generally loosely packed nature of the spar-cemented grains indicates cementation prior to burial of more than a few tens of feet (Jonas and McBride, 1977, p. 73). The subequant, subhedral morphology of the calcite crystals suggests that the magnesium/calcium ratio of the pore waters at the time of crystallization was less than about 2:1 (Folk, 1974, p. 176).

The third variety of calcite cement which is present in the study area is fine-grained (10-15 micron), very well-sorted, sparry calcite, which is abundant in lower-delta and basinal sediments. The fine grain size and well-sorted nature of this calcite is similar to that of microspar, which is produced by aggradational neomorphism of micrite (Folk, 1965). However, due to the complete lack of micrite in the Baca (with the exception of that in caliches) and the fact that lower-delta and lacustrine basinal sediments never contain more than 48 percent calcite (greater abundances of carbonate could not be accommodated

as pore filling in very loosely packed sandstones and would necessitate the former presence of carbonate mud matrix in the sediments), I believe that the fine-grained lacustrine calcite formed as simple pore fillings and not through neomorphism. Thus, the term microspar is not applicable to these carbonates. Fine-grained calcite is commonly stained red by hematite (Fig. 58) and occurs in both lacustrine mudstones and thin-frontal splay sandstones. Detrital grains within the frontal-splay sandstones are very loosely packed, which indicates that cementation took place prior to compaction. The lacustrine sediments are typically tightly and completely cemented with early-diagenetic spar, resulting in very low porosities and permeabilities which precluded alteration by later groundwaters.

The fine-grained, pore-filling sparry calcite crystals are generally well sorted, indicating precipitation in a uniform, stable, alkaline geochemical environment. The lack of vadose-zone cementation indicators such as gravitationally oriented and meniscate cements (Dunham, 1971) and the well-sorted nature of the calcite strongly suggest that the fine-grained spar formed below the water table or within the lacustrine environment. The loosely packed nature of the spar-cemented, frontal-splay sandstones implies that cementation took place before burial of more than a few tens of feet (Jonas and McBride, 1977, p. 73).

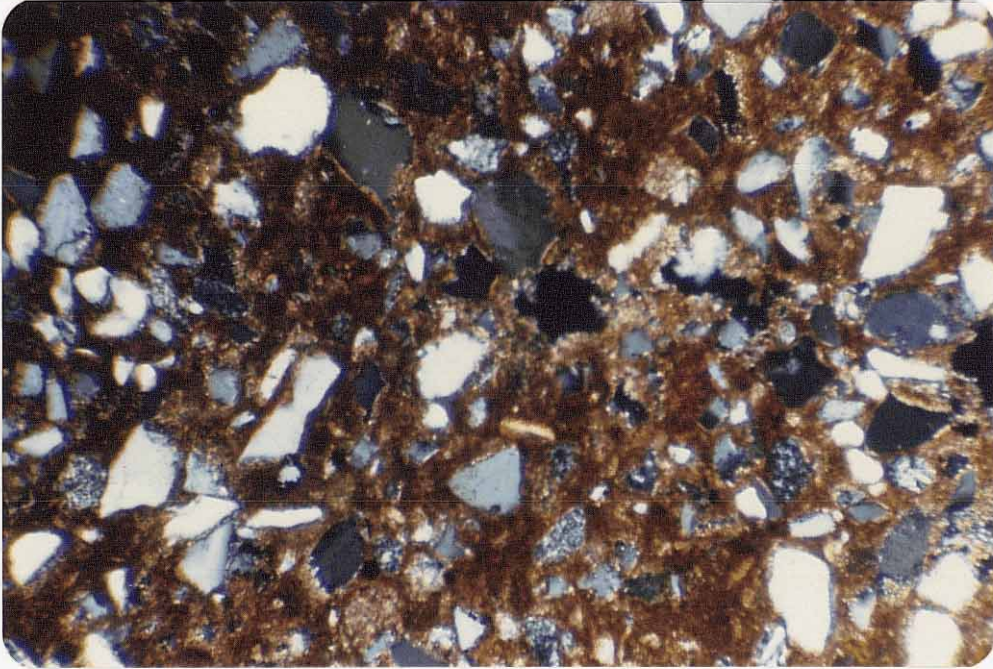


Figure 58. Hematite-stained fine-grained sparry calcite in a frontal-splay sandstone (sample 13). Note poorly compacted nature of this early-cemented lacustrine sandstone. Crossed nicols, field width=0.75 mm.

Subequant calcite crystal morphologies indicate precipitation from pore waters with magnesium/calcium ratios of less than about 2:1 (Folk, 1974, p. 176).

The boundary between upper delta sediments which are incompletely cemented with coarsely crystalline spar and lower-delta and basinal sediments which are tightly cemented with fine-grained calcite is sharp and generally corresponds to the approximate position of the original lake level during deltaic progradation. The contrast in extent of early calcite cementation between upper and lower delta sediments suggests that the lower-delta and basinal deposits were cemented within the lacustrine environment; if both upper and lower delta sediments were cemented below the water table following burial, one would expect both to exhibit similar degrees of cementation. The finer-grained nature of the lacustrine carbonates may be explained by: (a) inhibition of crystal growth by ions, such as magnesium, provided by clays in the lacustrine environment (Folk, 1979, oral commun.), or (b) rapid crystallization rates caused by high concentrations of carbonate within the closed-lake system. The presence of fine-grained spar only in lacustrine sandstones and not in non-lacustrine sandstones of similar grain size shows that carbonate crystal size was not strongly controlled by the diameter of the interstitial spaces. The incomplete cementation of upper-delta and

distal braided alluvial-plain sandstones by coarsely crystalline calcite probably occurred below the water table following shallow burial. Slow crystallization from dilute phreatic waters or the lack of substantial amounts of clay which could inhibit crystal growth may explain the relatively large calcite crystal size in these sandstones.

Quartz (0-9%, mean 1%, median 0.5% of bulk rock volume)

Following early-diagenetic calcite, quartz cements were the next to form in the Baca sandstones in the study area. The majority of the authigenic quartz in the Baca sandstones takes the form of simple syntaxial overgrowths (Fig. 59), but a small amount (less than 5%) occurs as radially oriented flamboyant megaquartz (K. Millikan, 1979, oral commun.) (Fig. 60). Quartz cements were only observed in upper-delta and distal braided alluvial-plain sandstones; early, complete calcite cementation precluded the formation of quartz and subsequent cements in the lacustrine sediments. Indeed, even in the non-lacustrine sandstones quartz and calcite occur antipathetically. Detrital quartz grains were often observed which exhibited syntaxial quartz overgrowths except along those portions of the grain boundary which are cemented with calcite spar (Fig. 61). Recognition of grains with older, reworked overgrowths was

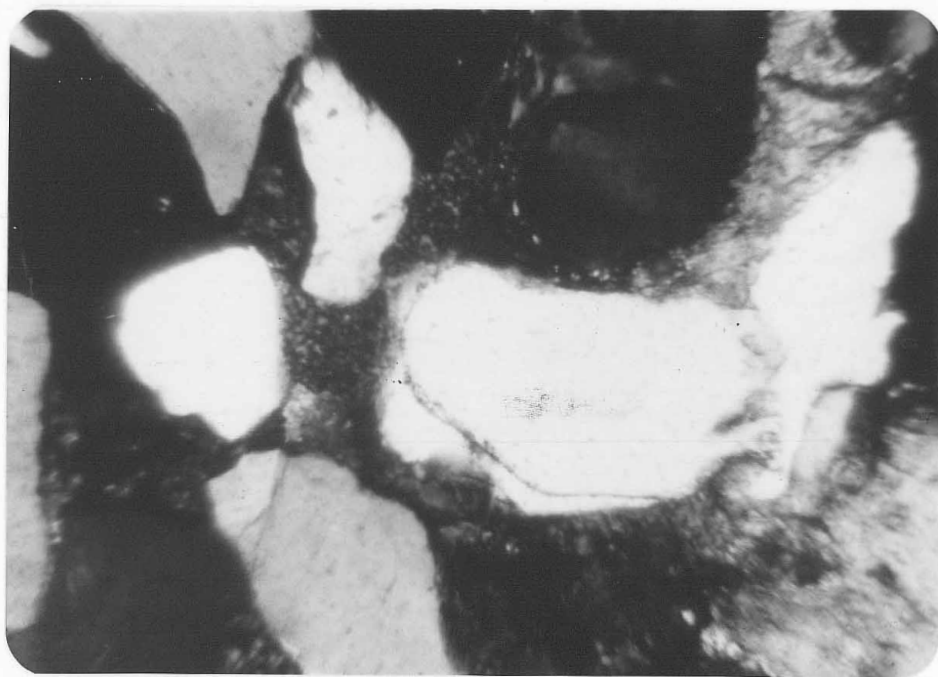


Figure 59. Syntaxial overgrowth on detrital quartz grain.
Sample 45, crossed nicols, field width=0.75 mm.

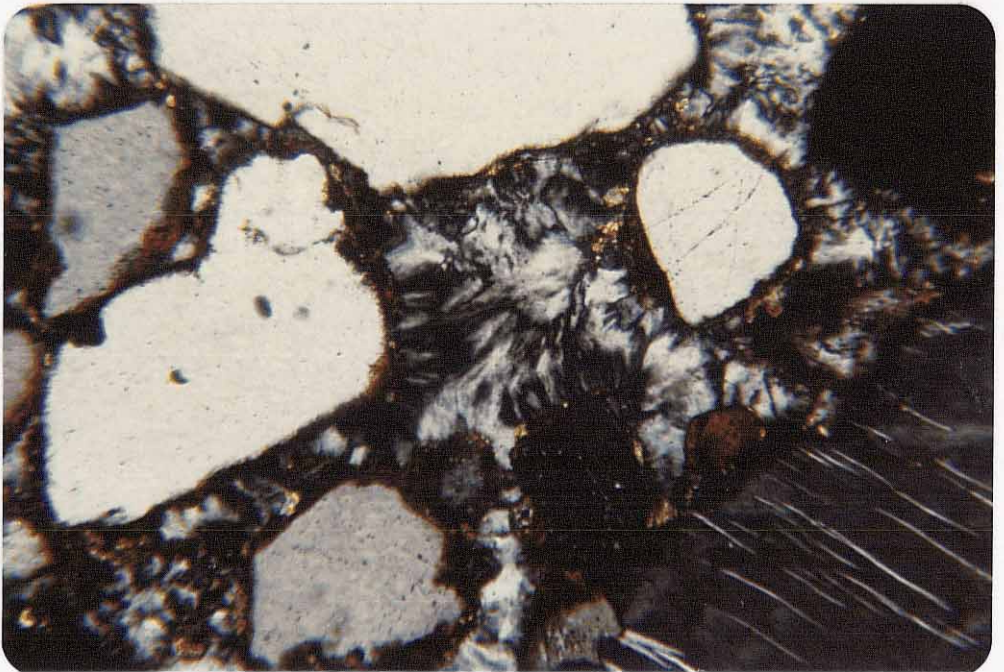


Figure 60. Flamboyant megaquartz cement. Sample M50, crossed nicols, field width=0.8 mm.

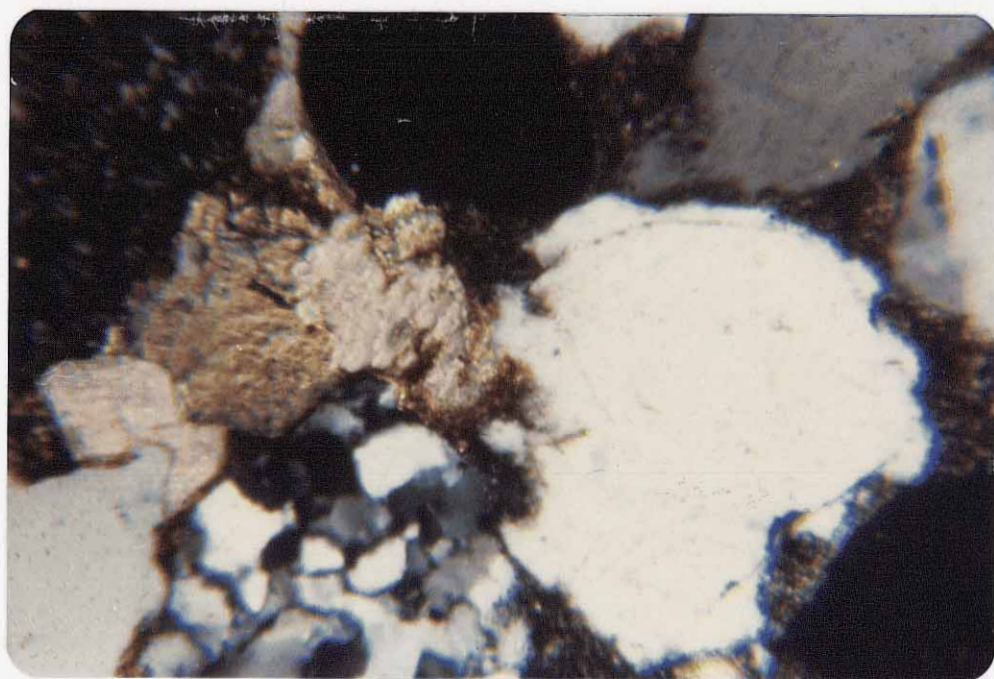


Figure 61. Inhibition of syntaxial quartz overgrowth by coarsely crystalline sparry calcite cement. Sample B, crossed nicols, width of field= 0.75 mm.

difficult. However, the occurrence of rare, isolated quartz grains with syntaxial overgrowths in the early-cemented lacustrine sediments indicates that a small percentage of the quartz overgrowths observed in the non-lacustrine rocks were probably reworked. The presence of minute hematite flecks (the primary source of red coloration in the Baca; see coloration section) beneath quartz overgrowths suggests that the hematite, or its hydrated iron-oxide precursor, formed prior to quartz cementation. The highest concentrations of authigenic quartz were observed near the top of the Baca stratigraphic section in the study area (Fig. 62), which suggests that much of the silica for these cements was derived from the overlying volcanics and, thus, implies that quartz cementation in the Baca took place following the inception of volcanism in early Oligocene time. A similar upward increase in authigenic quartz was observed by the writer in thin sections from Massingill's (1979) Baca measured section in the Bear Mountains vicinity (Fig. 63). The solubility of quartz increases with increasing pH and temperature (Jonas and McBride, 1977). The only conclusions which can be drawn concerning the geochemical nature of the interstitial waters during quartz precipitation is that temperatures were probably relatively low ($< 200^{\circ}\text{C}$?) and the pH was not strongly alkaline (< 10.5).

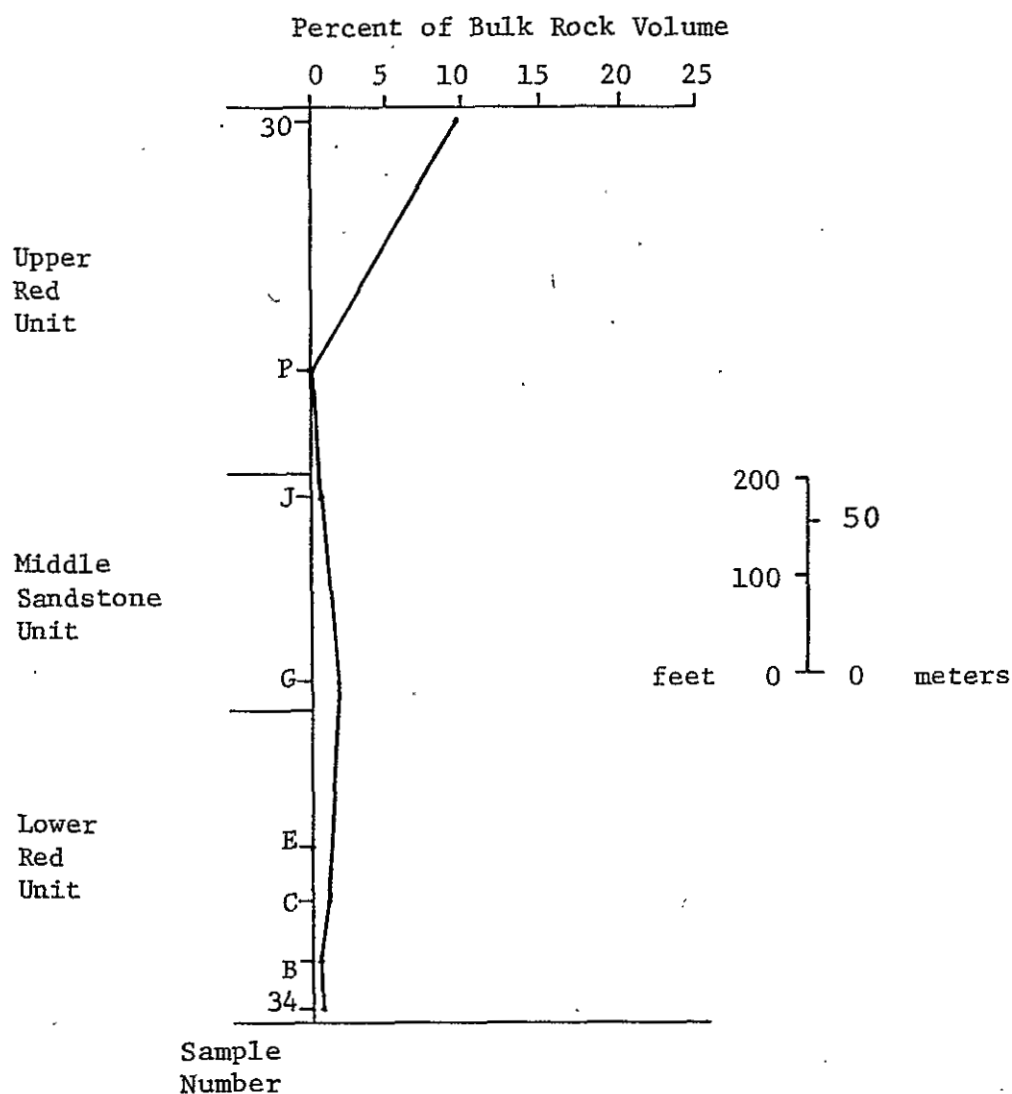


Figure 62. Plot of authigenic quartz content in study-area sandstones as a function of stratigraphic position.

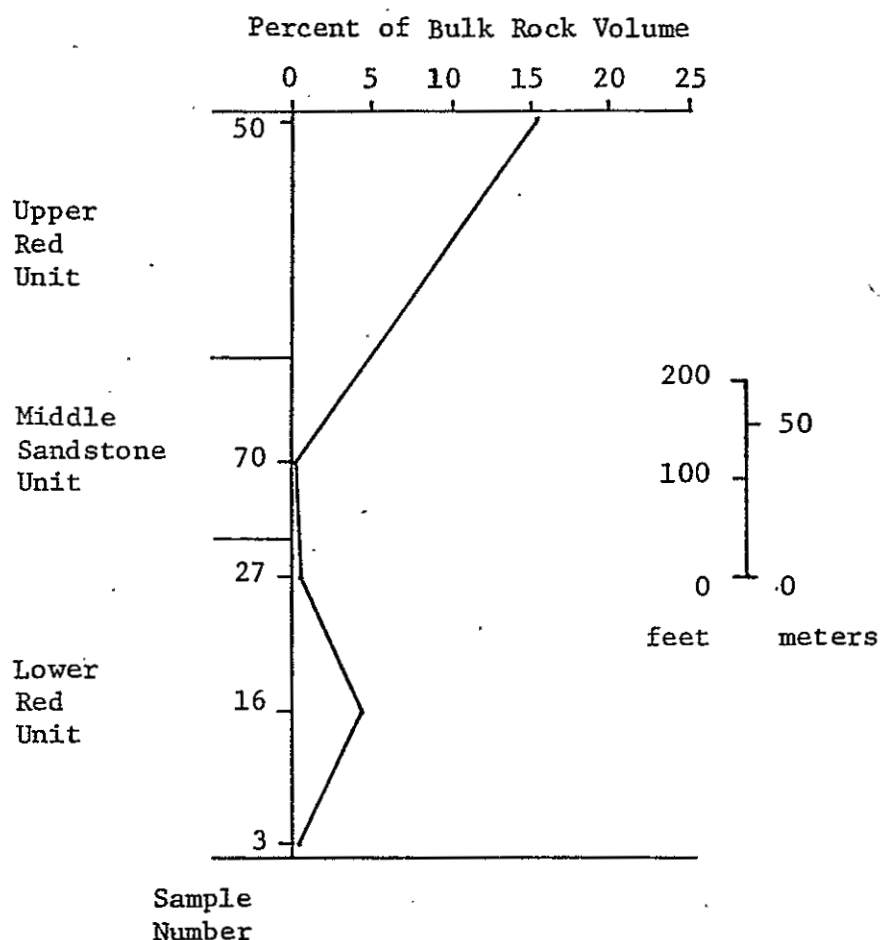


Figure 63. Plot of authigenic quartz content in Baca sandstones as a function of stratigraphic position. Data from point counts made by the writer on thin sections from Massingill's (1979) measured section in the Bear Mountains area.

Kaolinite (0-23%, mean 5%, median 4.5% of bulk rock volume)

Following quartz, kaolinite was the next cement in the diagenetic history of the Baca sediments in the study area. The distribution of authigenic kaolinite is the same as that of quartz; it occurs only in upper-delta and fluvial sandstones. Kaolinite occurs as a pore filling between grains which have not been previously cemented with calcite or quartz. Precipitation of both kaolinite and quartz in interstitial areas which were not tightly cemented by early, patchily distributed spar results in the common occurrence of both kaolinite and quartz within a given pore space. In other words, quartz and kaolinite often occur together, whereas calcite rarely occurs within a given pore space with either of these cements. The more closely packed nature of the kaolinite-cemented areas within sandstones relative to adjacent calcite-cemented areas indicates a period of compaction prior to kaolinite precipitation. In thin section, kaolinite appears as tiny flecks or vermicular stacks (Fig. 64, 65) as much as 30 microns in length and exhibits very low birefringence and low positive relief. X-ray diffraction data on the clay-sized fraction from one clay-cemented sandstone (sample 56) confirms the presence of kaolinite. The common vermicular habit of the kaolinite observed in thin section and its relatively late occurrence

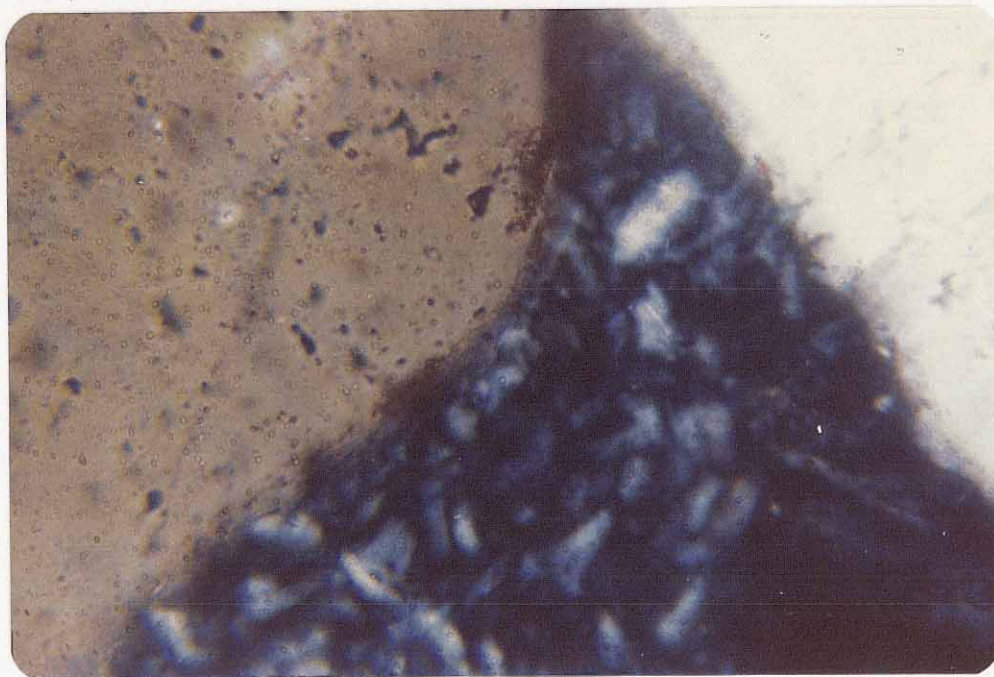


Figure 64. Authigenic kaolinite. Bluish tint is due to impregnation of kaolinite microporosity with blue epoxy. Sample 48, crossed nicols, field width=0.15 mm.

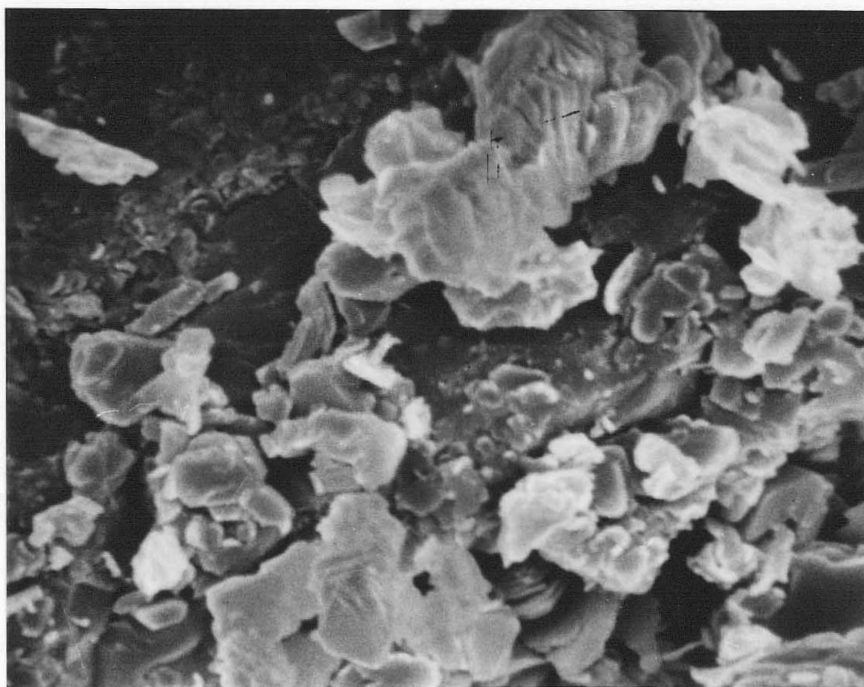


Figure 65. Scanning electron photomicrograph of vermicular stacks of kaolinite crystallites on a quartz sand grain. Sample 56, 5,000X.

in the diagenetic history of the Baca sediments indicate that the kaolinite is authigenic. In contrast to the other Baca sandstone cements, kaolinite contains appreciable microporosity, especially when arranged in vermicular stacks. This microporosity results in permeabilities as much as 8.8 mD (Jonas and McBride, 1977, p. 81-82), and thus may significantly enhance the aquifer characteristics of kaolinite-cemented sandstones. Microporosity produces the typical light-blue tint of kaolinite when observed in thin sections which have been impregnated with blue epoxy.

Kaolinite forms under slightly acidic conditions where there is an excess of silica but few potassium and magnesium ions in solution (Jonas and McBride, 1977). The common association of corroded feldspars and kaolinite cement in thin section, the instability of feldspar under acidic conditions requisite for kaolinite precipitation, and the presence of a few feldspar grains which have been replaced by kaolinite imply that secondary-porosity-producing cavernous dissolution of Baca feldspars took place synchronously with kaolinite cementation. The etching of garnets within kaolinite-cemented sandstones probably also took place at this time. Feldspar dissolution may have provided some of the silica necessary for kaolinite precipitation, however, due to the relatively small volumes of feldspar which have been dissolved, I do not feel that

feldspar dissolution could have supplied all of the silica.

Dolomite (0-10%, mean 1%, median 0% of bulk rock volume)

Dolomite was the final cementing agent in the Baca sandstones in the study area. Its occurrence is restricted to non-lacustrine sandstones, as is the case with quartz and kaolinite cements. Unlike the earlier cements, however, dolomite only occurs in the yellow-gray (non-red) Baca sandstones. In fact, oxidation of dolomite to limonite during modern outcrop weathering appears to be the predominant source of yellow coloration in these sandstones (see coloration section). Dolomite commonly contains small amounts (as much as a few percent) of iron (R. L. Folk, 1980, oral commun.). In thin section, dolomite generally occurs as well-formed rhombohedra which often exhibit alternating iron-rich and iron-poor zones (Fig. 66). It usually is not a simple pore filler, but appears as a replacement product of kaolinite, calcite, and, to a lesser extent, quartz (Fig. 67). Dolomite most often occurs as small, isolated rhombohedra within sandstones, except where it replaces relatively large calcite- or kaolinite-filled void spaces, in which case it appears as numerous, poorly developed, intergrown rhombohedral crystals.

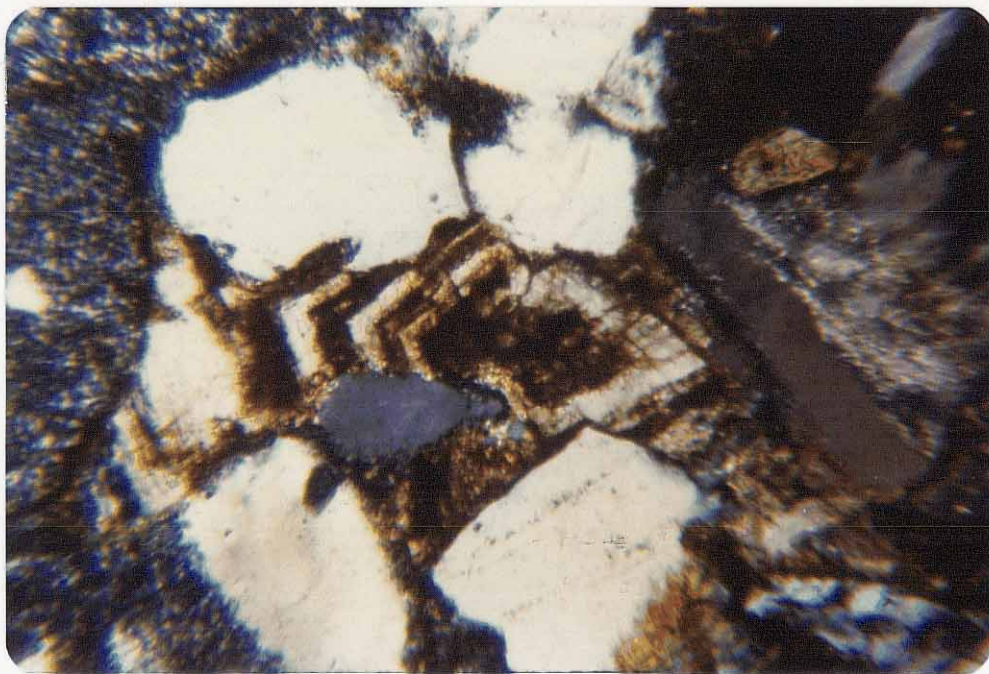


Figure 66. Dolomite cement showing alternating iron-rich and iron-poor zones. Sample B, crossed nicols, field width=0.75 mm.



Figure 67. Dolomite rhombohedron replacing adjacent quartz grain. Sample B, crossed nicols, field width= 0.75 mm.

The formation of dolomite within the Baca sandstones apparently is related both spatially and temporally to the intrusion of Miocene mafic dikes in the area. Figure 68 shows the coincidence in occurrence of yellow-gray, dolomite-bearing sandstones with the location of dikes in the study area. Dolomite forms in alkaline environments. The initial presence of small amounts of Fe^{2+} in the dolomite (as shown by recent limonitic alteration) implies reducing conditions at the time of precipitation. The following is a possible model for the formation of the Baca dolomite cements. During dike emplacement, oxidizing, carbonate-rich groundwaters were migrating through permeable Baca upper-delta and braided alluvial-plain sandstones. As these waters neared the intrusions, they progressively became reduced, presumably due to the introduction of reductants (H_2 , S^{2-}) by the dikes. These reducing groundwaters dissolved hematite and magnetite and altered ilmenite to leucoxene in the host sandstone (see heavy mineral section). At the same time, the groundwaters became heated by the nearby dikes, causing dolomite to precipitate (carbonate solubilities decrease with increasing temperatures). Much of the iron incorporated within the dolomite was probably derived from the above-described dissolution of heavy minerals. Thus, this model presents a geochemically viable, simple explanation for both the occurrence of yellow-gray,

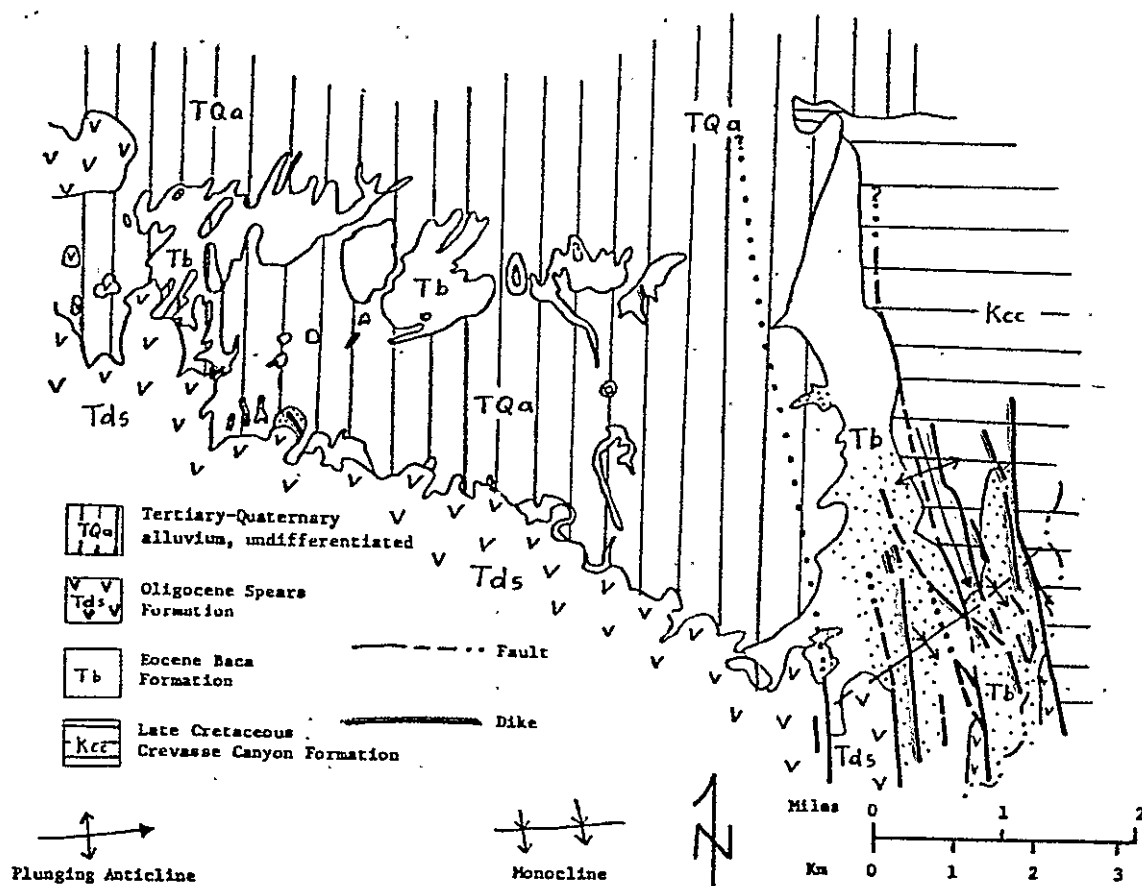


Figure 68. Generalized map of the study area showing coincidence of occurrence of dikes and areas in which Baca sandstones are yellow-gray in color (stippled areas).

dolomite-bearing sandstones in proximity to dikes, and the anomalous heavy-mineral suite within these yellow-gray sandstones.

Source of Coloration

There are two modes in the coloration of the Baca sediments in the study area (Fig. 69). The majority of the sediments average about 10R 6/2 (weak light red-orange). Upper-delta and distal braided alluvial-plain sandstones which are near mafic dikes are often non-red, averaging about 10YR 7/3 (very light yellow-orange).

Red Coloration

In the grossest sense, theories concerning the genesis of redbeds can be lumped into two basic schools of thought: soil-derived and diagenetic red coloration. The latter process is the most important in the red Baca sedimentary rocks in the study area.

Soil-derived Red Coloration. Soil-derived red coloration is one of the oldest and most well-rooted theories of redbed genesis, and was popularized by Krynine (1949, 1950) and Van Houten (1948). According to this

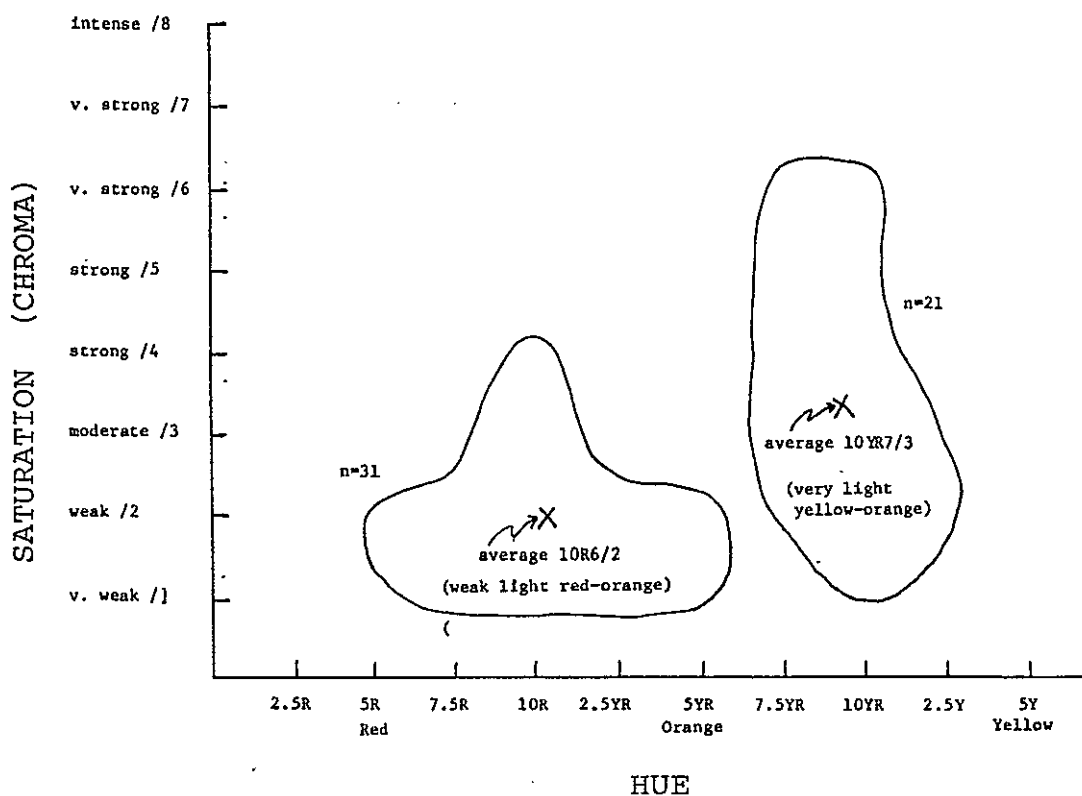


Figure 69. Distribution of coloration for 52 Baca sandstone samples from the study area. Values were determined by comparison with Munsell Soil Color Chart. Color terminology after Folk (1969).

theory, redbeds result from sediments which were derived from lateritic soils which formed in igneous or metamorphic terranes in tropical areas with seasonally high rainfall. In these areas, iron-bearing heavy minerals in the A horizon of lateritic soils become severely altered and leached by such processes as hydrolysis and attack by carbonic and humic acids. Destruction of these heavy minerals yields clay minerals (also derived from the weathering of feldspars) and hydrated iron oxides (limonite) which are transported downward by percolating groundwaters. In the B soil horizon illuviation takes place and these hydrated iron oxides and clay minerals form cutans (clay coats) on grains. Upon erosion, these soils provide large amounts of iron, in the form of grains coated with ferruginous clay, to the basin of deposition. When deposited, the sediment is yellowish brown in color due to the hydrated nature of the iron oxide (Van Houten, 1964). Post-depositional dehydration results in hematite forming within the cutans, giving the redbeds their coloration.

Diagenetic Red Coloration. Walker (1963, 1967) proposed that redbeds can form diagenetically by intrastratal dissolution of iron-bearing heavy minerals. By this method, any heavy-mineral-bearing sediment, regardless of the climate in the source area, can later become red if

the right set of conditions prevails in the basin of deposition. Igneous or metamorphic source rocks are necessary to provide the heavy minerals (Miller and Folk, 1955). After burial, the iron-bearing heavy minerals (particularly iron silicates) are leached by intrastratal solutions, yielding hydrated ferric oxides and clay minerals. Dehydration results in the formation of hematite which provides the red coloration. Dehydration can take place below the water table if the water is alkaline (Walker, 1974).

Diagenetically produced red coloration is primarily dependent upon conditions within the basin of deposition. According to Walker (1967, p. 366), these conditions include: (a) occurrence of iron-bearing detrital grains, (b) post-depositional conditions that favor the intrastratal dissolution of iron-bearing grains, (c) an interstitial Eh-pH environment that favors the formation of hydrated ferric oxides, (d) absence of subsequent reduction of ferric oxides, (e) enough time for dehydration to hematite to occur, and (f) relatively warm temperatures (above about 65-70 F).

Source of Red Coloration in the Baca Formation.

Through the petrographic microscope, the predominant source of red coloration in the Baca sandstones in the study area

appears to be small (0.5-3.0 micron) flecks of hematite which are uniformly distributed on the surfaces of sand grains. These flecks are present on both the corners and embayments of grains, but do not occur at contact points between grains (Fig. 70). Similar flecks are assumed to be the source of coloration of the red Baca mudstones, however, the birefringence of the clays and carbonate in these rocks made determination of the nature of the hematite impossible. Morphologically indistinct even under high power with the optical microscope, these flecks are usually seen with the scanning electron microscope to be plate-like in shape with ragged, irregular edges, although hematite crystals with euhedral terminations are not uncommon (Fig. 71). No clay cutans are associated with these flecks.

Three additional, relatively minor modes of occurrence of hematite were observed in the Baca sandstone thin sections. A few magnetite/ilmenite/specular hematite grains exhibited dissolution features and were surrounded by hematite halos. In two thin sections, minor amounts (< 1%) of pore-filling hematite cement were observed. This appears black in handspecimen, however, and thus does not contribute to the red coloration of the Baca Formation. Approximately two percent of the sand grains examined with the petrographic microscope displayed hematitic clay cutans. These cutans typically show the yellow birefringence of

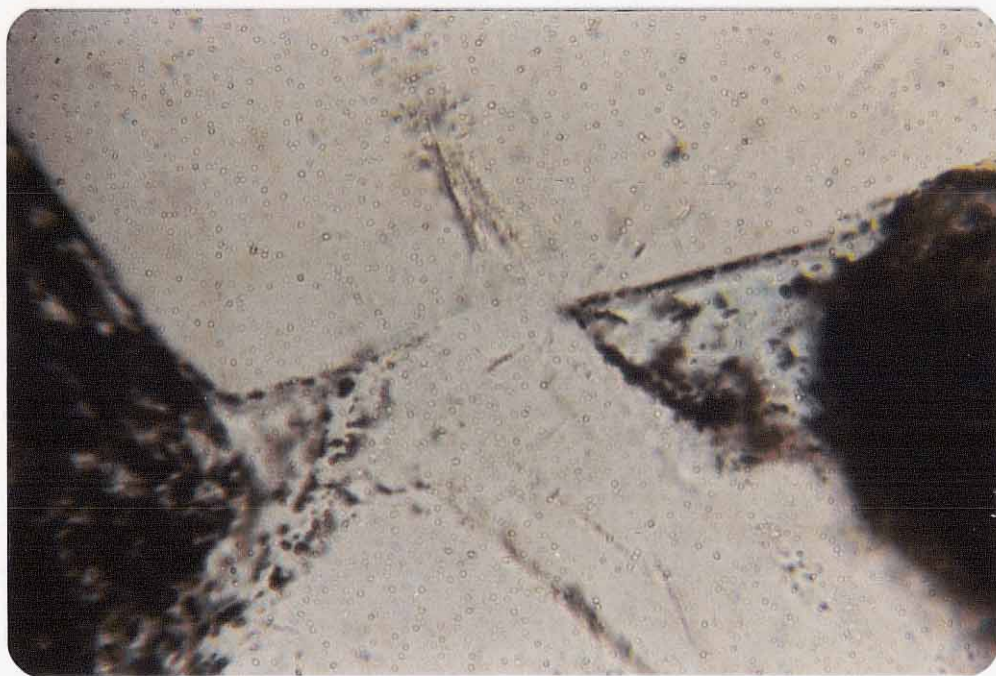


Figure 70. Hematite flecks uniformly distributed on Baca sand grains, except at contact points between grains. Sample P, plane light, field width=0.15 mm.

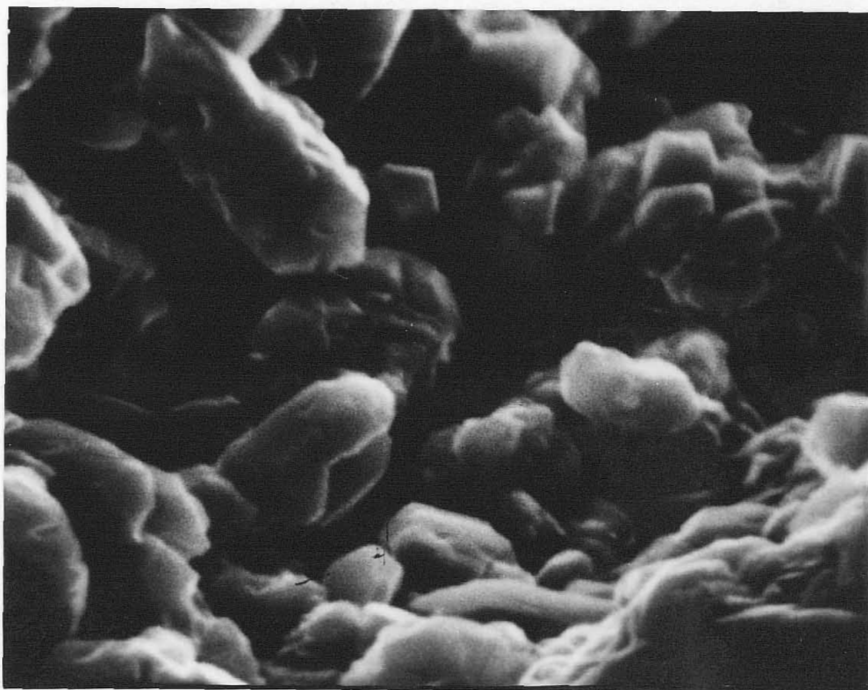


Figure 71. Scanning electron photomicrograph of euhedrally terminated hematite crystals on quartz sand grain. Sample P, 7,000X.

clay; hematite occurs as a diffuse stain within the clay coats. Possible sources of the clay-coated grains include soil zones in the source area or older Paleozoic or Mesozoic redbed sequences.

I believe that the majority of the red coloration in the Baca Formation was diagenetically produced. Evidence for this includes: (a) the presence of euhedral hematite crystals similar to those described in other diagenetically produced redbeds (Walker, 1967, p. 365); (b) uniform distribution of hematite flecks on both corners and embayments of grains and lack of flecks at contact points between grains indicates that the hydrated iron-oxide precursor to the hematite was precipitated post-depositionally; (c) the pore-filling nature of the hematite cement shows that post-depositional precipitation of iron oxides did occur; (d) paucity of augite and hornblende in heavy-mineral suites from sandstones derived from predominantly metamorphic and igneous source areas (as is the case with the Baca) indicates that intrastratal dissolution of these minerals took place (Walker, 1967, p. 365) (the generally fresh nature of the feldspars in early-cemented Baca sandstones shows that these heavy minerals were probably not destroyed within source-area soil zones); (e) general lack of clay-coated grains indicates that the red coloration did not form pedogenically; (f)

hematite halos around iron-bearing heavy-mineral grains indicate that intrastratal dissolution has occurred.

Intrastratal dissolution of iron-bearing heavy minerals provided the iron for the hematite colorant. A large portion of this iron, however, may have been supplied by authigenic iron sulfides which formed within the lake-bottom sediments. These iron sulfides are produced by anaerobic, sulfate-reducing bacteria that may have lived in the lacustrine sediments which probably became anoxic following shallow burial. Sulfate-reducing bacteria typically produce small (0.03-1.0 mm) pyrite framboids (Love, 1971). No such framboid-shaped hematite was observed, however, which indicates that if authigenic iron sulfides existed in the lacustrine sediments, they were not pseudomorphously replaced by hematite or its precursor. The lacustrine sediments are generally redder than associated non-lacustrine rocks, which implies higher concentrations of hematite in the lacustrine rocks and, thus, may indicate the former presence of authigenic iron sulfides in these rocks.

The presence of hematite flecks on the surfaces of sand grains within calcite-cemented portions of red, non-lacustrine sandstones and the occurrence of these flecks both on sand grains and interspersed within spar cement in lacustrine sediments indicates that iron mobilization took place very early (prior to and during calcite cementation)

in the diagenetic history of the Baca sediments. Dehydration of the hydrated-iron-oxide hematite precursor may have occurred during lake-level low stands or below the water table in an alkaline environment (Walker, 1974). The presence of caliches and other early-authigenic carbonates in the Baca implies that groundwaters were alkaline during the early portion of the diagenetic history of the sediments.

Folk (1976) states that redbeds undergo an evolutionary change in color through time (Fig. 72). Although the yellow-gray Baca sandstones fit well into this evolutionary sequence, the pale-red sandstones do not. Red Baca sandstones exhibit lower saturation values (average /2) than would be expected for an Eocene redbed sequence; according to Folk (1976) this saturation value is more typical of an Early Paleozoic sandstone. Moreover, the average value (lightness) of the red Baca sediments (6/) is somewhat light for an early Tertiary redbed sequence. The relatively coarsely crystalline nature of the Baca hematite is probably the cause for the large discrepancy between predicted and observed saturation values. The reason for this crystallinity is not known, but it may be related to the fact that the hematite formed diagenetically and is not soil-derived (R. L. Folk, 1980, oral commun.).

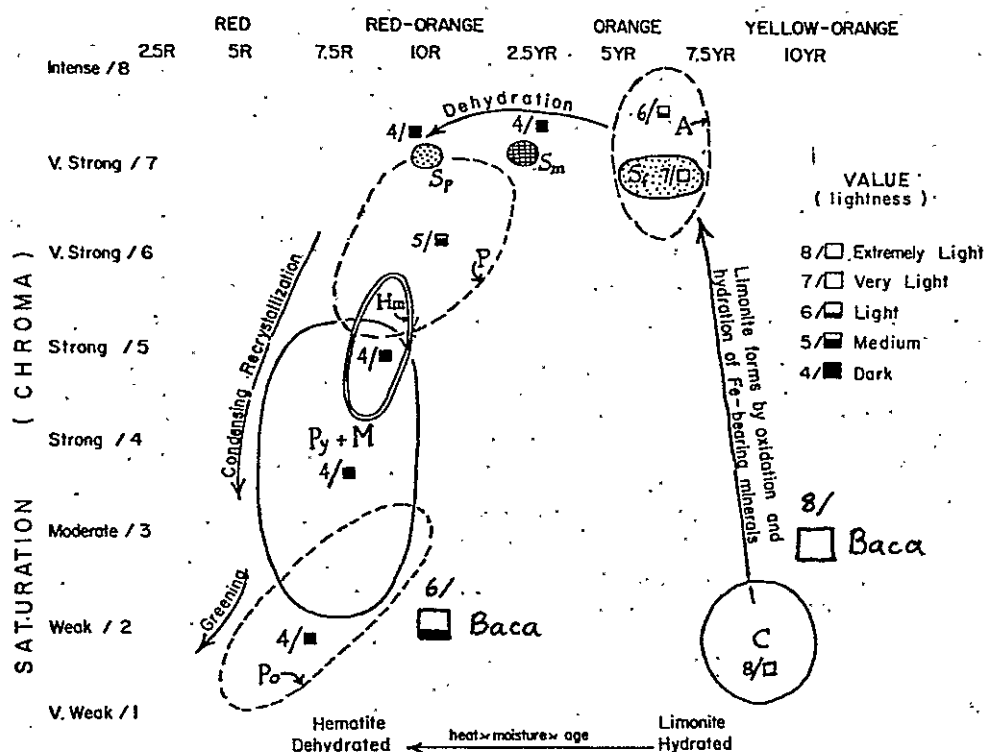


Fig. 72 Change of color with geologic age shown on a plot of hue vs. saturation. Third color dimension of lightness shown by the numbers 4/ etc. and degree of darkening of the squares. C, initial unweathered quartzose sand; A, Saharan sands, data from Alimen; Sf, Simpson Desert, surface fluff of Holocene age; Sm, Simpson Desert, modal color *en masse* of fine sands; Sp, Simpson Desert, color of hematite-clay cutans in pits, formed during Pleistocene lateritization; P, other Pleistocene sediments; Hm, color of powdered pure hematite; Py + M, color of Mesozoic and younger Paleozoic red rocks; Po, Older Paleozoic and Precambrian rocks. Processes that create these changes shown by the "evolutionary" arrows.

(Modified from Folk, 1976)

Yellow-gray Coloration

Permeable upper-delta and distal braided alluvial-plain sandstones which are located near mafic dikes are often yellowish-gray to orange in color (average 10YR 7/3). The majority of this coloration is due to alteration of iron-bearing carbonate cements to limonite during recent outcrop weathering, as was previously discussed in the dolomite section. Additionally, a significant portion of the non-red coloration in the Baca sandstones occurs as a diffuse limonitic stain within calcite and kaolinite cements and on detrital grains. In summary, the events leading to the development of yellowish to orange coloration in the Baca were: (a) oxidizing, alkaline groundwaters which migrated through permeable non-lacustrine sandstones became reduced due to interaction with reductants ($H_2S?$) associated with dike emplacement in Miocene time (These negative-Eh groundwaters dissolved hematite and magnetite and altered ilmenite to leucoxene in the host sandstones. Dissolved iron from these heavy minerals was incorporated into dolomite cements and formed diffuse stains within the sandstones); (b) Heating of groundwater by the dikes resulted in precipitation of dolomite; (c) Following late Tertiary uplift and erosional stripping, these reduced-iron-bearing sandstones were exposed to near-surface weathering

conditions, resulting in oxidation of the reduced iron to limonite, which gives rise to the present-day coloration of these sandstones.

Porosity

Porosity distributions played a very important role in the determination of the sequence of diagenetic events which affected the Baca sediments. Knowledge of the porosity distribution within the sediments may prove useful to explorationists in delineating probable pathways of migration of uranium-bearing groundwaters. Porosity determinations were made using point-count data from blue-epoxy-impregnated thin sections. Two types of porosity, primary and secondary, exist within the Baca sediments in the study area. Average overall porosity in the Baca (primary plus secondary porosity) is about 3.6%, and ranges from essentially zero to ten percent.

Primary Porosity

Primary porosity occurs as intergranular areas in Baca sandstones that have not been filled with cement. Lower-delta and lacustrine basinal sediments exhibited virtually no primary porosity, due to early and complete

cementation with fine-grained calcite. Primary porosity within non-lacustrine sandstones averages about 3.2%, and ranges from practically zero to ten percent. Of the non-lacustrine sandstones, the yellowish-gray sandstones contain greater primary porosity than do the red sandstones, the average values for these sandstones being about 5.1 and 1.5%, respectively. Microporosity in kaolinite cements may contribute slightly to the overall porosity of the Baca Formation.

Secondary Porosity

Secondary porosity is diagenetically produced and predominantly occurs as cavernous dissolution features within feldspars. Skeletalized magnetite/ilmenite/specular hematite grains within yellow-gray sandstones are a minor source of secondary porosity. Early-cemented lacustrine sediments exhibit virtually no secondary porosity. Within upper-delta and distal braided alluvial-plain sandstones, the average secondary porosity value is about 0.4%, and ranges from essentially zero to two percent. Secondary porosity within red, non-lacustrine sandstones averages about 0.2%, whereas that within yellow-gray sandstones averages about 0.7%. Cavernous dissolution of feldspars took place intrastratally, due to interaction with acidic

groundwaters (see feldspar and kaolinite sections). Skeletalization of magnetite/ilmenite/specular hematite grains within yellow-gray sandstones probably occurred during dolomite precipitation in an alkaline, reducing environment.

Diagenesis Summary

A flow chart depicting the diagenetic sequence of events for the Baca sediments in the study area is presented in Figure 73. The present-day characteristics of the sediments are highly dependent on their environment of deposition. Table 7 summarizes the distribution of cements, heavy minerals, porosity, and coloration among the various Baca facies. The lower-delta and lacustrine basinal sediments tend to be finer grained and less compacted than the non-lacustrine sediments. A plot of percent cement plus primary porosity vs. grain size (Fig. 74) indicates a trend towards increasingly looser packing in the fine-grained lacustrine sediments, and reflects the early, pre-compactional cementation of these sediments. Figure 74 also shows the presence of yellow coloration only in the coarse-grained, non-lacustrine sediments.

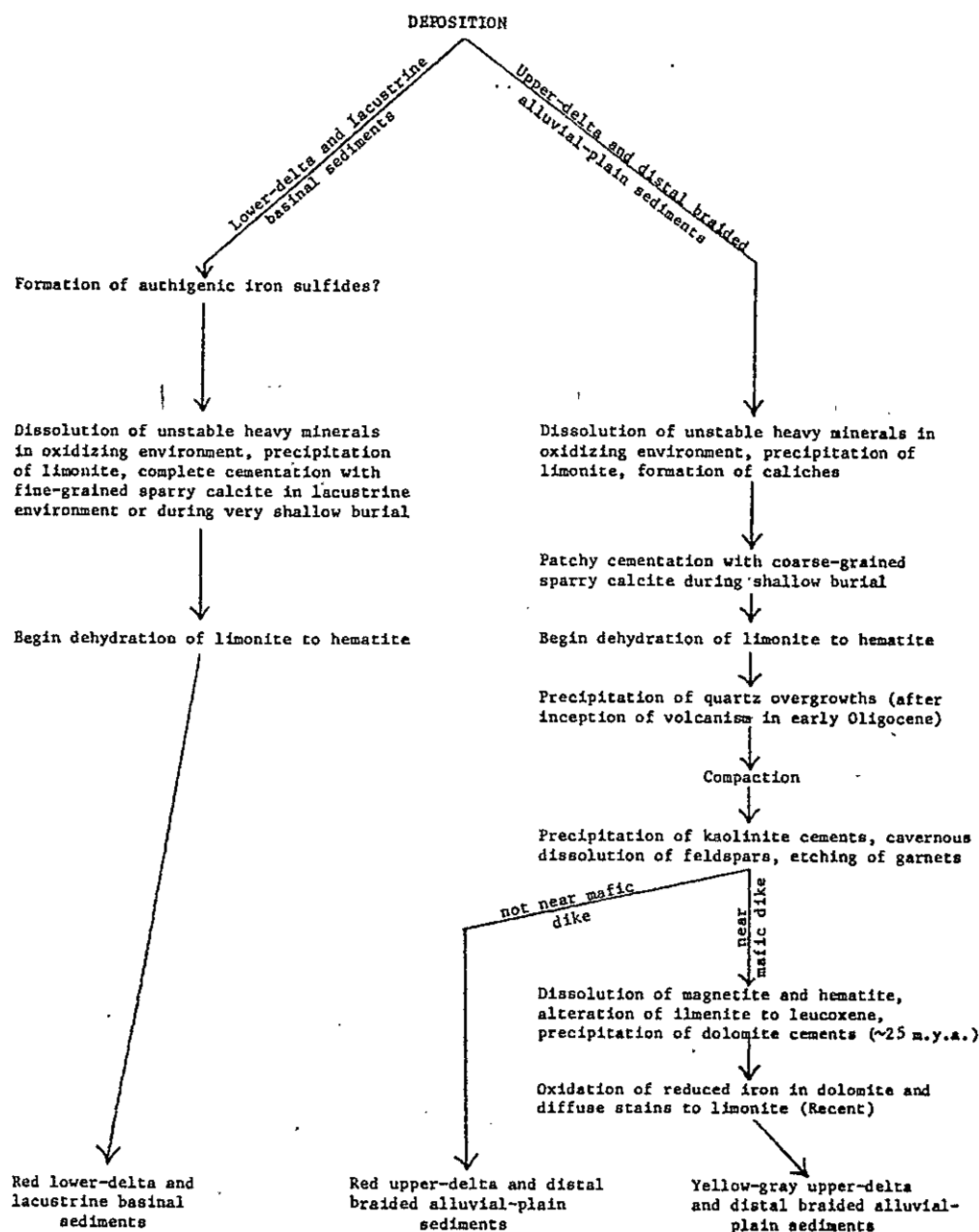


Figure 73. Diagenesis flowchart for the Baca sediments within the study area.

	COLOR	CEMENTS	POROSITY	DOMINANT HEAVY MINERALS
UPPER-DELTA AND DISTAL BRAIDED ALLUVIAL PLAIN SEDIMENTS	yellow-gray	coarse-grained sparry calcite, caliche, quartz, kaolinite, dolomite	primary: average 5.1% range 2-10% secondary: aver. 0.7% range 0-2%	leucoxene
	red	coarse-grained sparry calcite, caliche, quartz, kaolinite	primary: average 1.5% range 0-5% secondary: aver. 0.2% range 0-2%	magnetite/ilmenite/ specular hematite
LOWER-DELTA AND LACUSTRINE BASINAL SEDIMENTS	red	fine-grained sparry calcite, caliche	0	magnetite/ilmenite/ specular hematite

Table 7. Distribution of coloration, cements, porosity, and heavy minerals in relation to the various Baca facies.

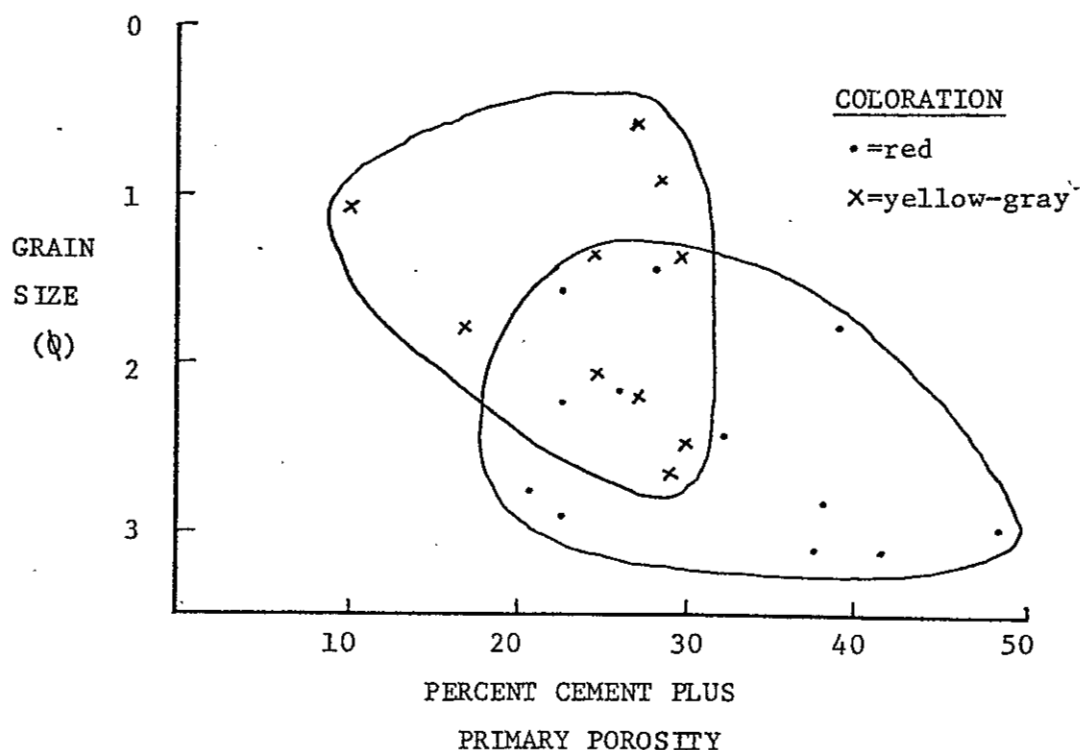


Figure 74. Plot of grain size vs. percent cement plus primary porosity showing tendency towards looser packing in the fine-grained lower-delta and lacustrine basinal sediments. Note the presence of yellow-gray coloration only in the coarser grained, non-lacustrine sandstones.

PALEOCLIMATE

Interpretations of the paleoclimate in west-central New Mexico during Baca time range from arid to semiarid (Snyder, 1971; Potter, 1970) to subhumid (Massingill, 1979; Johnson, 1978). Evidence from this study points to a hot, semiarid, possibly savanna-like climate in the study area during the Eocene. The probable closed nature of the Baca lacustrine system in the Bear-Gallinas Mountains vicinity is indicative of semiarid or arid conditions (Langbein, 1961). Rare paleocaliches within the Baca were pedogenically produced in an arid to semiarid environment. Goudie (1973) states that caliche formation is favored in semiarid climates where rainfall is seasonal (as in a savanna) and less than about 20 in (50 cm) annually. The presence of titanotheres, turtle, and crocodile fossils in the Baca exposures near Quemado and Datil (J. A. Schiebout, in progress) suggest a savanna-type climate. The common occurrence of root mottling and the lack of eolian features indicates vegetative stabilization of sediments and, thus, implies that arid conditions did not prevail, since sufficient water must have been available to support this vegetation. Modern ephemeral braided streams which are similar to the flashy-discharge Baca braided streams usually occur in arid and semiarid climates. However, the

pre-Miocene lack of abundant upland grasses may have caused high sediment yields, large amounts of runoff, and flashy river discharge characteristics even in wet climates (Schumm, 1968). The initial steps in the development of diagenetic red pigmentation are favored by high temperatures and an alkaline groundwater chemistry (Walker, 1967), which are commonly associated with semiarid climatic conditions. Feldspars within Baca sandstones were generally fresh upon deposition and suggest preservation by arid or semiarid climatic conditions.

ECONOMIC GEOLOGY

Uranium Occurrences

Uranium is the only known economically important resource which occurs in the Baca Formation. Potter (1970, p. 34-35) described three minor uranium occurrences associated with carbonaceous materials within the lower red and middle sandstone units in Baca Canyon. Uranium mineralization occurring near the contact between the Baca Formation and Cretaceous rocks in the Red Basin area north of Datil has been described by Griggs (1954) and Anonymous (1959). The Red Basin deposits may be economic and are currently being investigated by Gulf Minerals, Inc. Bachman, Baltz, and Griggs (1957) report several uranium occurrences along Jaralosa Creek, west of the Bear Mountains. One of these, the Hook Ranch prospect, lies within the study area and was examined by the writer. It consists of several exploration pits excavated into delta-front and lower delta-plain sandstones of the basal deltaic cycle of the upper red unit. The uranium-bearing sandstones are yellowish gray to gray, medium to very coarse grained, conglomeratic, and contain much carbonaceous materials. Carbonaceous debris ranges to as much as several centimeters in length and is more abundant in the prospect

sandstones than in non-mineralized Baca sandstones. One sandstone thin section (#73) from the Hook prospect was examined. It exhibited relatively high porosity (both primary and secondary) and contained calcite, kaolinite, and dolomite cements. Leucoxene was the predominant opaque heavy mineral. Alteration of ilmenite to leucoxene by oxygen-deficient groundwaters has been reported by Adams and others (1974) in the uraniferous sandstones of the Jurassic Morrison Formation.

Ore Genesis

Baca uranium deposits, such as the one at Hook Ranch, probably originated by concentration of uranium from very dilute, oxidizing groundwater solutions by the reducing action of carbonaceous debris and, possibly, by reaction with negative-Eh waters which were associated with the emplacement of mafic dikes. Reduction of uranium-bearing solutions by sulfide-rich groundwaters leaked upward along faults in south Texas has been reported by Galloway and Kaiser (1979). Uranium is highly soluble in oxidizing aqueous solutions, but precipitates under reducing conditions, usually to form complex organic compounds (Douros, 1967). The thick sequence of volcanic rocks overlying the Baca Formation probably were the source of the

uranium, although intrastratal dissolution of heavy minerals may also have been a source (Walker, 1975). Future uranium exploration efforts in the Baca in the Gallinas Mountains vicinity should be restricted to permeable, non-red upper-delta and braided alluvial-plain sandstones which have been altered by reducing groundwater solutions, and areas which contain anomalously high concentrations of carbonaceous materials.

SUMMARY OF BACA-EAGAR BASIN DEPOSITIONAL SYSTEMS

Johnson (1978) recognized humid alluvial-fan (renamed braided alluvial plain in this study), meanderbelt, and lacustrine depositional systems within the Baca-Eagar outcrop belt in west-central New Mexico and eastern Arizona. Within each of these depositional systems, Johnson delineated two or more component facies. Based on the facies distribution of Johnson (1978), the paleocurrent data from Snyder, (1971), Johnson (1978), Pierce and others (1979), and this study, and the Baca-Eagar tectonic framework proposed in this study, a hypothetical model for the basin-wide distribution of facies and paleocurrents is presented in Figure 75.

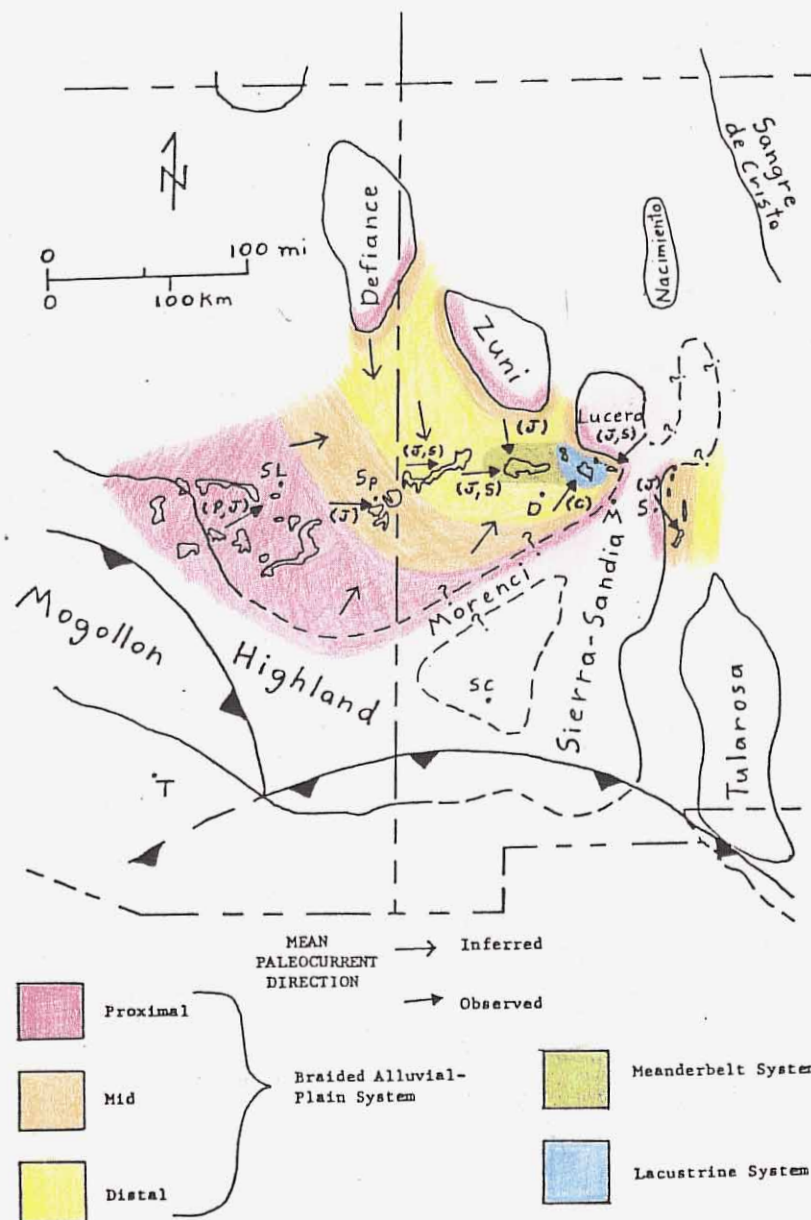


Figure 75. Hypothetical model for the distribution of facies and paleocurrents in the Baca-Eagar basin during early Baca time (high lake stand). Letters in parentheses indicate paleocurrent data sources. J=Johnson (1978), P=Pierce (1979), S=Snyder (1971), C=Cather (this study). Reference points same as Figure 10.

SUMMARY AND CONCLUSIONS

The sediments of the Eocene Baca Formation and correlative Eagar Formation and Mogollon Rim gravels of Arizona represent the basin-fill deposits of a large intermontane basin present in western New Mexico and eastern Arizona during Laramide time. The Baca-Eagar basin is bounded to the north by the Defiance, Zuni, and Lucero uplifts, to the southwest by the Mogollon Highland, to the southeast by the Morenci uplift, and to the east by the Sierra-Sandia uplift. These Laramide uplifts, particularly the Mogollon Highland, were the dominant contributors of detritus to the basin. All three styles of Laramide uplifts (Cordilleran foldbelt uplifts, asymmetrical basement-cored anticlinal uplifts, and Colorado Plateau monoclinal flexures) are present adjacent to the basin.

Within the study area, the Baca is about 940 ft (289 m) thick and can be subdivided into three informal members (lower red, middle sandstone, and upper red units) which reflect large-scale lake-level fluctuations in a large, closed lacustrine system which was present during Baca time in the Bear-Gallinas Mountains vicinity. These lake-level fluctuations were probably caused by climatic changes. A semiarid, savanna-type climate is proposed for west-central New Mexico during Baca time. Facies which were recognized

in the study area include distal braided alluvial-plain, fine-grained lacustrine delta, and lacustrine basinal facies. The distal braided alluvial-plain facies is dominantly comprised of fine to coarse sandstones and minor conglomerates which were deposited by low-gradient, flashy-discharge (ephemeral?) braided streams. Similar streams supplied sediment to the fine-grained lacustrine deltas, whose deposits are characterized by cyclical upward-coarsening sequences which represent alternate deltaic progradation and abandonment in a shallow lake. Lacustrine basinal sediments are similar to those of the lower prodelta portion of deltaic sequences and consist of red, calcareous mudstones intercalated with thin fine-sandstone and siltstone beds. The highly calcareous nature of the lacustrine sediments indicates a closed lake system. The characteristics of the lacustrine basin-center deposits, if any were present, is not known, as erosional stripping following late Tertiary uplift of the Colorado Plateau has removed all but the marginal lacustrine deposits. The "regional" paleocurrent direction in the study area appears to be towards the northeast; the eastward-directed paleocurrents in the eastern portion of the study area probably resulted from flow deflection by a Laramide monocline in that area.

The study area is located in the transition zone between the Colorado Plateau to the north and the Rio Grande rift system to the southeast. Three episodes of structural development have modified the area. A poorly defined monoclinial flexure of probable Laramide age is present in the southeastern portion of the study area. North-trending normal faults and associated drag folds and mafic dikes are common in the eastern part of the area and were produced by Neogene extension. Epeirogenic uplift of the Colorado Plateau during Neogene time resulted in the southward tilting of strata in the region.

Baca conglomerates in the study area exhibit a wide range of clast lithologies, including (in order of decreasing abundance) metaquartzite, limestone, chert, granite, sandstone and siltstone, schist, mudstone, and volcanic rocks. Conglomerate clasts are highly spherical and usually well rounded. The majority of the sandstones in the study area are lithic arkoses, feldspathic litharenites, and sublitharenites. Two genetic quartz types, common and metamorphic quartz, are present in subequal proportions. Orthoclase is the most common feldspar type, followed by microcline and plagioclase. Rock fragment varieties, listed in order of decreasing abundance, include metamorphic, chert, mudstone, granite/gneiss, volcanic, carbonate, sandstone and siltstone rock fragments. Upsection changes

in sandstone mineralogy indicate increasing contributions by Precambrian plutonic and metamorphic terranes, at the expense of sedimentary sources, during basal Baca sedimentation. The dominant source areas for the Baca Formation in the study area were the Morenci uplift and the western flank of that portion of the Sierra-Sandia uplift which lies to the south of the area. Baca sandstones exhibit two distinct heavy-mineral suites. The first is associated with red sandstones and consists predominantly of magnetite/ilmenite/specular hematite. Non-red (yellow-gray) Baca sandstones, on the other hand, contain a heavy-mineral suite which is dominated by leucoxene. Subordinate amounts of zircon, garnet, apatite, biotite, and muscovite are present in both of these suites. The anomalous heavy-mineral suite in the non-red sandstones was produced through interaction with negative-Eh groundwaters associated with dike emplacement and dolomite cementation during Miocene time. Illite is the dominant detrital clay mineral in the study area.


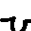
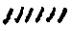







Four types of cement are present in the Baca sediments in the study area. These are, in order of decreasing abundance, calcite, kaolinite, quartz, and dolomite. Calcite cements, in the form of caliche, fine- and coarse-grained spar, were the first to precipitate. These formed during very shallow burial or within the

lacustrine environment. Quartz cements were the next to form and, as is the case with subsequent cements, are restricted to permeable upper-delta and braided alluvial-plain sandstones. Authigenic quartz content increases at the top of the Baca stratigraphic section, indicating that much of the silica was probably derived from overlying volcanic units. Kaolinite cements followed quartz precipitation, and are indicative of acidic groundwater conditions. Dolomite was the final cement, usually occurring as a replacement product of kaolinite and calcite. It only occurs in permeable sandstones which are near mafic dikes, and was precipitated from alkaline groundwaters during dike intrusion in Miocene time. Recent oxidation of dolomite to limonite is the predominant source of yellow coloration in the Baca. The widespread red coloration in the Baca is produced by early-diagenetic intrastratal dissolution of unstable heavy minerals, precipitation of limonite, and subsequent dehydration of limonite to produce the hematite colorant.

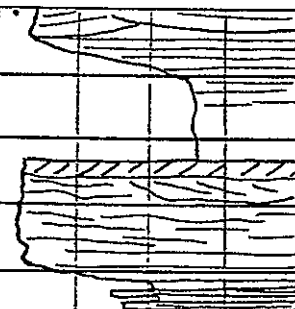
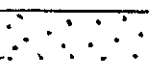
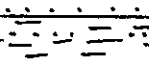

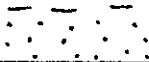
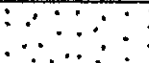
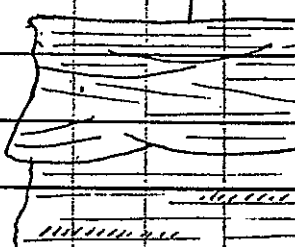

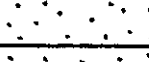
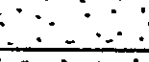
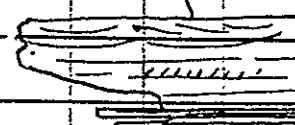
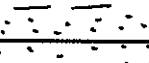
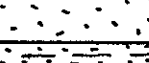
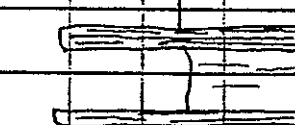
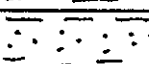
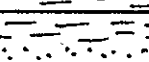

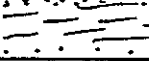

Uranium is the only known economically important resource in the Baca. The Hook Ranch uranium prospect is present in a deltaic sandstone unit in the eastern portion of the study area. The mineralized sandstones are dominantly gray in color and contain abundant carbonaceous debris. Uranium exploration efforts within the Baca in the

Gallinas Mountains vicinity should be restricted to non-red sandstones which are indicative of the former presence of reducing groundwaters, and areas which contain anomalously high concentrations of carbonaceous materials.

APPENDIX A

Baca Formation
Measured SectionExplanation
of SymbolsBioturbation  roots  burrowsSedimentary Structures ripple cross lamination tabular crossbedding trough crossbedding parallel stratification convolute stratificationLithology conglomerate sandstone mudstone

SEDIMENTARY STRUCTURES AND TEXTURES					BASIC ROCK TYPE	COLOR	BIOTURBATION	REMARKS	
GRAIN SIZE									
gran css fss silt clay									
								shallowly inclined prodelta foresets	
						5R 6 1/2	v	poorly exposed	
							Λ Λ		
						10YR 7 1/2			
					150				erosional base
							v	poorly exposed	
						5R 4 1/2	v		
						10YR 8 1/2			
								flaggy parting	
							v		
					100		5R 5 1/2	v	
								v	

SEDIMENTARY STRUCTURES AND TEXTURES		BASIC ROCK TYPE	COLOR	BIOTURBATION	REMARKS
GRAIN SIZE					
gran	css	fss	silt	clay	
			10R 6/2		poorly exposed
			5R 6/2		
			10R 6/2		poorly exposed
			5R 6/2	v	
250				10R 6/2	
			grades		large-scale trough crossbedding
				10YR 7/2	
				5R 6/2	
			10YR 7/2		poorly exposed
				v	
			5R 6/2		
				v	
200				10YR 7/2	
					

SEDIMENTARY STRUCTURES AND TEXTURES					BASIC ROCK TYPE	COLOR	BIOTURBATION	REMARKS
GRAIN SIZE								
gran css fss silt clay								
								abundant magnetite
650						5R 6 1/2		

APPENDIX B

Summary of Point-count Data for Study-area Sandstone Thin Sections

	SAMPLE NUMBER	DETRITAL CONSTITUENTS *														AUTHIGENIC CONSTITUENTS AND POROSITY **									
		grain size (φ)	metasilt	common quartz	metasilt/total qtz	orthoclase	microcline	plagioclase	metamorphic RF	carbonate RF	chert	chalcedony	volcanic RF	granite/gneiss RF	sandstone RF	silt stone RF	mudstone RF	unidentified RF	heavy minerals	detrital clay	quartz cement	calcite cement	kaolinite cement	dolomite cement	total porosity
A	1.3	26	51	.34	4	3	1	10	0	5	1	1	0	0	0	1	0	0	6	4.5	3	6	5	0	
B	1.6	39	36	.52	5	1	0	7	0	8	0	1	0	0	0	2	0	0	13	0.5	12	0.5	8	3	1.5
C	1.8	31	29	.52	10	2	1	13	0	11	0	0	0	0	4	0	2	0	1	2.5	6.5	1.5	6	t	
D	0.9	33	15	.69	23	6	1	13	0	4	0	1	2	1	0	1	0	1	0	0.5	3.5	6	10	2	0.5
E	2.4	29	34	.47	6	10	1	13	0	4	1	0	2	0	0	0	0	5	0	t	26	6	0	0.5	0
G	2.5	17	39	.31	17	2	3	7	0	3	1	6	2	0	0	0	0	1.5	0	1.5	20	4	0	5.5	0.5
H	1.3	31	38	.45	5	2	0	13	0	7	0	0	2	0	0	1	0	0	0	t	0	5	0.5	10	0.5
J	1.8	36	30	.55	11	1	1	8	0	4	0	1	3	0	0	5	0	0.5	2	0.5	19	6	0	3	0
L	2.8	42	39	.52	6	0	0	5	1	2	0	0	0	0	0	5	0	1.5	0	0	38	0	0	0	0
N	0.6	51	12	.81	17	4	2	5	0	6	t	1	0	0	2	1	0	1	0	t	4	12	8	3.5	1
P	2.2	34	37	.48	8	1	0	11	3	4	1	t	1	1	0	1	2	4	0	0	11	11	0	0.5	0
8	3.1	25	48	.34	14	2	0	5	t	1	0	3	2	0	0	0	0	1	0	0	38	0	0	0	0
13	2.9	20	59	.26	8	1	0	3	2	6	0	1	0	0	0	0	0	1	0	0	48	0	0	0	0
24	2.8	19	43	.30	14	1	0	14	1	3	0	0	1	1	0	1	4	4	0	2.5	10	2	0	5	t

* percent of framework grains

** percent of bulk rock volume

APPENDIX B (continued)

	SAMPLE NUMBER	DETRITAL CONSTITUENTS *															AUTHIGENIC CONSTITUENTS AND POROSITY **									
		grain size (φ)	metagartz	common quartz	metagtz/total qtz	orthoclase	microcline	plagioclase	metamorphic RF	carbonate RF	chert	chalcedony	volcanic RF	granite/gneiss RF	sandstone RF	siltstone RF	mudstone RF	unidentified RF	heavy minerals	detrital clay	quartz cement	calcite cement	kaolinite cement	dolomite cement	total porosity	secondary porosity
	30	2.9	28	34	.45	17	5	0	11	0	1	0	1	0	0	3	3	4	9.5	2	2	0	5.5	1		
	32	1.6	28	22	.55	15	7	1	19	0	2	0	0	2	0	5	0	1.5	0	0	32	3.5	1.5	0	0	
	34	2.0	13	58	.19	4	3	0	2	0	17	0	0	2	0	0	2	1	0	1	41	0	0	0	0	
	36	2.0	25	39	.40	8	2	0	14	0	0	1	4	0	0	3	0	2	0	2	10	8	0	7	1	
	37	3.1	37	43	.46	5	1	0	9	3	1	0	1	0	0	1	1	4	0	0	42	0	0	0	0	
	39	1.8	23	30	.44	19	9	2	7	0	4	0	0	4	1	0	1	3	0.5	0	0.5	38	0.5	0	t	t
	45	1.6	31	32	.49	11	3	0	6	2	5	0	4	3	1	0	3	0	2	0	1	12	10	0	5	t
	47	2.5	27	31	.46	7	3	1	20	0	1	0	0	7	0	0	0	3	8	7	0.5	5	5.5	0	1	0
	48	2.2	28	35	.42	19	4	1	12	0	0	0	0	2	0	1	0	1	4.5	0	3	2	10	0	6	2
	49	2.1	29	41	.42	8	1	0	9	8	3	0	0	0	0	0	2	0	1	0	0	38	0	0	0.5	t
	56	2.2	49	35	.59	6	3	0	3	0	3	0	0	2	0	0	0	0	t	0	1.5	0	23	0	3	2
	69	2.6	37	43	.47	7	3	2	17	0	5	0	1	0	0	0	2	1	1.5	0	0.5	21	5	0	10	1
TOTAL	range	0.6-3.1	13-51	12-59	.19-.81	4-23	0-10	0-3	2-20	0-8	0-17	0-6	0-7	0-1	0-2	0-5	0-4	0-8	0-13	0-9.5	0-48	0-23	0-10.5	0-10	0-2	
	mean	2.1	30	37	.46	11	3.1	0.7	9.6	0.7	4.4	0.2	1.0	1.4	0.2	0.1	1.5	0.8	1.9	1.0	1.2	18	5.0	1.1	3.2	0.4

* percent of framework grains
 ** percent of bulk rock volume

REFERENCES CITED

- Adams, S. S., Curtis, H. S., and Hafen, P. L., 1974, Alteration of detrital magnetite-ilmenite in continental sandstones of the Morrison Formation, New Mexico: in Formation of uranium ore deposits, Proceedings of a symposium, Athens, Greece.
- Allen, J. R., and Balk, R., 1954, Mineral resources of Fort Defiance and Tohatchi quadrangles, Arizona and New Mexico: N. Mex. Bur. Mines and Min. Res., Bull. 36., 192 p.
- Anonymous, 1959, Uranium deposits in the Datil Mountains-Bear Mountains region, New Mexico: N. Mex. Geological Society Guidebook, 10th Field Conf. p. 135-143.
- Armstrong, R. L., 1968, Sevier orogenic belt of Nevada and Utah: Geol. Soc. Am. Bull., v. 79, p. 429-458.
- Assereto, R., and Folk, R. L., 1976, Brick-like texture and radial rays in Triassic pisolites of Lombardy, Italy: a clue to distinguish ancient aragonitic pisolites: Sed. Geol., v. 16, p. 205-222.
- Axelsson, V., 1967, The Laiture delta: a study of deltaic morphology and processes: Geogr. Ann. Ser. A, v. 49, p. 1-127.
- Bachman, G. O., Baltz, E. H., and Griggs, R. L., 1957, Reconnaissance of geology and uranium occurrences of the upper Alamosa Creek valley, Catron County, New Mexico: U. S. Geol. Surv. Trace Elements Inv., Rept. 521.
- Basu, A. B., Young, S. W., Suttner, L. J., James, W. C., and Mack, G. H., 1975, Re-evaluation of the use of undulatory extinction and polycrystallinity in detrital quartz grains for provenance interpretation: Jour. Sed. Petrology, v. 45, p. 873-882.
- Bates, C. C., 1953, Rational theory of delta formation: Am. Assoc. Petroleum Geologists Bull., v. 37, p. 2119-2162.
- Begle, E., 1978, The weathering of granite, Llano region, central Texas: Univ. Texas (Austin), Unpub. M. A. thesis, 163 p.

- Blatt, H., 1967, Original characteristics of clastic quartz grains: Jour. Sed. Petrology, v. 37, p. 401-424.
- Boothroyd, J. C., and Ashley, G. M., 1975, Processes, bar morphology, and sedimentary structures on braided outwash fans, northeastern Gulf of Alaska, in McDonald, B. C., and Jopling, A. V., eds., Glaciofluvial and Glaciolacustrine Sedimentation: Soc. Econ. Paleontologists and Mineralogists, Spec. Pub. no. 23, p. 193-222.
- Bull, W. B., 1972, Recognition of alluvial-fan deposits in the stratigraphic record, in Rigby, J. K., and Hamblin, W. K., eds., Recognition of Ancient Sedimentary Environments: Soc. Econ. Paleontologists and Mineralogists, Spec. Pub. no. 16, p. 63-83.
- Burchfiel, B. C., and Davis, G. A., 1972, Structural framework and evolution of the southern part of the Cordilleran orogen, western United States: Am. Jour. Sci., v. 272, p. 97-118.
- Callender, J. F., and Zilinski, R. E., Jr., 1976, Kinematics of Tertiary and Quaternary deformation along the eastern edge of the Lucero uplift, central New Mexico: N. Mex. Geol. Soc., Spec. Pub. no. 6, p. 53-61.
- Cameron, K. L., and Blatt, H., 1971, Durabilities of sand size schist and "volcanic" rock fragments during fluvial transport, Elk Creek, Black Hills, South Dakota: Jour. Sed. Petrology, v. 41, p. 565-576.
- Cant, D. J., and Walker, R. G., 1976, Development of a braided-fluvial facies model for the Devonian Battery Point Sandstone, Quebec: Canad. Jour. Earth Sciences, v. 13, p. 102-119.
- Chaiffetz, M. S., 1979, (abs.) Palynological age and paleoecology of the Baca Formation, northwestern Socorro County, central-western New Mexico: Geol. Soc. Am. Abs. Prog., p. 268.
- Chapin, C. E., and Seager, W. R., 1975, Evolution of the Rio Grande rift in the Socorro and Las Cruces areas: N. Mex. Geol. Soc., Guidebook, 26th field conf., p. 297-321.

- _____, Chamberlin, R. N., Osburn, G. R., White, D. W., Sandford, A. R., 1978, Exploration framework of the Socorro geothermal area, New Mexico: N. Mex. Geol. Soc., Spec. Pub. no. 7, p. 115-130.
- _____, Osburn, G. R., Hook, S. C., Massingill, G. L., Frost, S. J., 1979, Coal, uranium, oil and gas potential of the Riley- Puertecito area, Socorro County, New Mexico: N. Mex. Bur. Mines and Min. Res., Open File Rept., 33 p.
- Coney, P. J., 1971, Cordilleran tectonic transitions and motion of the North American plate: *Nature*, v. 233, p. 462-465.
- _____, 1976, Plate tectonics and the Laramide orogeny: N. Mex. Geol. Soc., Spec. Pub. no. 6, p. 5-10.
- _____, 1978, Mesozoic-Cenozoic Cordilleran plate tectonics: *Geol. Soc. Am., Mem.* 152, p. 33-50.
- Cooley, M. E., and Davidson, E. S., 1963, The Mogollon Highlands- their influence on Mesozoic and Cenozoic erosion and sedimentation: *Ariz. Geol. Soc. Digest*, v. 6, p. 7-35.
- Costello, W. R., and Walker, R. G., 1972, Pleistocene sedimentology, Credit River, southern Ontario: a new component of the braided river model: *Jour. Sed. Petrology*, v. 42, p. 389-400.
- Couples, G., and Stearns, D. W., 1978, Analytical solutions applied to structures of the Rocky Mountains foreland on local and regional scales: *Geol. Soc. Am. Mem.* 151, p. 313-335.
- Crowell, J. C., 1955, Directional current structures from the Prealpine Flysch, Switzerland: *Geol. Soc. Am. Bull.*, v. 66, p. 1351-1384.
- Davis, G. H., 1978, Monocline fold pattern of the Colorado Plateau: *Geol. Soc. Am., Mem.* 151, p. 215-233.
- _____, 1979, Laramide folding and faulting in southeastern Arizona: *Am. Jour. Sci.*, v. 279, p. 543-569.
- Dickenson, W. R., and Snyder, W. S., 1978, Plate tectonics of the Laramide orogeny: *Geol. Soc. Am., Mem.* 151, p. 355-365.

- Dobkins, J. E., Jr., and Folk, R. L., 1970, Shape development on Tahiti-Nui: Jour. Sed. Petrology, v. 40, p. 1167-1203.
- Dodge, C. N., 1973, Pebbles of the Chinle and Morrison Formations: N. Mex. Geol. Soc. Guidebook, 24th Field Conf., p. 114-121.
- Dott, R. H., 1973, Paleocurrent analysis of trough cross stratification: Jour. Sed. Petrology, v. 43, p. 779-784.
- Douros, J. D., 1967, The relationship of microorganisms to uranium and other mineral deposits: Denver Research Inst., Univ. of Denver.
- Drewes, H., 1978, The Cordilleran orogenic belt between Nevada and Chihuahua: Geol. Soc. Am. Bull., v. 89, p. 641-657.
- Dunham, R. J., 1971, Meniscus cement: in Bricker, O. P., ed., Carbonate Cements, Johns Hopkins Press, Baltimore, Md., p. 297-300.
- Eardley, A. J., 1962, Structural geology of North America: Harper and Row, Pub., New York, 743 p.
- Epis, R. C., and Chapin, C. E., 1975, Geomorphic and tectonic implications of the post-Laramide, late Eocene erosion surface in the southern Rocky Mountains: Geol. Soc. Am., Mem. 144, p. 45-74.
- Fisher, W. L., Brown, L. F., Jr., Scott, A. J., and McGowen, J. H., 1969, Delta systems in the exploration of oil and gas: Univ. Texas, Austin, Bur. Econ. Geology, Research Colloquium, 212 p.
- _____, and Brown, L. F., 1972, Clastic depositional systems-a genetic approach to facies analysis: Univ. Texas, Austin, Bur. Econ. Geology, Annotated Outline and Bibliography, 211 p.
- Fitzsimmons, J. P., 1959, The structure and geomorphology of west-central New Mexico: N. Mex. Geol. Soc., Guidebook Tenth Field Conf., p. 112-116.
- Folk, R. L., 1959, Practical petrographic classification of limestones: Am. Assoc. Petroleum Geologists, v. 43, p. 1-38.

- _____, 1969, Toward greater precision in rock-color terminology: Geol. Soc. Am. Bull., v. 80, p. 725-728.
- _____, 1974, Petrology of sedimentary rocks: Austin, Hemphill Publishing Co., 182 p.
- _____, 1974, Reddening of desert sands, Simpson Desert, Australia: Jour. Sed. Petrology, v. 46, p. 604-615.
- _____, 1976, Reddening of desert sands, Simpson Desert, Australia: Jour. Sed. Petrology, v. 46, p. 604-615.
- _____, and Pittman, J. S., 1971, Length-slow chalcedony: a new testament for vanished evaporites: Jour. Sed. Petrology, v. 41, p. 1045-1058.
- Foster, R. W., 1978, Selected data from deep drill holes along the Rio Grande rift in New Mexico: N. Mex. Bur. Mines and Mineral Res., Circ. 163, p. 236-237.
- Galloway, W. E., 1977, Catahoula Formation of the Texas coastal plain: depositional systems, composition, structural development, ground-water flow history, and uranium distribution: Univ. Texas, Austin, Bur. Econ. Geol. Rept. Inv. no. 87, 59 p.
- _____, and Kaiser, W. R., 1979, Catahoula Formation of the Texas coastal plain: origin, geochemical evolution, and characteristics of uranium deposits: Univ. Texas, Austin, Bur. Econ. Geol., Open File Rept., 139 p.
- Gardener, J. H., 1910, The Carthage coal field, New Mexico: U. S. Geol. Survey Ann. Rept. no. 5, p. 69-123.
- Gilbert, G. K., 1885, The topographic features of lake shores: U.S. Geol. Survey Ann. Rept. no. 5, p. 69-123.
- Givens, D. B., 1957, Geology of the Dog Springs quadrangle, New Mexico: N. Mex. Bur. Mines and Min. Res. Bull. 58, 40 p.
- Gole, C. V., and Chitale, S. V., 1966, Inland delta building activity of Kosi River: Proc. Am. Soc. Civil Engineers, Jour. of Hydraulics Div., HY-2, p. 111-126.

- Gorham, T. W., and Ingersoll, R. V., 1979, Evolution of the Eocene Galisteo Basin, north-central New Mexico: N. Mex. Geol. Soc. Guidebook, 30th Field Conf., p. 219-224.
- Goudie, A., 1973, Duricrusts in tropical and subtropical landscapes: Oxford, Clarendon Press, 174 p.
- Griggs, R. L., 1954, A reconnaissance for uranium in New Mexico, 1953: U. S. Geol. Survey Circ. 354, 9 p.
- Grover, N. C., and Howard, C. S., 1938, The passage of turbid water through Lake Mead: Am Soc. of Civil Engineers Trans., v. 103, p. 720-732.
- Hantzschel, W., 1975, Treatise on invertebrate paleontology, Part W, Trace fossils and problematica: 2nd ed., Lawrence, Univ. of Kansas, 269 p.
- Harms, J. C., and Fahnestock, 1965, Stratification, bed forms, and flow phenomena (with an example from the Rio Grande), in Middleton, G. V., ed., Primary sedimentary structures and their hydrodynamic interpretation: Soc. Econ. Paleontologists and Mineralogists, Spec. Pub. 12, p. 84-115.
- Harrell, J. A., and Eriksson, K. A., 1979, Empirical conversion equations for thin-section and sieve derived size distribution parameters: Jour. Sed. Petrology, v. 49, p. 273-280.
- Hayes, P. T., 1978, Cambrian and Ordovician rocks of southeastern Arizona and southwestern New Mexico: N. Mex. Geol. Soc. Guidebook, 29th Field Conf., p. 165-173.
- High, L. R., and Picard, M. D., 1974, Reliability of cross-stratification types as paleocurrent indicators in fluvial rocks: Jour. Sed. Petrology, v. 44, p. 158-168.
- Hjulstrom, F., 1952, The geomorphology of the alluvial outwash plains (sandurs) of Iceland, and the mechanics of braided rivers: Internat. Geog. Union, 17th Cong., Proc., Washington, p. 337-342.
- Hooke, R. L., 1967, Processes on arid region alluvial fans: Jour. Geology, v. 75, p. 453-456.

- Hunt, C. B., 1956, Cenozoic geology of the Colorado Plateau: U. S. Geol. Survey Prof. Paper 279, 99 p.
- Jacobs, R. C., 1957, Geology of the central front of the Fra Cristobal Mountains, New Mexico: N. Mex. Geol. Soc. Guidebook, 8th Field Conf., p. 256-257.
- Johnson, B. D., 1978, Genetic stratigraphy and provenance of the Baca Formation, New Mexico and the Eagar Formation, Arizona: Univ. Texas (Austin), unpub. M. A. thesis, 150 p.
- Jonas, E. C., and McBride, E. F., 1977, Diagenesis of sandstone and shale: Application to exploration for hydrocarbons: Univ. Texas, Austin, Continuing Education Program, Pub. no. 1, 165 p.
- Jones, B. F., 1965, The hydrology and mineralogy of Deep Springs Lake, Inyo County, California: U. S. Geol. Survey Prof. Paper 502-A, 56 p.
- Kelley, V. C., 1951, Tectonics of the San Juan basin: N. Mex. Geol. Soc. Guidebook, 2nd Field Conf., p. 124-131.
- _____, 1955, Regional tectonics of the Colorado Plateau and relationships to the origin and distribution of uranium: Univ. New Mexico Pub. Geol. no. 5, 120 p.
- _____, and Clinton, N. J., 1960, Fracture systems and tectonic elements of the Colorado Plateau: Univ. New Mexico Pub. Geol. no. 6, 104 p.
- _____, and Silver, C., 1952, Geology of the Caballos Mountains with special reference to regional stratigraphy and structure and to mineral resources, including oil and gas: Univ. New Mexico Pub. Geol. no. 4, 286 p.
- Kessler, L. G., 1971, Characteristics of the braided stream depositional environment with examples from the South Canadian River, Texas: Earth Sciences Bull., v. 7, p. 25-35.
- Kottlowski, F. E., 1967, Rocks that shape the enchanting landscape: N. Mex. Bur. Mines and Min. Res. Scenic Trips to the Geologic Past, no. 8, p. 33-38.

- Krynine, P. D., 1946, Microscopic morphology of quartz types: *Annals of the 2nd Pan Am. Cong. of Mining Engineering and Geol.* (Petropolis, Brazil), p. 35-49.
- _____, 1949, The origin of red beds: *New York Acad. Sciences Trans. Ser. 2*, v. 11, p. 60-68.
- _____, 1950, The origin of redbeds (abs.): *Am Assoc. Petroleum Geol. Bull.*, v. 34, p. 1770.
- Langbein, W. B., 1961, Salinity and hydrology of closed lakes: *U. S. Geol. Survey Prof. Paper* 412, 50 p.
- Lee, W. T., and Knowlton, F. H., 1917, Raton Mesa and other regions in Colorado and New Mexico: *U. S. Geol. Survey Prof. Paper* 101, 437 p.
- Love, L. G., 1971, Early diagenetic polyframboidal pyrite, primary and redeposited, from the Wenlockian Denbigh Grit Group, Conway, North Wales, U. K.: *Jour. Sed. Petrology*, v. 44, p. 1038-1044.
- Massingill, G. L., 1979, Geology of the Riley-Puertecito area, southeastern margin of the Colorado Plateau, Socorro County, New Mexico: *Univ. Texas (El Paso)*, unpub. Ph. D. dissert., 301 p.
- Mayerson, D., 1979, Geology of the Corkscrew Canyon-Abbe Spring area, Socorro County, New Mexico: *N. Mex. Inst. Mining and Tech.*, unpub. M. S. thesis, 125 p.
- McBride, E. F., and Yeakel, L. S., 1963, Relation between parting lineation and rock fabric: *Jour. Sed. Petrology*, v. 33, p. 779-782.
- McGowen, H. J., 1970, Gum Hollow fan delta, Nueces Bay, Texas: *Univ. Texas, Austin, Bur. Econ. Geol. Rept. Inv. no.* 69, 91 p.
- McKee, E. D., Crosby, E. J., and Berryhill, H. L., Jr., 1967, Flood deposits, Bijou Creek, Colorado, June 1965: *Jour. Sed. Petrology*, v. 37, p. 829-851.
- Meckel, L. D., 1967, Tabular and trough cross-bedding: Comparison of dip azimuth variability: *Jour. Sed. Petrology*, v. 37, p. 80-86.

- Miall, A. D., 1977, Review of the braided stream depositional environment: *Earth Sci. Review*, v. 13, p. 1-62.
- Miller, D. N., and Folk, R. L., 1955, Occurrence of detrital magnetite and ilmenite in red sediments: new approach to the significance of redbeds: *Am. Assoc. Petroleum Geol. Bull.*, v. 39, p. 338-345.
- Mothersill, J. S., 1975, Lake Chad: geochemistry and sedimentary aspects of a shallow polymictic lake: *Jour. Sed. Petrology*, v. 45, p. 295-309.
- Normark, W. R., and Dickson, F. H., 1976, Man-made turbidity currents in Lake Superior: *Sedimentology*, v. 23, p. 815-831.
- O'Brien, B. R., 1956, Geology of the Cienega Amarilla area, Catron County, New Mexico and Apache County, Arizona: Univ. Texas (Austin), unpub. M. A. thesis, 76 p.
- Palmquist, J. C., 1978, Laramide structures and basement block faulting: Two examples from the Big Horn Mountains, Wyoming; *Geol. Soc. Am. Mem.* 151, p. 125-138.
- Pierce, H. W., Damon, P. E., and Shafiqullah, M., 1979, An Oligocene (?) Colorado Plateau edge in Arizona: *Tectonophysics*, v. 61, p. 1-24.
- Potter, S. C., 1970, Geology of Baca Canyon, Socorro County, New Mexico: Univ. of Arizona, unpub. M. S. thesis, 54 p.
- Powers, M. C., 1953, A new roundness scale for sedimentary particles: *Jour. Sed. Petrology*, v. 28, p. 108-110.
- Rust, B. R., 1972a, Structure and process in a braided river: *Sedimentology*, v. 18, p. 221-245.
- _____, 1972b, Pebble orientation in fluvial sediments: *Jour. Sed. Petrology*, v. 42, p. 384-388.
- Sales, J. K., 1968, Crustal mechanics of Cordilleran foreland deformation: a regional and scale model approach: *Am Assoc. Petroleum Geol. Bull.*, v. 52, p. 2016-2044.

- Sandberg, P. A., 1975, New interpretations of Great Salt Lake ooids and of ancient non-skeletal carbonate mineralogy: *Sedimentology*, v. 22, p. 497-537.
- Schumm, S. A., 1968, Speculation concerning paleohydrologic controls of terrestrial sedimentation: *Geol. Soc. Am. Bull.*, v. 79, p. 1573-1588.
- Silver, L. T., 1978, Precambrian formations and Precambrian history in Cochise County, southeastern Arizona: *N. Mex. Geol. Soc. Guidebook*, 29th Field Conf., p. 157-164.
- Sirriner, G. K., 1956, Geology of the Springerville-St. Johns area, Apache County, Arizona: Univ. Texas (Austin), unpub. Ph. D. dissert., 248 p.
- Smith, N. D., 1970, The braided stream depositional environment: Comparison of the Platte River and some Silurian clastic rocks, north central Appalachians: *Geol. Soc. Am. Bull.*, v. 81, p. 2993-3014.
- _____, 1975, Sedimentary environments and late Quaternary history of a low-energy mountain delta: *Canad. Jour. Earth Sciences*, v. 12, p. 2004-2013.
- Smithson, S. B., Brewer, J., Kaufman, S., Oliver, J., and Hurich, C., 1978, Nature of the Wind River thrust, Wyoming, from COCORP deep-reflection data and from gravity data: *Geology*, v. 6, p. 648-652.
- Sneed, E. D., and Folk, R. L., 1958, Pebbles in the lower Colorado River, Texas: a study in particle morphogenesis: *Jour. Geol.*, v. 66, p. 114-150.
- Snyder, D. O., 1971, Stratigraphic analysis of the Baca Formation, west central New Mexico: Univ. New Mexico, unpub. Ph. D. dissert., 158 p.
- Stearns, D. W., 1978, Faulting and forced folding in the Rocky Mountain foreland: *Geol. Soc. Am. Mem.* 151, p. 1-35.
- Stokes, W. L., 1947, The primary lineation in fluvial sandstones: A criteria of current direction: *Jour. Geol.*, v. 55, p. 52-54.
- Sumner, W., 1980, Geology of the Water Canyon-Jordan Canyon area, Socorro County, New Mexico: *N. Mex. Inst. Mining and Tech.*, unpub. M. S. thesis, 142 p.

- Surdam, R. C., and Wolfbauer, C. A., 1975, Green River Formation, Wyoming: a playa-lake complex: Geol. Soc. Am. Bull., v. 86, p. 335-345.
- Swirydczuk, K., Wilkinson, B. H., and Smith, G. R., 1979, The Pliocene Glens Ferry Oolite: lake-margin carbonate deposition in southwestern Snake River plain: Jour. Sed. Petrology, v. 49, p. 995-1004.
- Theakstone, W. H., 1976, Glacial lake sedimentation, Austerdalsisen, Norway: Sedimentology, v. 23, p. 671-688.
- Thom, W. T., Jr., 1955, Wedge uplifts and their tectonic significance, in Poldervaart, A., ed., Crust of the Earth: Geol. Soc. Am. Spec. Paper 62, p. 369-376.
- Tonking, W. H., 1957, Geology of the Puertecito quadrangle, Socorro County, New Mexico: N. Mex. Bur. Mines and Min. Res. Bull. 41, 67 p.
- Tweto, O., 1975, Laramide (Late Cretaceous-early Tertiary) orogeny in the southern Rocky Mountains: Geol. Soc. Am. Mem. 144, p. 1-44.
- Van Houten, F. B., 1948, Origin of red-banded early Cenozoic deposits in the Rocky Mountain region: Am. Assoc. Petroleum Geol. Bull., v. 32, p. 2083-2126.
- _____, 1962, Cyclic sedimentation and the origin of analcime-rich Upper Triassic Lockatong Formation, west central New Jersey and adjacent Pennsylvania: Am. Jour. Sci., v. 260, p. 561-576.
- _____, 1964, Origin of red beds--some unsolved problems, in Nairn, A. E. M., ed., Problems in Paleoclimatology: New York, Interscience Pub., Inc., p. 647-661.
- Walker, T. R., 1963, (abs.) In situ formation of red beds in an arid to semiarid climate: Geol. Soc. Am. Spec. Paper 76, p. 174-175.
- _____, 1967, Formation of red beds in modern and ancient deserts: Geol. Soc. Am. Bull. v. 78, p. 353-368.

- _____, 1974, Formation of red beds in moist tropical climates: A hypothesis: Geol. Soc. Am. Bull., v. 85, p. 633-638.
- _____, 1975, (abs.) Intrastratal sources of uranium in first-cycle, nonmarine redbeds: Am. Assoc. Petroleum Geol. Bull., v. 59, p. 925.
- Weber, R. H., 1971, K/Ar ages of Tertiary igneous rocks in central and western New Mexico: Isochron/West, N. Mex. Bur. Mines and Min. Res. Pub., p. 42.
- Williams, G. E., 1971, Flood deposits of the sand-bed ephemeral streams of central Australia: Sedimentology, v. 17, p. 1-40.
- Williams, P. F., and Rust, B. R., 1969, The sedimentology of a braided river: Jour. Sed. Petrology, v. 39, p. 649-679.
- Willard, M. E., 1959, Tertiary stratigraphy of northern Catron County, New Mexico: N. Mex. Geol. Soc. Guidebook, 10th Field Conf., p. 92-99.
- _____, and Givens, D. B., 1958, Reconnaissance geologic map of Datil thirty-minute quadrangle: N. Mex. Bur. Mines and Min. Res. Geologic Map 5.
- _____, and Weber, R. H., 1958, Reconnaissance geologic map of Canon Largo thirty-minute quadrangle: N. Mex. Bur. Mines and Min. Res. Geologic Map 6.
- Wilpolt, R. H., MacAlpin, A. J., Bates, R. L., and Vorbe, G., 1946, Geologic map and stratigraphic sections of the Paleozoic rocks of Joyita Hills, Los Pinos Mountains, and northern Chupadera Mesa, Valencia, Torrance, and Socorro Counties, New Mexico: U. S. Geol. Survey Oil and Gas Inv. Prelim. Map 61.
- _____, and Wanek, 1951, Geology of the region from Socorro and San Antonio east to Chupadera Mesa, Socorro County, New Mexico: U. S. Geol. Survey Oil and Gas Inv. Map OM-121.
- Winchester, D. E., 1920, Geology of the Alamosa Creek Valley, Socorro County, New Mexico; With special reference to the occurrence of oil and gas: U. S. Geol. Survey Bull. 716-A.

Woodward, L. A., Kaufman, A., and Anderson, J. B., 1972, Nacimientos fault and related structures, northern New Mexico: Geol. Soc. Am. Bull., v. 83, p. 2383-2396.

_____, 1973, Structural framework and tectonic evolution of the Four Corners region of the Colorado Plateau: N. Mex. Geol. Soc. Guidebook, 24th Field Conf., p. 94-98.

_____, 1976, Laramide deformation of the Rocky Mountain foreland; geometry and mechanisms: N. Mex. Geol. Soc. Spec. Pub. no. 6, p. 11-17.

VITA

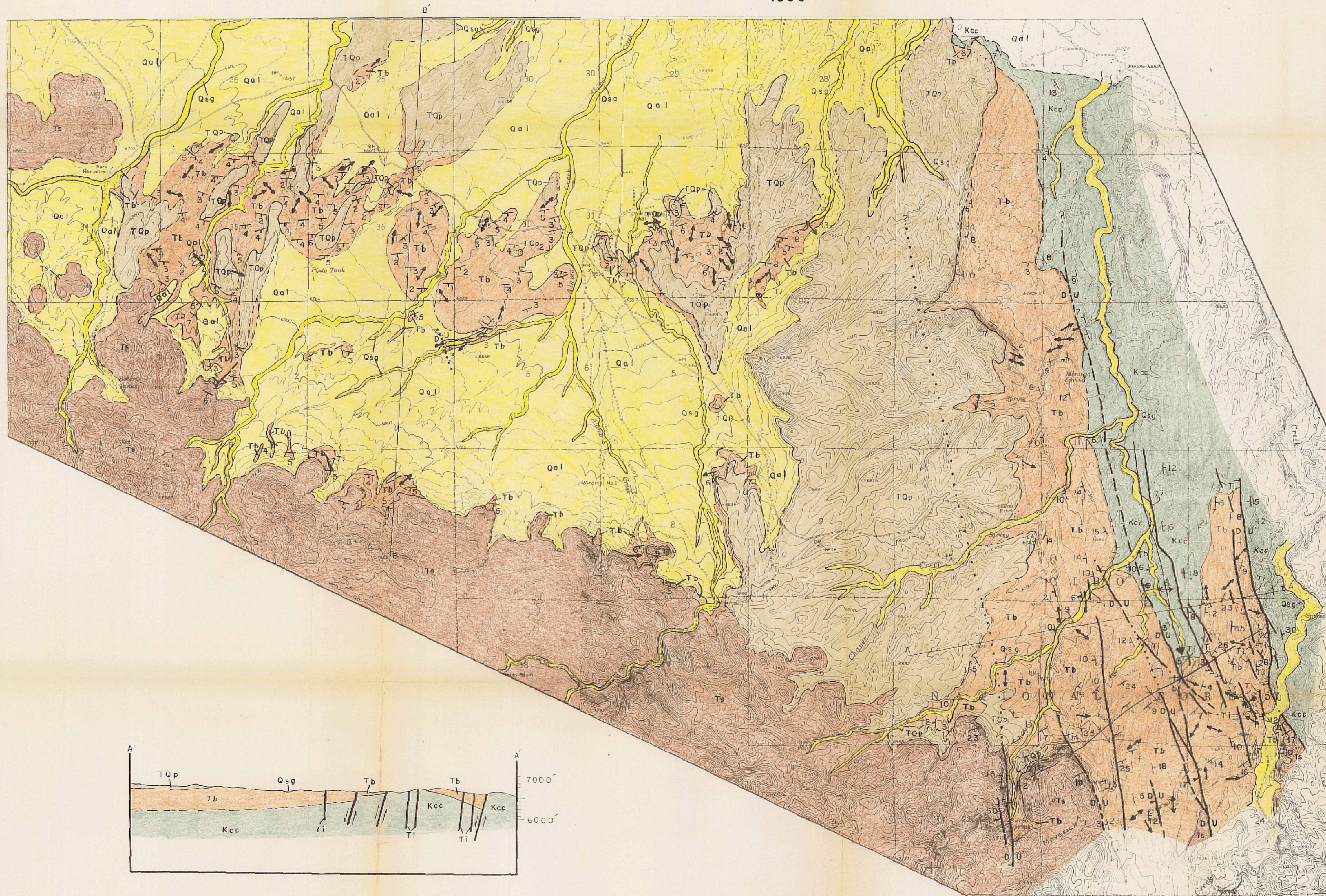
Steven Martin Cather was born in Van Nuys, California on July 25, 1953, the son of Franklin Eugene and Betty Joel Cather. After graduating from El Camino Real High School in Woodland Hills, California, he entered California State University at Northridge and began his studies in geology. In June, 1974, with the intent of escaping the overpopulated madness of Los Angeles, he migrated to the hinterlands of New Mexico, where he was enrolled as a transfer student at New Mexico Institute of Mining and Technology in Socorro. There he graduated with a Bachelor of Science degree in geology in May, 1976. For the majority of the year following his graduation, he was employed in two short-term uranium geology jobs with Kerr-McGee Corporation and Houston Oil And Minerals, Inc. In September, 1977, he entered the graduate school at the University of Texas at Austin. While working towards the Master of Arts degree in geology, he was employed as a teaching assistant by the Department of Geological Sciences. He is presently employed by the New Mexico Bureau of Mines and Mineral Resources.

Permanent address: 111 Clancy, Truth or Consequences, N. M.

This thesis was typed by Steve Cather on the DECsystem-20 computer at NMIMT.

Geologic Map and Sections of the Southern Portion of the
Alamo Reservation and Vicinity, Socorro County, New Mexico

Geology by Steve Cather
Drafting by Debbie Vetterman
1980

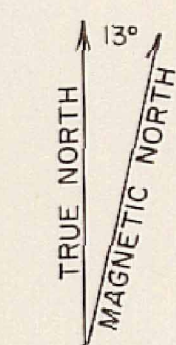
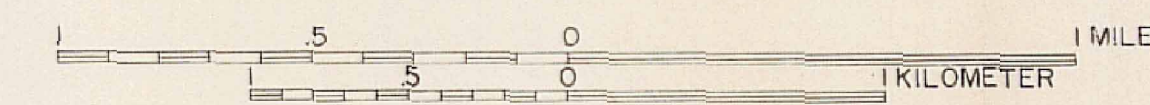
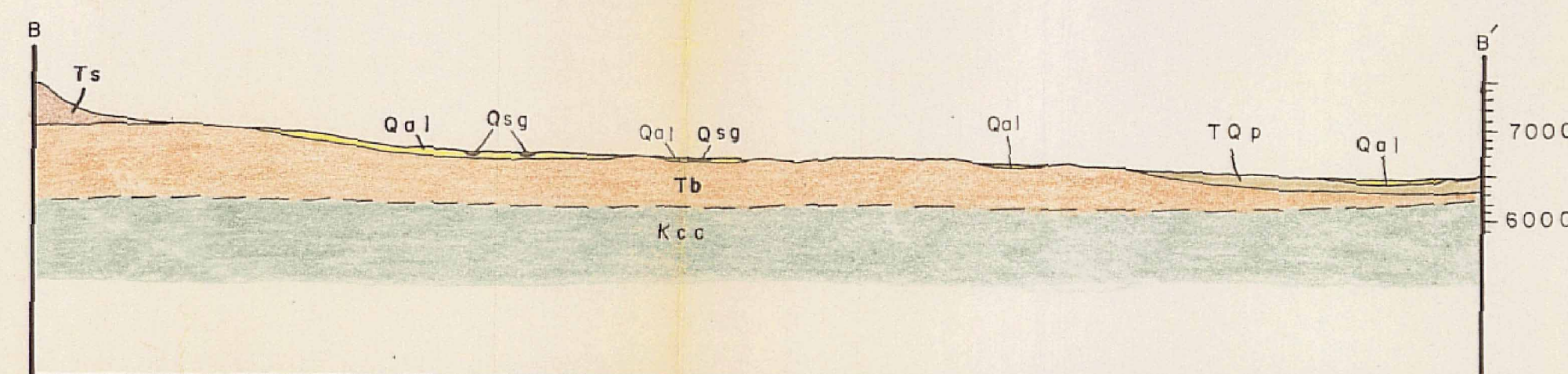
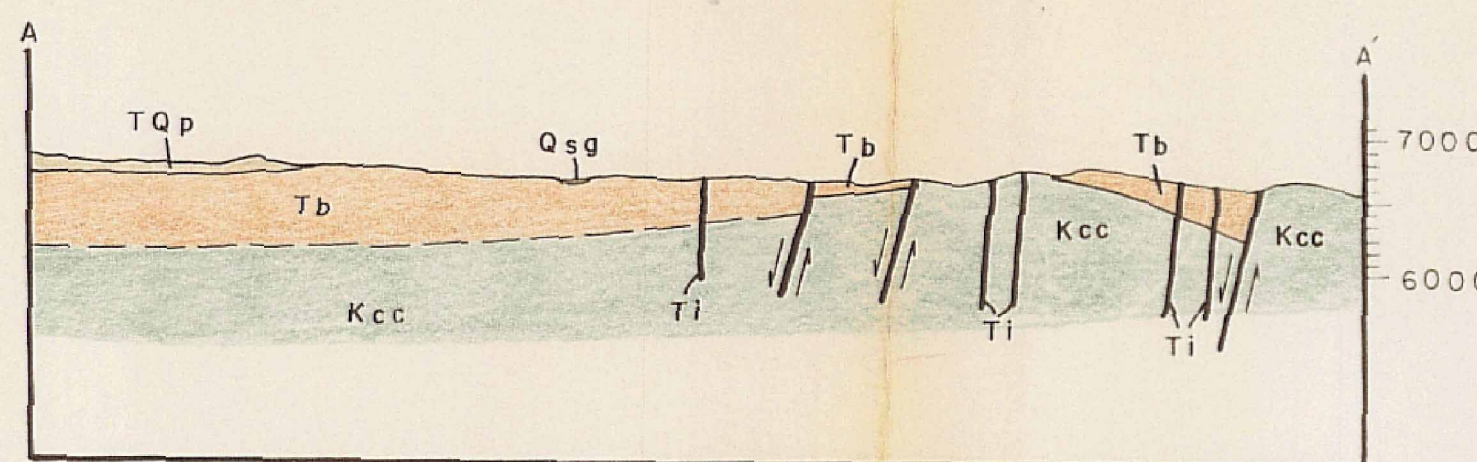


EXPLANATION

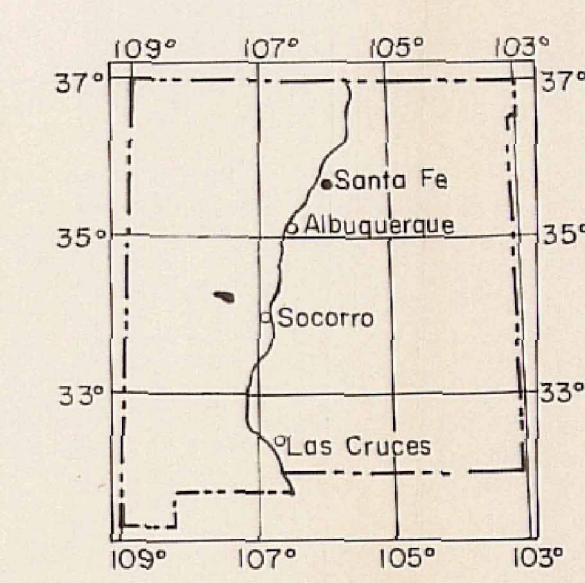
- | | | |
|------------|--|--|
| Quaternary | Qsg | recent stream sands and gravels |
| | Qal | alluvial fan and valley fill sediments |
| | TQp | piedmont gravels |
| Tertiary | Miocene
Tm | mafic dikes |
| | Oligocene
Ts | Spears Formation |
| | Eocene
Tb | Baca Formation |
| Cretaceous | Kcc | Crevasse Canyon Formation |

SYMBOLS

- | | |
|--|---|
| | Strike and dip of bedding |
| | Horizontal bed |
| | Contact (dashed where approximated, dotted where inferred). |
| | Fault (dashed where approximated, dotted where inferred), showing direction and amount of dip of fault plane, upthrown and down-thrown sides. |
| | Plunging Anticline |
| | Monocline |
| | Unidirectional paleocurrent indicator |
| | Bidirectional paleocurrent indicator |



APPROXIMATE MEAN DECLINATION



INDEX MAP